GAZİANTEP UNIVERSITY GRADUATE SCHOOL OF NATURAL & APPLIED SCIENCES

STRUCTURAL BUCKLING OPTIMIZATION OF STIFFENED PLATES

M. Sc.THESIS
IN
CIVIL ENGINEERING

BY
TALHA EKMEKYAPAR
JULY 2008

Structural Buckling Optimization of Stiffened Plates

M.Sc.Thesis
in
Civil Engineering
University of Gaziantep

Supervisor
Prof. Dr. Mustafa Özakça

by

Talha EKMEKYAPAR

July 2008

T.C.
GAZİANTEP UNIVERSITY
GRADUATE SCHOOL OF
NATURAL & APPLIED SCIENCES
CIVIL ENGINEERING

Name of the thesis: Structural Buckling Optimization of Stiffened Plates
Name of the student: Talha EKMEKYAPAR
Exam date: 03.07.2008

Approval of the Graduate School of Natural and Applied Sciences

Prof. Dr. Sadettin ÖZYAZICI
Director

I certify that this thesis satisfies all the requirements as a thesis for the degree of Master of Science/Doctor of Philosophy.

Assoc. Prof. Dr. Mustafa GÜNAL
Head of Department

This is to certify that we have read this thesis and that in our opinion it is fully adequate, in scope and quality, as a thesis for the degree of Master of Science/Doctor of Philosophy.

Prof. Dr. Mustafa ÖZAKÇA
Supervisor

Examining Committee Members

Prof. Dr. H. İbrahim GÜZELBEY ______________________

Prof. Dr. Mustafa ÖZAKÇA ______________________

Assoc. Prof. Dr. Mustafa GÜNAL ______________________

Assist. Prof. Dr. Abdülkadir ÇEVİK ______________________

Assist Prof. Dr. Bahattin KANBER ______________________

ABSTRACT

STRUCTURAL BUCKLING OPTIMIZATION OF STIFFENED PLATES

EKMEKYAPAR, Talha
M.Sc. in Civil Engineering
Supervisor: Prof. Dr. Mustafa ÖZAKÇA
July 2008, 123 pages

In this thesis, structural buckling optimization of stiffened plates was studied. Two types of stiffeners were used. First, straight stiffeners and second T shaped stiffeners. Examined plate types have common length, width and volume constraints. In each stiffener type, some combinations of pad elements, substiffener elements and variable plate skin were used. Buckling analyses of plates were carried out using a Fortran computer code which is based on Finite Strip (FS) method and developed by Özakça[1]. Optimization of plates was carried out with same program, which uses Sequential Quadratic Programming (SQP) as optimization tool. By these applications the effectiveness of 16 plate types using straight and T shaped stiffener types were investigated. Totally 315 runs were carried out for this purpose. The buckling optimization results are fluctuating in a wide range due to used elements combinations listed above and number of stiffeners. Improvements due to used element type and number of stiffeners are listed and compared according to stiffener types.

Key Words: Stiffened plates, Buckling analysis, Structural optimization, Finite strip

ÖZET

TAKVİYELİ PLAKALARIN YAPISAL BURKULMA OPTİMİZASYONU

EKMEKYAPAR Talha
Yüksek Lisans Tezi, İnşaat Mühendisliği Bölümü
Tez Yöneticisi: Prof. Dr. Mustafa ÖZAKÇA
Temmuz 2008, 123 sayfa

Bu tezde takviyeli plakaların yapısal burkulma optimizasyonu çalışılmıştır. İki tip takviye elemanı çeşidi kullanılmıştır. Bunlar düz takviyeler ve T şeklindeki takviyelerdir. İncelenen plaka tiplerinin uzunluk, genişlik ve hacim ortak kısıtları vardır. Her çeşit takviyeli plaka tipinde yastık, ara takviye elemanı ve lineer değişen plaka elemanlarından oluşan bazı kombinasyonlar kullanılmıştır. Plakların burkulma analizleri Özakça [1] tarafından geliştirilen Sonlu Şeritler metodu tabanlı bir FORTRAN yazılımıyla gerçekleştirilmiştir. Plakaların optimizasyon işlemi de aynı program tarafından Ardışık Karesel Programlama algoritması kullanılarak gerçekleştirilmiştir. Bu çerçevede düz ve T şeklinde takviye elemanları kullanarak 16 tip plakanın burkulmaya karşı etkileri irdelenmiştir. Bu amaçla 315 tane plağın analizi ve optimizasyonu yapılmıştır. İncelenen plakların burkulma optimizasyon sonuçları kullanılan eleman kombinasyonuna ve takviye elemanları sayısına göre geniş bir aralık içinde dalgalanmaktadır. Eleman tiplerine ve takviye elemanlarının sayısına göre burkulma yükündeki iyileşmeler gözlenip kullanılan eleman ve takviye elemanı tipi ile ilişkilendirilip karşılaştırmalar yapılmıştır.

Anahtar Kelimeler: Takviyeli plakalar, Burkulma analizi, Yapısal optimizasyon, Sonlu şeritler.

Acknowledgements

I would like to express my sincere deepest gratitude to my supervisor Prof. Dr. Mustafa Özakça, for his guidance, advice, encouragement and sharing his extensive experience during the preparation of this thesis.

Also I wish to initiate my thanks to Dr. Nildem Tayşi for her suggestions and replies to my inquiries.

Finally, I would like to express my gratitude to my wife Tuğba EKMEKYAPAR for her encouragement and patience.

CONTENTS

Page

LIST OF FIGURES

LIST OF TABLES

LIST OF SYMBOLS

FE	Finite Element
FS	Finite Strip
SQP	Sequential quadratic programming
DVs	Design variables

Scalar

A	Area
b	Length of strip
C_p, S_p	Cosine and sine function
$C(0)$	Order of continuity
d	Displacement
E	Young's modulus
$F(\mathbf{s})$	Objective function to be minimized
$g_j(\mathbf{s})$	Inequality constraint function
$h_k(\mathbf{s})$	Equality constraint function
J	Jacobian
ℓ	The arc length parameter of the curve
(m,n)	Mode and half-sine wave
N_i	Shape function associated with node i
R	Radius of curvature
s	Design variables
t	Thickness
u_ℓ, v_ℓ, w_ℓ	Displacement components in ℓ, y and n-direction
u,v,w	Global displacement parameters
u^p, v^p, w^p	Displacement amplitudes of p^{th} harmonic
V	Volume of the structure

U	Total strain energy
V_g	Potential energy of volume
P_{cr}	Critical buckling load
P_0	Initial load

Vector

$\mathbf{d}$	Vector of unknown displacements (eigenvector)
$\mathbf{d}_i^p$	Vector of nodal degrees of freedom
$\mathbf{d}_i^e$	Displacement (eigenvector) vector associated with element *e* and node *i*
$\overline{\mathbf{d}}_i^p$	Displacement (eigenvector) vector at node *i* and harmonic *p*
$\mathbf{s}$	Design variable vector
$\boldsymbol{\varepsilon}_m$	Inplane strains
$\boldsymbol{\varepsilon}_b$	Bending strains
$\boldsymbol{\varepsilon}_s$	Transverse shear strains
ε_ℓ^{nl}, ε_y^{nl}, $\gamma_{\ell y}^{nl}$	Second order strains
$\boldsymbol{\sigma}_m^p, \boldsymbol{\sigma}_b^p, \boldsymbol{\sigma}_s^p$	Membrane, bending and shear stress resultant vectors
$\sigma_\ell^0, \sigma_y^0, \tau_{\ell y}^0$	Applied inplane stresses

Matrix

$\mathbf{B}$	Strain-displacement matrix
$\mathbf{B}_{mi}^e$	Membrane strain-displacement matrix for element *e* and node *i*
$\mathbf{B}_{bi}^e$	Bending strain-displacement matrix for element *e* and node *i*
$\mathbf{B}_{si}^e$	Shear strain-displacement matrix for element *e* and node *i*
$\mathbf{B}_{mi}^p$	Membrane strain-displacement matrix for node *i* and harmonic *p*
$\mathbf{B}_{si}^p$	Shear strain-displacement matrix for node *i* and harmonic *p*

$\mathbf{B}_{si}$	Shear strain displacement matrix
$\mathbf{D}$	Matrix of rigidities
$\mathbf{D}_m$, $\mathbf{D}_b$, $\mathbf{D}_s$	Matrices of membrane, bending and shear rigidities
$\mathbf{J}$	Jacobian matrix
$\mathbf{K}_{ij}^{e}$	Stiffness matrix associated with element e and node I and j
$[\mathbf{K}]^{pp}$	Global stiffness matrix associated with harmonic p
$[\mathbf{K}_{ij}^{e}]^{pq}$	Stiffness matrix linking nodes i and j and harmonics p and q
$\mathbf{K}_{mij}^{e}$	Membrane stiffness matrix for element e and node i and j
$\mathbf{K}_{bij}^{e}$	Bending stiffness matrix for element e and node i and j
$\mathbf{K}_{sij}^{e}$	Shear stiffness matrix for element e and node i and j
$\mathbf{N}$	Shape function matrix

Greek Symbols

α	Angle between local and global axes
δ_{ι}	Mesh density
Δs_k	Small perturbation of design variables s_k
$\varepsilon_{\ell}, \varepsilon_{y}$	Strain in ℓ direction and longitudinal strain
$\gamma_{\ell y}, \gamma_{yn}$	Shear strain
κ	Shear modification factor
κ_{ℓ}	Curvature in the ℓ-direction
κ_{y}	Longitudinal curvature
$\kappa_{\ell y}$	Twisting curvature
λ^{p}	Load factor (eigenvalues)
ν	Poisson's ratio
ϕ, ψ	Rotation of the midsurface normal in the ℓn and yn plane
ϕ^{p}, ψ^{p}	Rotation amplitude for the p^{th} harmonic term
ξ	Isoparametric element natural (curvilinear) coordinate
σ	Stress component
$\partial\ell$	Partial differential of ℓ

CHAPTER 1

INTRODUCTION

1.1 General Information

Weight saving for a structural element without loss of any strength is the crucial aim of structural engineering. Because of their high strength to weight ratio stiffened plates have wide use in most of structural engineering domains. Two dimensional behavior of flat plates is strengthened in third direction against bending by adding longitudinal stiffeners to flat plate surface. Stiffened plates widely used in ships, aircrafts and other heavily loaded thin walled structures.

An axially loaded structure converts its in-plane energy to bending energy with increasing load and at a certain load value, buckling situation arises. So buckling phenomena is an inevitable situation for axially heavily compressed loaded structural elements. In design procedure of those types of structures, buckling case must be considered and should be avoided and negotiated.

The first buckling studies are carried out in eighteenth century by Leonhard Euler. He proved that there was a critical load for buckling of a slender column which bends to sideways with very large displacements before reaching the ultimate stress capacity of used material. Further studies about buckling showed that Euler's analytical formulas are exactly true for column applications. But because of the two dimensional action, the buckling behavior of plates are different and complex when compared with columns. Also when straight plates are stiffened with longitudinal stiffeners their response against axial loads become more complex. Analytical solutions for those types of structures become insufficient and tedious. In this regard, numerical solutions are inevitable.

There are several numerical methods, which are applicable in structural analysis domain. The most powerful of them is the Finite Element (FE) method, which is developed in 1960's. By the development of FE method, researchers endeavored to apply this powerful method in all parts of structural analysis. Observations verified that FE method gives excellent results compared with analytical solutions. In this regard, some researches are carried out for complex buckling problems.

In the following years, Finite Strip (FS) method is developed by Cheung [4] and the method has the capability of solving structural analysis problems that have prismatic shape and simple boundary conditions. FS forges fewer equations to be solved than FE. As result of this reduction, FS method is faster than FE method. The extensively comparison between FE and FS is introduced in Chapter 2.

To use available amount of material efficiently and obtain very high critical buckling load it is not enough to add stiffener elements to flat plate surface for strengthening them against buckling behavior. For this purpose, it is necessary to optimize the stiffened plate cross section dimensions subject to constant volume constraint. To know which shape gives the highest response of critical buckling load is a very complex task. Some mathematical or heuristic optimization methods should be properly adapted to structural analysis methods to obtain maximum critical buckling load.

1.2 Stiffened Plate Terminology

The structural elements of stiffened plates that examined in this thesis are shown in Figure 1.1.

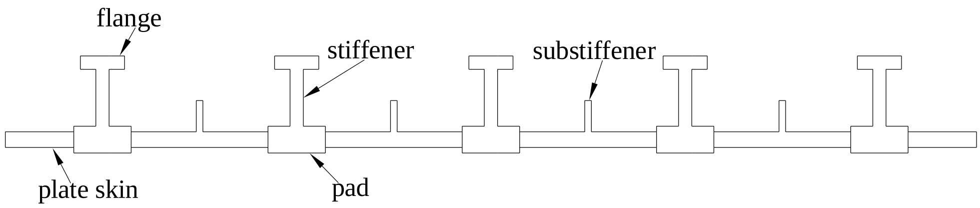

Figure 1.1 Structural plate elements

The effect of these structural plate elements on the critical buckling load is examined using the combinations of those elements. Number of stiffeners is also changed in the range of two to eight, for instance, Figure 1.1 shows stiffened plate with five stiffeners.

1.3 Principle Objectives

The crucial motivation of the thesis is structural size and structural shape optimization of stiffened plates including some combinations of structural elements shown above using a powerful computer code. The specific objectives may be expressed as follows:

- Maximizing the critical buckling load of considered stiffened plates.
- Investigating the performance of each structural element on the critical buckling load.
- Observing the change in element shape during optimization procedure to remark the efficiency of each structural element.
- Obtaining the best geometric shape and thickness variation for the considered stiffened plate.

1.4 About Computer Program

A free vibration analysis using FS method and shape optimization with Sequential Quadratic Programming (SQP) programs for straight folded plates and shells were developed by Özakça [1]. Then Özakça and coworkers [33] included buckling analysis subroutines of folded plates and shells into program. The latest version of program is used in FS analysis and structural optimization of stiffened plates.

1.5 Layout of Thesis

The contents of each chapter are expressed as:

- Chapter 2 contains literature survey about buckling analysis and shape optimization.
- Chapter 3 includes a condensed derivation of FS equations.
- Optimization process, definition of elements and design variables, structural optimization flowchart are presented in Chapter 4.
- Chapter 5 deals with results of analyses and remarks according to results.
- In Chapter 6, conclusions based on the present thesis are underlined.
- Finally, recommendations for future work are expressed.

CHAPTER 2

LITERATURE SURVEY

2.1 Introduction

Plates are straight, plane structures whose thicknesses are small compared to their other dimensions. More familiar examples of plates are table tops, side panels, roof of buildings, turbine disks, bulkheads, containers, airfoils and tank bottoms. Because of two-dimensional actions of plates, they have wide use in most fields of engineering. Although two-dimensional behavior of plates has several advantages as a structural element, this behavior requires more complex analysis methods. Powerful methods such as finite element and finite strip methods should be performed according to problem behavior and structure type.

2.2 Basics of Buckling

The equilibrium of plate is stable when the applied in plane forces are small and the deformations are created without lateral displacements. If the magnitude of these in-plane forces increases to a certain value, an important change occurs in the deformation path of plates. Then lateral displacements begin to introduce with in-plane displacements. In this situation, the stable equilibrium of plate becomes unstable and the plate is said to have buckled. The load that causes this condition is called as critical buckling load. The importance of the critical load is the initiation of a lateral deflection pattern, when the load is further increased, rapidly causes to very large deflections and eventually to complete failure of the plate. This is a dangerous condition, which must be considered during design procedure of structural plate elements and must be avoided [2].

Szilard [2] defined the main principle of buckling behavior of structures by a simple analogy involving the various states of equilibrium of a rigid sphere shown in Figure 2.1. The equilibrium condition of a sphere is called stable if it rests in a large concave bowl (Case1). If we disturb this sphere by small displacement, δx, after some oscillations in concave bowl it returns to its original position. If we consider same sphere is resting on a plane surface (Case 2), the equilibrium state is called as neutral and a small displacement, δx, does not affect the potential of sphere.

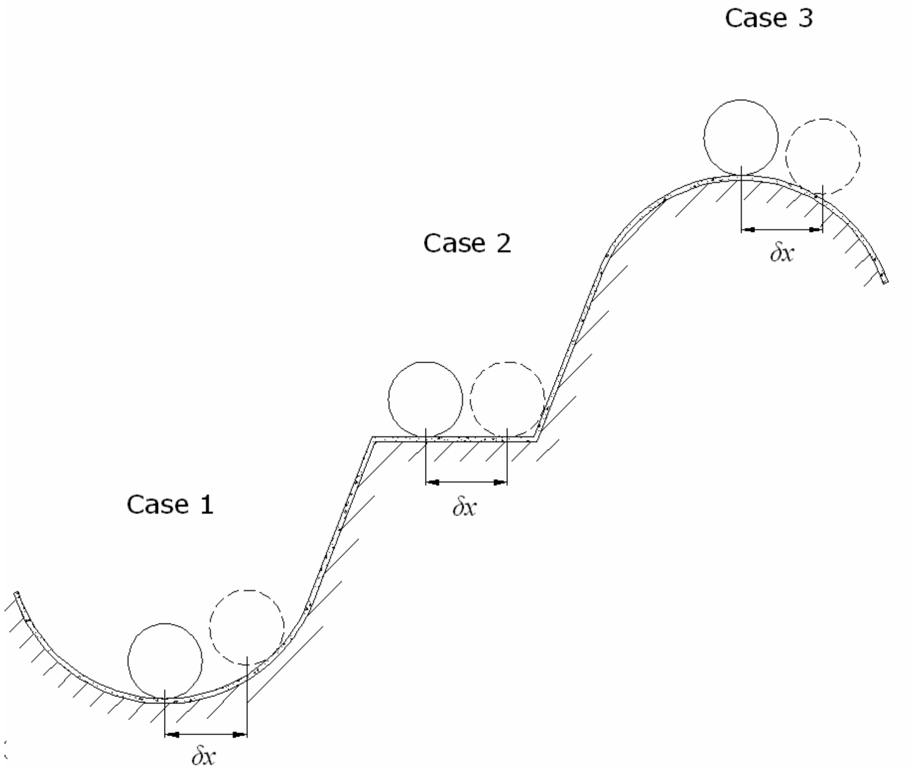

Figure 2.1 Various states of equilibrium [2]

If the sphere rests on another sphere (Case 3), in that case the state of equilibrium is called as unstable. A small disturbance (δx) causes complete and inevitable lost of equilibrium and failure. It is important to note that in the classical buckling theory the path leading from a stable to an unstable equilibrium always passes through a neutral state of equilibrium [2].

2.3 Buckling Analysis Methods

The solution of plate buckling problems by analytical methods is applicable when plate geometry, loading conditions and boundary conditions are simple. Otherwise, it is nearly impossible and tedious to solve this type of problems. The analytical solutions of various types of plates are extensively studied by Timoshenko [3]. Since computer applications are included structural analysis domain, extensive researches are performed about plate buckling analysis and several methods are developed. The most significant characteristic of developed computer applications is the capability of solving complex geometry, boundary and loading conditions. Another important characteristic of these applications is very high speed computation when compared analytical methods. In this regard, the most popular methods to solve plate buckling problems are the Finite Element (FE) and Finite Strip (FS) methods.

The FE method, as the most powerful and most preferred tool of solution in structural analysis, is well known, established and verified in all types of structural problems. For structures that have regular geometric plans and simple boundary conditions applying FE increases the solution time of problem and unnecessary. Plenty number of element requirement creates large matrix equations and increases the cost of solution. Also in many times, higher dimensional analysis is required for considered structural problem. To obtain more accurate results refinement of elements is required, thus a simple problem becomes a large complex one. Furthermore, it is a crucial point of view for a researcher to generate computer codes for that type of analysis. Researcher must generate much extended subroutines even wants to solve a problem, which has simple geometry and simple boundary conditions. The used computer also must be a high performance computer to solve large FE equations quickly. The above observations are especially true for static analysis of three dimensional solids and spatial structures and for eigenvalue problems in vibration and buckling analysis. An alternative method which can reduce the computational effort and core requirements, but at the same time retaining to some extent the versatility the FE analysis, is evidently desirable for the afore mentioned class of structures [4].

These requirements can be satisfied fully by FS, which is recently developed by Cheung [4]. In this method, the structure is divided into strips (in two dimensions) or prisms (in three dimensions). In this application, the geometry of the structure is usually constant along one or two coordinate axes so that the width of a strip or the cross section of the prism or layer will not change from one end to the other [4].

Cheung [4] defines the FS method as a special form of the FE procedure that uses the displacement approach. Unlike the standard FE, method uses polynomial displacement functions in all directions. The FS method calls for use of simple polynomials in some directions and continuously differentiable smooth series in the other direction, with the stipulation that such series should satisfy a priori the boundary conditions at the end of the strips or prisms [4].

A two dimensional plate geometrically modeled with four noded square FEs and FSs in Figure 2.2 to illustrate differences of two methods in analysis model.

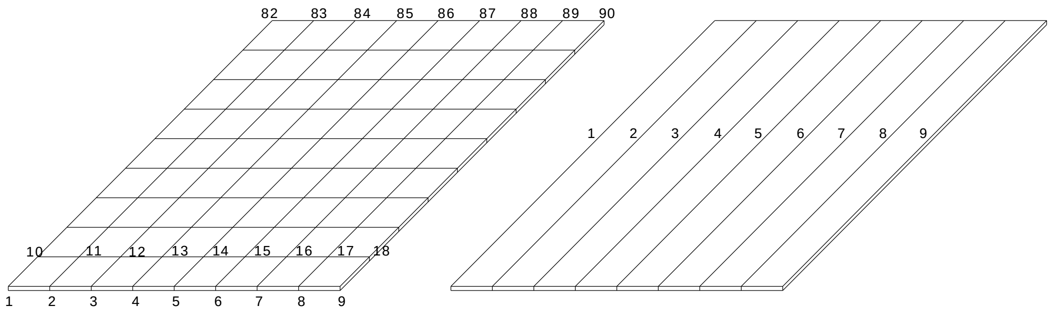

Figure 2.2 FE and FS models of a two dimensional plate

In the FE model, there are totally 90 nodes and 72 elements. If a researcher wants to run a computer code using FE method he/she must designate all nodes coordinates as input data. For instance:

Node	X	Y
1	0.0	0.0
2	5.0	0.0
3	10.0	0.0
.	.	.
.	.	.
.	.	.
90	40.0	45.0

Also element connectivity data of all elements must be designated to computer code as input data. For instance:

Element	Nodes			
1	1	2	11	10
2	2	3	12	11
3	3	4	13	12
.	.	.	.	.
.	.	.	.	.
.	.	.	.	.
72	80	81	90	89

Nevertheless, in FS model it is adequate that to designate only cross section geometry of plate. In FS model, there are eight strips should be defined. It is enough that designate nine coordinates and two noded, eight elements connectivity to computer code for this model. Examples of input data are specified below:

Node	X
1	5
2	10
3	15
.	.
.	.
.	.
9	40

Element	Nodes	
1	1	2
2	2	3
3	3	4
.	.	.
.	.	.
.	.	.
8	8	9

Also the computational times of two applications are different. FE method analysis uses 72 elements but FS analysis needs only eight strips. For this reason, FE analysis takes a long time versus FS.

Cheung [4] tabulated a general comparison between FE method and FS method to detail applications, inputs and outputs of two methods that presented at Table 2.1

FE analysis applications to plate buckling analysis have been carried out by following researchers; Allman [5], Przemieniecki [6] and Fafard et al. [7]. For complex boundaries, Anderson et al. [8] approximated curved boundaries with a large number of straight-edged triangular elements.

Sheikh et al. [9] investigated stability of tee-shaped steel stiffened plate under uniaxial compression using FE. They investigated the effect of five dimensionless parameters (the transverse slenderness of the plate, the slenderness of the web and flange of the stiffener, the ratio of torsional slenderness of the stiffener to the transverse slenderness of the plate, and the stiffener to-plate area ratio) on stability of stiffened plates.

Sridharan and Zeggane [10] studied the interaction of local and overall buckling in plate structures and stiffened shells by FE using a specially formulated shell element. Grondin et al. [11] investigated the stability of stiffened plates with tee-shaped stiffeners using FE. They validated the model using results of tests on full size stiffened plate specimens. Some of investigated parameters are plate aspect ratio, plate to stiffener cross-sectional area ratio and plate slenderness ratio.

Some other studies are available for different mechanical properties of stiffened plates. For example Jiang [12] carried out an investigation of bending and buckling of unstiffened, sandwich and hat-stiffened orthotropic, rectangular plates using first order shell elements and first and second order three dimensional solid elements by FE.

Table 2.1 Comparison between FE and FS methods [4]

	Finite Element	*Finite Strip*
Applicability to structures	*Applicable to any geometry, boundary conditions and material variation. Extremely versatile and powerful.*	*In static analysis, more often used for structures with two opposite simply supported ends and with or without intermediate elastic supports, especially for bridges. In dynamic analysis it is used for structures with all boundary conditions but without discrete supports.*
Required equ. to be solved	*Usually large number of equations and matrix with comparatively large bandwidth. Can be very expensive and at times impossible to work out solution because of limitation in computing facilities.*	*Usually much smaller number of equations and matrix with narrow bandwidth, especially true for problems with an opposite pair of simply supported ends. Consequently much shorter computing time for solution of comparable accuracy.*
Input data	*Large quantities of input data and easier to make mistakes. Requires automatic mesh and load generating schemes.*	*Very small amount of input data because of the small number of mesh lines involved due to the reduction in dimensional analysis.*
Output data	*Large quantities of output because as a rule all nodal displacements and element stresses are printed. Also many lower order elements will not yield correct stresses at the nodes and stress averaging or interpolation techniques must be used in the interpretation of results.*	*Easy to specify only those locations at which displacements and stresses are required and then output accordingly.*
Required computer effort	*Requires a large amount of core and is more difficult to program. Very often, advanced techniques such as mass condensation or subspace iteration have to be resorted to for eigenvalue problems in order to reduce core requirements.*	*Requires smaller amount of core and easier to program. Because only the lowest few eigenvalues are required (for most cases anyway) , the first two to three terms of the series will normally yield sufficiently accurate results matrix can usually be solved by standard eigenvalue subroutines.*

The FS method first developed by Cheung [13] in 1968. The main principle of FS is reducing partial differential equations into ordinary differential equations or partial differential equations of a lower order [4]. In FS the reduction is achieved either by assuming that the separation of variable approach can be applied in expressing the interpolation functions of unknowns or by carrying out suitable transformations. The FS theory and applications have been extensively discussed in text by Cheung [3]. Dawe et al [14-15] also have some investigations about buckling, postbuckling and free vibration of plates using FS.

Smith and Sridharan [16] investigated stability analysis of plate structures under arbitrary loading. They analyzed sample problems and compared economy of the method with FE method. Tham and Szeto [17] investigated buckling of arbitrary shaped plates by FS. They formulated plates using spline FSs. Then formulated eigenvalue matrix equation for buckling analysis and solved by same procedure as that of the standard FE method and presented some numerical examples to demonstrate the versatility and accuracy of the method.

Dawe and Peshkam [18] studied the prediction of buckling stresses and natural frequencies of vibration of long prismatic plate structures which may be formed of fibre-reinforced, composite, laminated material with very general properties.

Cheung [19] investigated free vibration and buckling analysis of plates with abrupt changes in thickness and complex support conditions. He modeled the stepped plate by FS and verified method by presenting numerical results. Xie and Ibrahim [20] investigated buckling mode localization of randomly misplaced rib-stiffened plates under compressive loads. They agreed FS solutions with those obtained from analytical solutions.

Takahasni and Nakazawa [21] studied vibration and buckling of plate girders by FS using small deflection theory. They obtained natural frequencies and buckling stresses of the simply supported plate girder and the effect of the flange plate on natural frequencies of the web plate is investigated.

Hinton [22] studied buckling of initially stressed Mindlin plates using thick finite strip method. He obtained some further results for initially stressed rectangular plates with two opposite edges simply supported and various support conditions on remaining sides. Hinton et al [23] investigated buckling analysis of prismatic folded plate structures supported on diaphragms at two opposite edges. They carried out analysis using variable thickness finite strips based on Mindlin-Reissner assumptions which allow for transverse shear deformation effects.

Özakça et al [24] investigated structural shape optimization of prismatic folded plates under buckling load consideration. They determined buckling loads using linear, quadratic and cubic, variable thickness, C(0) continuity, Mindlin-Reissner finite strips. Following studies, Özakça et al [25] investigated the post-buckling of sub-stiffened or locally tailored aluminium panels. They investigated post-buckling performance of panels with sub-stiffening or local tailoring of the skin thickness using linear variable thickness FS analysis.

2.4 Optimization Methods

Since the inception of engineering it is the most significant aim of structural engineers that constructing structures which are lightest and strongest. So in that point some changes in plate dimensions and shape should be made. Very low in-plane load carrying capacity of straight plates can be increased to very high values by adding stiffener elements to plate surface. Including only stiffener elements are not adequate to use plate volume very efficiently. In this regard size and shape optimization procedures should be carried out to increase in-plane load carrying capacity of such structures, efficiently.

In engineering science mathematical programming methods are the early and powerful methods that engineers use since the inception of computer applications. Structural optimization using two dimensional representations was first investigated by Zienkiewicz and Campbell [26]. Since then much work has been reported.

Levy and Ganz [27] analyzed plates that optimized using variational calculus to obtain the optimality condition which states that the thickness is proportional to the strain energy density and truncated Fourier series solution was used to obtain an optimal shape.

Hojjat and Kok [28] developed prototype knowledge based expert system for optimum design of steel plate girders used in highway bridges. They developed a mathematical optimization algorithm for minimum weight design of plate girders using generalized geometric programming technique.

Jarmai et al [29] investigated optimal design of cylindrical orthogonally stiffened shell member of an offshore fixed platform truss, loaded by axial compression and external pressure using various mathematical programming the methods. In optimization and design they used ring stiffeners of welded box section and stringers of halved rolled I-type sections.

Bedair [30] developed approaches for minimum weight design of stiffened plates. He described an alternative energy based approach for stability analysis of multi-stiffened plates under uniform compression and idealized the structure as assembled plate and beam elements are rigidly connected at their junctions. Then he derived strain energy components for the plate and the stiffener elements in terms of out-of and in-plane displacement functions and used sequential quadratic programming to find the buckling load of the structure for given plate/stiffener geometric proportions.

Two main fundamental aims of computer applications are creating algorithms that have short run time and capability of finding optimal solutions. Since, the magnificent improvement of computers some other alternative algorithms are developed for optimization problems that called heuristic methods and improved in last three decades. The most significant characteristic of heuristic methods is the fast running times of those algorithms.

Bisagni and Lanzi [31] investigated post buckling optimization procedure for the design of composite stiffened panels subjected to compression loads using neural networks. To overcome too expensive analyses from a computational point of view, he developed an optimization procedure. It is based on a global approximation strategy, where the structure response is given by a system of neural networks trained by means of finite element analyses, and on genetic algorithms that results particularly profitable due to presence of integer variables.

Kang and Kim [32] studied minimum weight design of compressively loaded composite plates and composite stiffened panels under constrained post buckling strength. As an optimization technique, they used a modified Genetic Algorithm to find optimum points.

CHAPTER 3

BUCKLING ANALYSIS OF PLATES

3.1 Introduction

Most of the structures are constructed using plates have regular geometric shapes along longitudinal direction. Analyzing such structures with classical methods or FE method is extravagant and the cost of the solutions can be very high as we discussed in previous chapter. Also designating the geometric positions of FEs and element connectivity properties of such structures to computer applications is time consuming and tedious. If such structures also have simple boundary conditions it is suitable that to apply FS method for buckling analysis to simplify solution procedure.

3.2 Structural Plate Theories

The plate theories are divided in two groups; thin plate theory and thick plate theory. The plate theories are also basis for shell and stiffened plates.

Thin shell theories neglect transverse shear and rotary inertia effects and consequently may yield incorrect results, especially for higher values of the ratio of the thickness-to-minimum span and also for higher modes. In addition, many structures may not be considered as a ‘thin plate’, in this regard transverse shear strains in plates can not be ignored. Therefore, the plate theory is more suitable in general, and the elements developed based on the Mindlin-Reissner plate theory are more practical and useful for real life problems. For example, in plate analysis, the buckling loads are overestimated for all buckling modes in shear-weak situations and for the higher buckling modes in shear-stiff cases. In such circumstances, the effects of shear deformation and rotatory inertia should be taken into account.

Mindlin-Reissner shell theory allows for transverse shear deformation effects. The main assumptions are that:

- displacements are small compared to the shell thicknes,
- stress normal to the mid-surface is negligible,
- normals to the mid-surface before deformation remain straight but not necessarily normal to the mid-surface after deformation.

It is well known that displacement-based Mindlin-Reissner finite strips require only $C(0)$ continuity of the displacements and independent normal rotations between adjacent elements. This provides an important advantage over FS based on classical Kirchhoff-Love thin shell theory where $C(1)$ continuity is strictly required. Thus, it is simple to formulate Mindlin-Reissner shell elements. However, several difficulties can be emerged when Mindlin-Reissner shell elements are used in thin shell situations. The success of the Mindlin-Reissner formulation presented here for both thick and thin shell analysis lays in the use of reduced integration techniques for the numerical computation of stiffness matrix. This simply implies that the shear terms contributing to the stiffness matrix are numerically integrated with a lower order Gaussian quadrature than that needed for their exact computation, whereas the rest of the stiffness matrix is exactly calculated. Care has been taken to avoid mechanism or spurious zero-energy modes [33].

3.3 Finite Strip Formulation

In this section, the Mindlin-Reissner finite strip formulation for prismatic plates and shells in right planform will be specified.

3.3.1 Strain energy

If we consider the buckling of the Mindlin-Reissner shell strip shown in Figure 3.1 translations in the ℓ, y and n directions can be represented by the displacement components u_ℓ, v_ℓ and w_ℓ. The displacement components u_ℓ and w_ℓ may be written in terms of global displacements *u* and *w* in the *x* and *z* directions as

$$u_\ell = u\,cos\,\alpha + w\,sin\,\alpha$$

$$w_\ell = -u\,sin\,\alpha + w\,cos\,\alpha \tag{3.1}$$

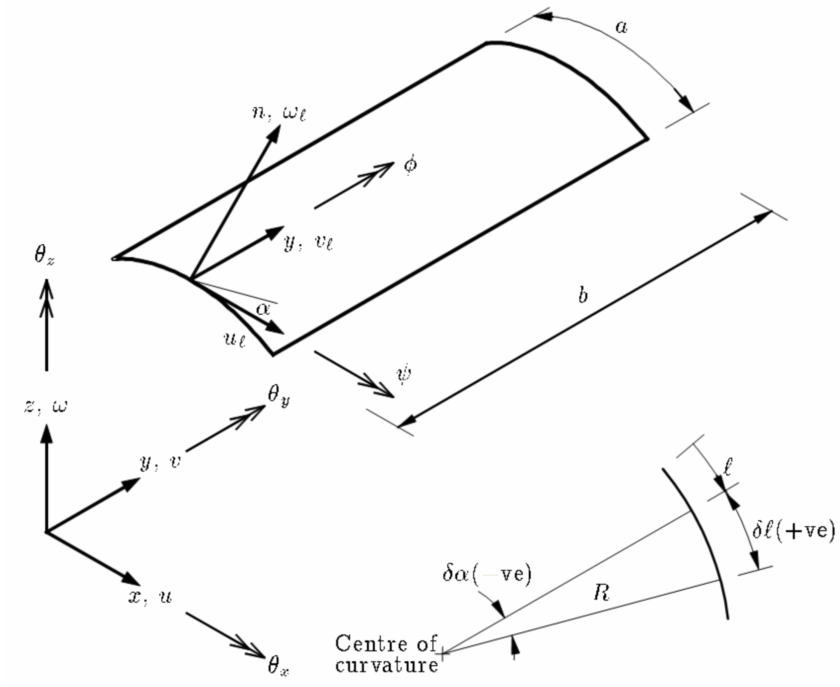

Figure 3.1 Definition of Mindlin-Reissner finite strips

The strain energy for a typical curved Mindlin-Reissner strip e of length b shown in Figure 3.1 is given in terms of the global displacements u, v, w and the rotations ϕ and ψ of the mid-surface normal in the ℓn and yn planes respectively by the expressions (3.1)

$$U^e = \frac{1}{2}\int_0^b\int_{\ell^e}\left(\boldsymbol{\varepsilon}_m^T\mathbf{D}_m\boldsymbol{\varepsilon}_m + \boldsymbol{\varepsilon}_b^T\mathbf{D}_b\boldsymbol{\varepsilon}_b + \boldsymbol{\varepsilon}_s^T\mathbf{D}_s\boldsymbol{\varepsilon}_s\right)d\ell dy \tag{3.2}$$

The strain terms $\boldsymbol{\varepsilon}_m$, $\boldsymbol{\varepsilon}_b$ and $\boldsymbol{\varepsilon}_s$ are in-plane strains, bending strains and transverse shear strains respectively. These strain terms are given in global coordinate system in Table 3.1.

Table 3.1 Strain terms and strain displacement matrices

Strain terms	*Derived equations*
$\boldsymbol{\varepsilon}_m = [\varepsilon_\ell, \varepsilon_y, \gamma_{\ell y}]^T$	$\left[\dfrac{\partial u}{\partial \ell}\cos\alpha + \dfrac{\partial w}{\partial \ell}\sin\alpha, \quad \dfrac{\partial v}{\partial y}, \quad \dfrac{\partial u}{\partial y}\cos\alpha + \dfrac{\partial w}{\partial y}\sin\alpha + \dfrac{\partial v}{\partial y}\right]^T$
$\boldsymbol{\varepsilon}_b = [\kappa_\ell, \kappa_y, \kappa_{\ell y}]^T$	$\left[-\dfrac{\partial \phi}{\partial \ell}, \quad -\dfrac{\partial \psi}{\partial y}, \quad -\left(\dfrac{\partial \phi}{\partial y} + \dfrac{\partial \psi}{\partial \ell}\right) - \left(\dfrac{\partial u}{\partial y}\cos\alpha + \dfrac{\partial w}{\partial y}\sin\alpha\right)\dfrac{d\alpha}{d\ell}\right]^T$
$\boldsymbol{\varepsilon}_s = [\gamma_{\ell n}, \gamma_{yn}]^T$	$\left[-\dfrac{\partial u}{\partial \ell}\sin\alpha + \dfrac{\partial w}{\partial \ell}\cos\alpha - \phi, \quad -\dfrac{\partial u}{\partial y}\sin\alpha + \dfrac{\partial w}{\partial y}\cos\alpha - \psi\right]^T$

Considering an isotropic material has elastic modulus E, Poisson's ratio ν and thickness t, the matrix of membrane rigidities, flextural rigidities and shear rigidities are $\boldsymbol{D_m}$, $\boldsymbol{D_b}$ and $\boldsymbol{D_s}$ respectively and they are given in Table 3.2

Table 3.2 Membrane, flextural and shear rigidities

Rigidities	*Derived equations*
$\boldsymbol{D_m}$	$\dfrac{Et}{(1-\nu^2)}\begin{bmatrix} 1 & \nu & 0 \\ \nu & 1 & 0 \\ 0 & 0 & (1-\nu)/2 \end{bmatrix}$
$\boldsymbol{D_b}$	$\dfrac{Et^3}{12(1-\nu^2)}\begin{bmatrix} 1 & \nu & 0 \\ \nu & 1 & 0 \\ 0 & 0 & (1-\nu)/2 \end{bmatrix}$
$\boldsymbol{D_s}$	$\dfrac{\kappa^2 Et}{2(1+\nu)}\begin{bmatrix} 1 & 0 \\ 0 & 1 \end{bmatrix}$

κ^2 is the shear modification factor and is usually taken as $5/6$ for an isotropic material. Details of derivations can be found in [33]

3.3.2 Potential energy of the applied inplane stresses

If inplane strain energy of a structure converted to bending energy by applied in plane loads, buckling phenomena arises.

The potential energy of the applied inplane stresses $\sigma_\ell^0, \sigma_y^0$ and $\tau_{\ell y}^0$ arises from the action of the applied stresses on the corresponding second order strains $\varepsilon_\ell^{nl}, \varepsilon_y^{nl}, \ \gamma_{\ell y}^{nl}$ are taken from Dawe and Peshkam [10]. The potential energy of the shell of volume V_g is

$$V_g = \int_v \left(\sigma_\ell^0 \varepsilon_\ell^{nl} + \sigma_y^0 \varepsilon_y^{nl} + \tau_{\ell y}^0 \gamma_{\ell y}^{nl}\right) dV \tag{3.4}$$

integrating through the thickness, this becomes

$$V_g^e = \frac{1}{2}\int_0^b\int_{\ell^e}\left(t\left\{ \sigma_\ell^0\left[\left(\frac{\partial u}{\partial \ell}\right)^2 + \left(\frac{\partial v}{\partial \ell}\right)^2 + \left(\frac{\partial w}{\partial \ell}\right)^2\right] + \sigma_y^0\left[\left(\frac{\partial u}{\partial y}\right)^2 + \left(\frac{\partial v}{\partial y}\right)^2 + \left(\frac{\partial w}{\partial y}\right)^2\right]\right\} \right.$$
$$\left. + \frac{t^3}{12}\left\{ \sigma_\ell^0\left[\left(\frac{\partial \phi}{\partial \ell}\right)^2 + \left(\frac{\partial \psi}{\partial \ell}\right)^2\right] + \sigma_y^0\left[\left(\frac{\partial \phi}{\partial y}\right)^2 + \left(\frac{\partial \psi}{\partial y}\right)^2\right]\right\}\right) d\ell dy \tag{3.5}$$

3.3.3 Finite strip idealization

Using $n-$noded, $C(0)$ strips, the global displacements and rotations of strips may be interpolated within each strip in terms of truncated Fourier series along direction y, in which both the material and geometrical properties of the plate are taken to be constant, i.e.

$$u(\ell, y) = \sum_{p=p_1}^{p_2} u^p(\ell) S_p; \qquad v(\ell, y) = \sum_{p=p_1}^{p_2} v^p(\ell) C_p$$

$$w(\ell, y) = \sum_{p=p_1}^{p_2} w^p(\ell) S_p; \qquad \phi(\ell, y) = \sum_{p=p_1}^{p_2} \phi^p(\ell) S_p$$

$$\psi(\ell, y) = \sum_{p=p_1}^{p_2} \psi^p(\ell) C_p \tag{3.6}$$

where $C_p = \cos(p\pi y/b)$ and $S_p = \sin(p\pi y/b)$, u^p, v^p, w^p, ϕ^p and ψ^p are displacement and rotation amplitudes for the p^{th} harmonic term.

The next step is to discretise the displacement and rotation amplitudes (which are functions of the $\ell-$coordinate only) using an $n-$noded finite element representation so that within a strip e the amplitudes can be written as

$$u^p(\ell) = \sum_{i=1}^{n} N_i u_i^p; \qquad v^p(\ell) = \sum_{i=1}^{n} N_i v_i^p; \qquad w^p(\ell) = \sum_{i=1}^{n} N_i w_i^p$$

$$\phi^p(\ell) = \sum_{i=1}^{n} N_i \phi_i^p; \qquad \psi^p(\ell) = \sum_{i=1}^{n} N_i \psi_i^p$$

$$\mathbf{u} = \sum_{p=p_1}^{p_2} \sum_{i=1}^{n} \mathbf{N}_i^p \mathbf{d}_i^p \tag{3.7}$$

where

$$\mathbf{u} = [u, v, w, \phi, \psi]^T \tag{3.8}$$

$$\mathbf{d}_i^p = [u_i^p, v_i^p, w_i^p, \phi_i^p, \psi_i^p]^T$$

and

$$\mathbf{N}_i^p = \begin{bmatrix} N_i S_p & 0 & 0 & 0 & 0 \\ 0 & N_i C_p & 0 & 0 & 0 \\ 0 & 0 & N_i S_p & 0 & 0 \\ 0 & 0 & 0 & N_i S_p & 0 \\ 0 & 0 & 0 & 0 & N_i C_p \end{bmatrix} \tag{3.9}$$

$N_i(\xi)$ is the shape function associated with node i. These elements are essentially isoparametric so that

$$x = \sum_{i=1}^{n} N_i x_i; \qquad y = \sum_{i=1}^{n} N_i y_i; \qquad t = \sum_{i=1}^{n} N_i t_i \tag{3.10}$$

where x_i and y_i are typical coordinates of node i and t_i is the thickness at node i. The shape functions N_i used in this study is given in Table 3.3

Table 3.3 Shape functions

Shape functions	
Linear	$N_1 = \frac{1}{2}(1-\xi)$ $N_2 = \frac{1}{2}(1+\xi)$
Quadratic	$N_1 = \frac{\xi}{2}(\xi-1)$ $N_2 = 1-\xi^2$ $N_3 = \frac{\xi}{2}(\xi+1)$
Cubic	$N_1 = \frac{9}{16}\left(\frac{1}{9}-\xi^2\right)(\xi-1)$ $N_2 = \frac{27}{16}(1-\xi^2)\left(\frac{1}{3}-\xi\right)$ $N_3 = \frac{27}{16}(1-\xi^2)\left(\frac{1}{3}+\xi\right)$ $N_4 = -\frac{9}{16}\left(\frac{1}{9}-\xi^2\right)(\xi+1)$

Note also that the Jacobian is defined as;

$$J = \frac{d\ell}{d\xi} = \left[\left(\frac{dx}{d\xi}\right)^2 + \left(\frac{dy}{d\xi}\right)^2\right]^{1/2} ;\; d\ell = Jd\xi \tag{3.11}$$

where

$$\frac{dx}{d\xi} = \sum_{i=1}^{n} \frac{dN_i}{d\xi} x_i ; \qquad \frac{dy}{d\xi} = \sum_{i=1}^{n} \frac{dN_i}{d\xi} y_i \tag{3.12}$$

Also, it is possible to write that

$$\sin\alpha = \frac{dy}{d\xi}\frac{1}{J}; \qquad \cos\alpha = \frac{dx}{d\xi}\frac{1}{J} \tag{3.13}$$

and

$$\frac{dN_i}{d\ell} = \frac{dN_i}{d\xi}\frac{1}{J} \tag{3.14}$$

3.3.4 Stiffness matrix

Stiffness matrix $\mathbf{K}^e$ of strip elements can be evaluated considering the strain energy of the Mindlin-Reissner strip. The strain energy of a strip element can be expressed as

$$U^e = \frac{1}{2}\sum_{p=p_1}^{p_2}\sum_{q=q_1}^{q_2}\sum_{i=1}^{n}\sum_{j=1}^{n}\mathbf{d}_i^p[\mathbf{K}_{ij}^e]^{pq}\mathbf{d}_j^q \tag{3.15}$$

where the typical submatrix of the stiffness $\mathbf{K}^e$ of strip e linking nodes i and j and harmonics p and q has the form

$$[\mathbf{K}_{ij}^e]^{pq} = \int_0^b\int_{-1}^{+1}\left([\mathbf{B}_{mj}^p]^T\mathbf{D}_m\mathbf{B}_{mj}^q + [\mathbf{B}_{bj}^p]^T\mathbf{D}_b\mathbf{B}_{bj}^q + [\mathbf{B}_{sj}^p]^T\mathbf{D}_s\mathbf{B}_{sj}^q\right)J\,d\xi\,dy \tag{3.16}$$

The membrane strains $\boldsymbol{\varepsilon}_m$ may then be expressed as

$$\boldsymbol{\varepsilon}_m = \sum_{p=p_1}^{p_2}\sum_{i=1}^{n}\mathbf{B}_{mi}^p\mathbf{d}_i^p$$

The flexural strains or curvatures $\boldsymbol{\varepsilon}_b$ can be written as

$$\boldsymbol{\varepsilon}_b = \sum_{p=p_1}^{p_2}\sum_{i=1}^{n}\mathbf{B}_{bi}^p\mathbf{d}_i^p$$

The transverse shear strains $\boldsymbol{\varepsilon}_s$ are approximated as

$$\boldsymbol{\varepsilon}_s = \sum_{p=p_1}^{p_2}\sum_{i=1}^{n}\mathbf{B}_{si}^p\mathbf{d}_i^p$$

Where $\mathbf{B}_{mi}$, $\mathbf{B}_{bi}$ and $\mathbf{B}_{si}$ are the membrane, bending and shear strain matrices respectively and (strain displacement) matrices and given in Table 3.4

Table 3.4 Strain displacement terms

Strain disp. terms	*Derived equations*
$\mathbf{B}_{mi}^{p}$	$\begin{bmatrix} (dN_i/d\ell)S_p\cos\alpha & 0 & (dN_i/d\ell)S_p\sin\alpha & 0 & 0 \\ 0 & -\bar{p}N_iS_p & 0 & 0 & 0 \\ \bar{p}N_iC_p\cos\alpha & (dN_i/d\ell)C_p & \bar{p}N_iC_p\sin\alpha & 0 & 0 \end{bmatrix}$
$\mathbf{B}_{bi}^{p}$	$\begin{bmatrix} 0 & 0 & 0 & -(dN_i/d\ell)S_p & 0 \\ 0 & 0 & 0 & 0 & \bar{p}N_iS_p \\ (\bar{p}N_iC_p\cos\alpha)/R & 0 & (\bar{p}N_iC_p\sin\alpha)/R & -\bar{p}N_iC_p & (-dN_i/d\ell)C_p \end{bmatrix}$
$\mathbf{B}_{si}^{p}$	$\begin{bmatrix} -(dN_i/d\ell)S_p\sin\alpha & 0 & (dN_i/d\ell)S_p\cos\alpha & -N_iS_p & 0 \\ -\bar{p}N_iC_p\sin\alpha & 0 & \bar{p}N_iC_p\cos\alpha & 0 & -N_iC_p \end{bmatrix}$

Where $\bar{p} = p\pi/b$.

3.3.5 Geometric stiffness matrix

Geometric stiffness matrix $\mathbf{K}_{\sigma}^{e}$ can now be formed which is associated with the potential energy V^{e} of the applied inplane stresses σ_{ℓ}^{0} and σ_{y}^{0}. The potential energy of a strip can be expressed as

$$V^{e} = \frac{1}{2}\sum_{p=p_1}^{p_2}\sum_{q=q_1}^{q_2}\sum_{i=1}^{n}\sum_{j=1}^{n}\mathbf{d}_i^{p}[\mathbf{K}_{\sigma ij}^{e}]^{pq}\mathbf{d}_j^{q} \tag{3.17}$$

where a typical sub-matrix $\mathbf{K}_{\sigma}^{e}$ of strip e linking nodes i and j, harmonics p and q has the form

$$[\mathbf{K}_{\sigma ij}^{e}]^{pq} = \int_0^b\int_{-1}^{+1}\Big(t[\mathbf{S}_{ui}^{p}]^T\mathbf{H}\mathbf{S}_{uj}^{q} + t[\mathbf{S}_{vi}^{p}]^T\mathbf{H}\mathbf{S}_{vj}^{q} + t[\mathbf{S}_{wi}^{p}]^T\mathbf{H}\mathbf{S}_{wj}^{q}\Big)$$

$$+\left(\frac{t^3}{12}[\mathbf{Q}_i^{p}]^T\mathbf{H}\mathbf{Q}_j^{q} + \frac{t^3}{12}[\mathbf{R}_i^{p}]^T\mathbf{H}\mathbf{R}_j^{q}\right)Jd\xi\, dy \tag{3.18}$$

$\mathbf{S}_u$, $\mathbf{S}_v$, $\mathbf{S}_w$, $\mathbf{Q}_i$, $\mathbf{R}_i$ and $\mathbf{H}$ the matrices of the geometric stiffness matrix are defined in Table 3.5

Table 3.5 Matrices of geometric stiffness matrix

Terms	Matrices
$\mathbf{S}_{ui}^{p}$	$\begin{bmatrix} (dN_i/d\ell)S_p & 0 & 0 & 0 & 0 \\ N_i(p\pi/b)C_p & 0 & 0 & 0 & 0 \end{bmatrix}$
$\mathbf{S}_{vi}^{p}$	$\begin{bmatrix} 0, & (dN_i/d\ell)C_p & 0 & 0 & 0 \\ 0 & -N_i(p\pi/b)S_p & 0 & 0 & 0 \end{bmatrix}$
$\mathbf{S}_{wi}^{p}$	$\begin{bmatrix} 0 & 0 & (dN_i/d\ell)S_p & 0 & 0 \\ 0 & 0 & N_i(p\pi/b)C_p & 0 & 0 \end{bmatrix}$
$\mathbf{Q}_{i}^{p}$	$\begin{bmatrix} 0 & 0 & 0 & (dN_i/d\ell)S_p & 0 \\ 0 & 0 & 0 & 0 & -N_i(p\pi/b)S_p \end{bmatrix}$
$\mathbf{R}_{i}^{p}$	$\begin{bmatrix} 0 & 0 & 0 & 0 & (dN_i/d\ell)C_p \\ 0 & 0 & 0 & N_i(p\pi/b)C_p & 0 \end{bmatrix}$
H	$\begin{bmatrix} \sigma_\ell^0 & 0 \\ 0 & \sigma_y^0 \end{bmatrix}$

Matrix $\mathbf{K}_\sigma^e$ is depend on an element's geometry, displacement field, and state of stress. Thus, $\mathbf{K}_\sigma^e$ is independent of elastic properties of material. However, by introducing the stress-strain relation $\mathbf{K}_\sigma^e$ can alternatively be written in terms of elastic properties and strains or deformations.

$$[\mathbf{K}^{pp} + \lambda^p \mathbf{K}_\sigma^{pp}]\overline{\mathbf{d}}^p = 0 \tag{3.19}$$

where λ^p is the load factor (eigenvalues) by which the inplane stress σ_ℓ^0 and σ_y^0 are multiplied to produce instability and $\overline{\mathbf{d}}^p$ (eigenvectors) is the associated buckling mode. In the present studies the eigenvalues are evaluated using the subspace iteration algorithm.

We seek the lowest value of λ^p which provides equation 3.19. The lowest value of λ^p generates critical buckling load of structure.

$$\boldsymbol{P}_{cr} = \lambda^p \boldsymbol{P}_0 \tag{3.20}$$

The details of derivation of FS equations derivation can be seen from reference [33].

3.4 Examples

3.4.1 Verification by literature data (NASA sets)

To verify accuracy of present formulation for the buckling analysis of stiffened plates, several examples for which solutions are available have been considered. In all cases, the boundary conditions at the ends of the structure, i.e. at $y = 0$ and $y = b$, correspond to 'hard' simple diaphragm supports-in other words $v = \omega = \phi = 0$. Note that in a typical finite strip solution a set of m modes and associated buckling factors is obtained for each harmonic term half wave n. In all cases, reduced integration is used to evaluate the stiffness matrix and the shear correction factor is assumed $\kappa^2 = 0.8333$.

We now consider the buckling of stiffened panels with diaphragm ends subject to various combinations of longitudinal compression and shear.

The isotrophic panels subjected to longitudinal compression analyzed by Stroud et. al [32] and Peshkam and Dawe [18] is now considered. Stroud et al. [34] used a program called EAL (Engineering Analysis Language) and Peshkam and Dawe [18] used a Mindlin-Reissner superstrip procedure involving a very fine mesh of cubic strips to study these problems. We use these finite element and superstrip results to check the present formulation. The geometry of the square planform with side length $a = 762\ mm$ and six repeating elements is shown in Figure 3.2.

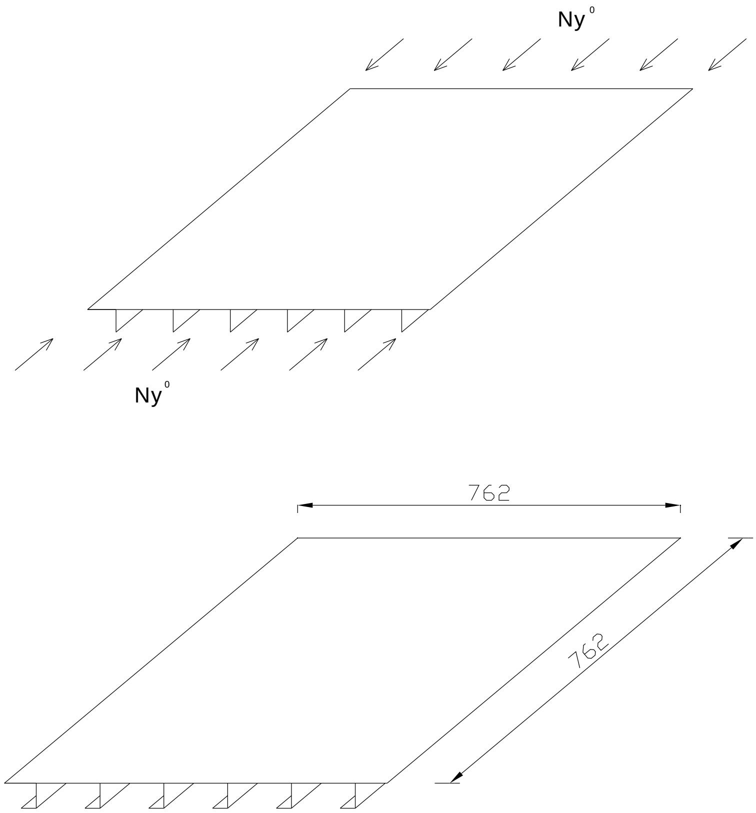

Figure 3.2 Isotropic stiffened panels from the NASA set [33]

The panels subjected to prebuckling load distribution for each plate flat in NASA examples when $N_y^0 = 175.13\, kN/m$ is shown in Table 3.6. The following (aluminum) material properties are assumed: elastic modulus $E = 72.44 N/m^2$ and Poisson's ratio $v = 0.32$. The subdivisions chosen for blade stiffened panel are indicated in Figure 3.4. Table 3.7 shows the results for the various subdivisions and strip types for Panel-I. A very good agreement is found between the finite element (EAL) and the superstrip solutions.

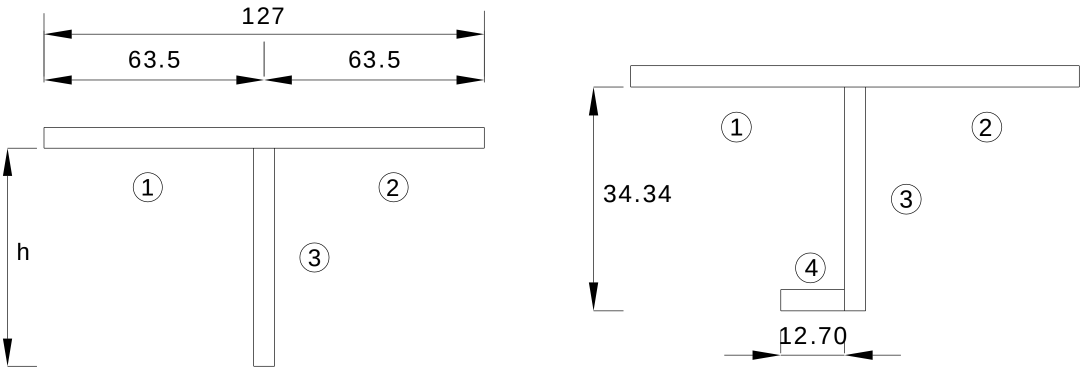

(a) (b)

Figure 3.3 Details of repeating elements in isotropic stiffened panels (a) Panel I and II $-h = 34.34$ for Panel I and $h = 50.04$ for Panel II and (b) Panel III.

Table 3.6 Prebuckling load distribution for each plate flat in NASA panels when $N_y = 175.13 kN / m$

Panel	Internal load distribution N_y^0 (kN /m)			
	Flat 1	Flat 2	Flat 3	Flat 4
I	145.57	101.90	147.57	
II	133.31	154.64	133.31	
III	139.46	139.46	96.29	96.29

Table 3.7 Buckling factors for blade-stiffened panel I

Number of point	Buckling factors		
	Linear strips	Quad. strips	Cubic strips
79	0.94331	0.97102	0.97083
109	0.95550	0.97098	0.97096
181	0.96590	0.97096	0.97096
217	0.96707	0.97095	0.97094
EAL sol.	0.9759	0.9759	0.9759
Superstrip	0.9709	0.9709	0.9709

In Panel-II a mesh of 73 cubic strips is used and the resulting buckling factor of 0.29499 compares well with the values of 0.2965 and 0.2944 obtained using the finite element and superstrip solutions respectively. The lowest buckling load is obtained with $p_1 = p_2 = 7$. This agrees with the shape of the buckling modes obtained using the finite element and superstrip solutions.

In Panel-III a mesh of 84 cubic strips is used and results in a buckling factor of 1.34887 compares again with the values of 1.356 and 1.3454 obtained using the FE and superstrip solutions respectively. The panel buckles with seven longitudinal half sine waves. This is in agreement with FE and superstrip lowest buckling mode.

3.4.2 Verification in SAP2000

For the verification of computer code used in this thesis three optimized plates also analyzed with SAP2000 finite element structural analysis and design computer program. The relations of two program’s results are expresses below.

a) *Straight stiffened plate with four stiffeners size optimization:* The optimum dimensions and obtained buckling load of this plate can be seen from Table 5.3. PLATEV_1 gave 107.542 kN and SAP2000 resulted 107.941 kN. The difference between two critical buckling loads is 0.37 %.

b) *Straight stiffened plate with eight stiffeners size optimization:* The optimum thickness and obtained critical buckling load of plate can be seen from Table 5.3. PLATEV_1 found 219.833 kN of critical buckling load and SAP2000 analysis resulted 219.504 kN. The difference between two critical buckling loads is 0.15 %.

c) *Straight stiffened plate with five stiffeners and pads under stiffeners size optimization:* The optimum thicknesses and critical buckling load of plate can be seen from Table 5.9. PLATEV_1 found 175.648 kN of critical buckling load and SAP2000 analysis resulted 175.971 kN. The difference between two critical buckling loads is 0.18 %.

CHAPTER 4

OPTIMIZATION PROCEDURE

4.1 Introduction

The general principle by Maupertuis proclaims *"If there occur some changes in nature, the amount of action necessary for this change must be as small as possible"*. In this view, the main purpose of optimization is obtaining the best outcome of a given problem while assuring some restrictions. In this regard to consume limited resources that maximizes the objective. The objective varies depending on problem types and desired functions of problem.

The importance of minimum weight design of structures was first recognized by the aerospace industry where aircraft structural designs are often controlled more by weight than by cost considerations. In other industries dealing with civil, mechanical and automotive engineering systems, cost may be the primary consideration although the weight of the system does affect its cost and performance. A growing realization of the scarcity of raw materials and a rapid depletion of our conventional energy sources is being translated into a demand for lightweight, efficient and low cost structures [35].

Critical buckling load capacity of stiffened plates can be increased to very high values by using properly dimensioned stiffened plate elements. In this point it is necessary to mention about the essentiality of structural optimization procedure. This procedure involves iterative solutions and require reanalyzing of problem several times before obtaining the optimum solution. In this study objective function is maximization of the critical buckling load capacity of stiffened plates while satisfying constant volume constraint.

4.2 Structural Optimization Algorithm

The basic algorithm for structural shape optimization is given in Figure 4.1

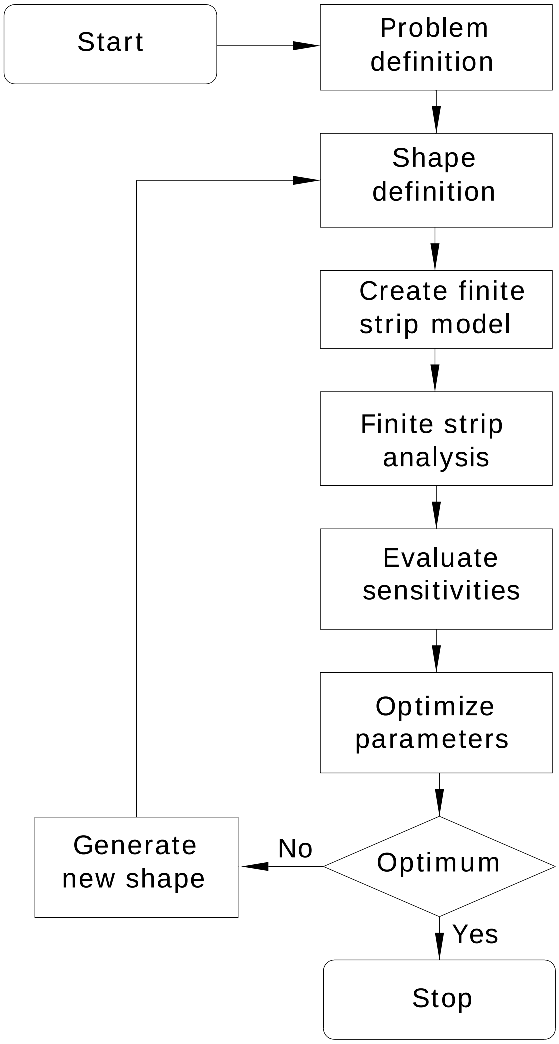

Figure 4.1 Structural optimization flowchart

Özakça et al [24] summarized the basic algorithm of structural optimization, using FS as an analysis method and sequential quadratic programming as an optimization method, in following steps.

1- *Problem definition*: Consider the case of the structural optimization of a panel structure in which we wish to maximize the critical buckling load subject to the constraints that the total volume of the panel should remain constant and first ten buckling loads should be greater than critical buckling load. Other types of constraints such as bounds on the design variables must also be introduced.

2- *Shape definition*: The shape of the panel cross section is defined in some convenient form that allows us to examine the sensitivities of the design to small changes in shape. Here, we describe the geometry of the plate cross section using parametric cubic spline segments with the coordinates specified at certain key points.

3- *Create finite strip model*: The next step is to generate a mesh of suitable FSs. Here, an unstructured mesh generator with mesh density specified at some key points and then interpolated through the segments appropriately is used. In order to ensure the accuracy of the FS model, it is necessary make sure derefinement does not occur during the analysis in each optimization iteration. This means that, the strip size distribution (mesh density) remains unchanged during redesign. As the structural shape changes during the optimization process, the remeshing is based on predetermined mesh density at every iteration. As with normal finite strip analysis also the boundary conditions and material properties must be defined.

4- *Finite strip analysis*: Next we carry out a FS analysis and in the present work the structure is modeled using linear, variable thickness, Mindlin-Reissner, $C(0)$ FSs.

5- *Sensitivity analysis*: The sensitivities of the buckling loads and volume of the current design to small changes in the design variables are then evaluated. These design sensitivities are generally nonlinear implicit functions of the design variables and are therefore difficult and expensive to calculate. The numerical accuracy of sensitivity analysis affects the search directions that are used in optimization algorithms.

6- *Optimize parameters*: Using the objective and constraint functions and their derivatives, the sequential quadratic programming (SQP) optimization algorithm is employed to optimize the parameters or design variables. The new set of values will result in a modified design. Furthermore, the constraints must be satisfied if the new design is to be deemed acceptable. If a convergence criterion for optimization algorithm is satisfied, then the optimum solution has been found and the solution process is terminated.

7- *Update optimization model*: After the optimization, it is necessary to update the geometric model, i.e. the coordinates and/or thicknesses of the primary design variables in structural optimization. This is the only part of the original input data which has to be updated with for each optimization iteration. If no convergence has been achieved, the new geometry is sent to the mesh generator which automatically generates a new analysis model and the whole process is repeated from step 2.

4.2.1 Mathematical definition of optimization problem

Problems of structural optimization are characterized by various objectives and constraints, which are generally nonlinear functions of the design variables. These functions can be discontinues and non convex. Each objective and constraint choice defines a different optimization problem, and solution can be found using several mathematical programming methods.

In general the constraint functions are grouped in to three classes: equality constraints h_j, inequality constraints g_i, and the geometric (regional) constraints defined by the upper and the lower bounds of the design variables.

However, all optimization problems can be expressed in standard mathematical terms as:

minimize (or maximize)

$$F(\mathbf{s}) \tag{4.1}$$

subject to:

$$\begin{aligned} & g_i(s) \le 0 \qquad i = 1,\dots m \\ & h_j(s) = 0 \qquad j = 1,\dots l \\ & s_k^l \le s_k \le s_k^u \quad k = 1,\dots n_{dv} \end{aligned} \tag{4.2}$$

The notion of improving or optimizing a structure implicitly presupposes some freedom to change the structure. The potential for change is typically expressed in terms of ranges of permissible changes of a group of parameters. Such parameters are usually called design variables in structural optimization terminology. Design variables can be cross-sectional dimensions or member sizes; they can be parameters controlling the geometry of the structure and its material properties, etc. In which, **s** is the design variables vector.

The notion of optimization also implies that there are some merit function *F*(**s**) or functions ***F*(s)**=[F_1**(s)**, F_2**(s),** F_3**(s)**,…..] that can be improved and can be used as a measure of effectiveness of the design. The common terminology for such functions is objective functions. For structural optimization problems, weight, displacements, stresses, vibration frequencies, buckling loads, and cost or any combination of these can be used as objective functions.

In optimization process of structures, there are limits about design variables. Sometimes design constraints may be dimensions of structural elements, weight of structure, vibration frequency, and displacement of a point, $g_i(s)$ and $h_j(s)$ are the constraint functions. Finally, s_k^l and s_k^u represent the lower and the upper bounds of the design variables, *m* is the number of design variables used.

In this study objective function is maximization of critical buckling load of stiffened plates. Design variables are stiffened plate cross sectional elements' dimensions that are defined clearly in Chapter 5. When maximizing critical buckling load of stiffened plates first constraint is an equality constant material volume constraint. Optimized plates widths and lengths are constant. Also there are upper and lower limits inequality constraints of design variables.

Buckling load constraint $g(s)$ can be expressed as

$$g(s) = 1 - \frac{(\sigma_{cr})_i}{(\sigma_{cr})_{max}} \tag{4.3}$$

where $(\sigma_{cr})_{max}$ defines the upper limit on buckling load and $(\sigma_{cr})_i$ describing the buckling load of the current design. Similarly

$$g(s) = \frac{V_i}{V_{max}} - 1 \tag{4.4}$$

defines the volume constraint. V_i and V_{max} are the current value and upper limit of the volume respectively.

4.2.2 Shape definition

4.2.2.1 Structural shape definition

The designation of geometric model and control the parameters of optimization procedure for an appropriate flow algorithm is complex and requires attention. The cross section of typical stiffened plate structure is shown in Figure 4.2.

To form cross section geometry of stiffened plates to introduce computer code the segments must be generated one by one. Generating a straight segment can be done by entering its two key points' geometrical coordinates as input data.

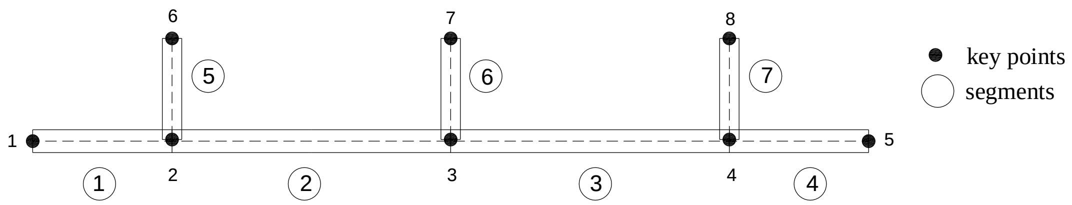

Figure 4.2 Geometric representation of stiffened plate

Defined number of key points to form the cross sectional shapes of the stiffened plates are important for computational algorithm. More key points mean more design variables for computer code. So increasing the defined number of key points cause increasing computational time.

For the applicability to real life, increasing the efficiency of computational effort and symmetrical behavior of structural elements it is a necessary situation to link the design variables at two or more key points. By linking of design variables, the length of a considered segment can be assigned as a design variable and symmetry of shape in an axis can be easily achieved. In this regard, the number of design variables for optimization is considerably reduced.

4.2.2.2 Structural thickness definition

The thicknesses of the stiffened plate elements are specified at some or all of the key points for the desired initial element shape of the structure and then interpolated by program.

4.2.3 Mesh generation for finite strip analysis

After defining the geometry, the next step is to generate a proper finite element mesh for the cross section of stiffened plate. This meshing procedure can be carried out with an automatic mesh generator for desired mesh density. Automatic mesh generator has the capability of meshing the arbitrary complex geometry given no input other than the geometric representation of the domain to be meshed and an associated mesh density distribution. Mesh generation should be robust, versatile, and efficient to obtain more accurate results. Here, we use a mesh generator which allows refinement of finite element meshes. It also allows for a significant variation in mesh spacing throughout the region of interest. The mesh generator can generate meshes of two three and four noded elements and strips.

It is very significant factor for obtaining more accurate results to mesh the cross section properly. In this regard mesh operation should be carried out considering critical points in cross section. Also meshes in segments should be compatible with each other. Figure 4.3 shows a mesh example of stiffened plates.

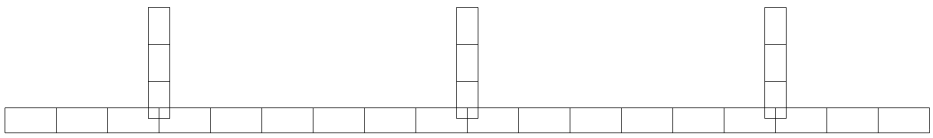

Figure 4.3 Mesh representation of plates

The mesh density is a piecewise linear function of the values of mesh size δ at some points along the mid-surface of the structure.

4.2.4 Structural finite strip analysis

It is the important factor for optimization methods to reach optimum solution in minimum computational time. So efficiency of the optimization methods are based on the computational time required in the process. Most of the numerical optimization methods have iterative procedures. So the number of structural analyses required to complete the optimum solution is large. In this regard, to reduce the cost of problem the efficient and inexpensive structural analysis method should be used.

In such case, FS method is the best approach to the problems. As discussed in Chapter 3 the FS method has proven to be an inexpensive and useful tool in analysis of structures having regular prismatic type geometries and simple supported on diaphragms at two opposite edges with the remaining edges arbitrarily restrained. Theory and implementation of finite strip method for buckling analyses are given in Chapter 3 and details can be seen from reference [33].

4.2.5 Sensitivity analysis

Sensitivity analysis is a crucial part of optimization procedure. After FS analysis completed the sensitivities of the current design should be evaluated to small changes in the design variables. We calculate the sensitivities of items such as buckling load based on finite differences.

Sensitivity analysis is based on the systematic calculation of the derivatives of the response for the FS model with respect to parameters forming the model geometry *i.e.* the design variables which may be length, thickness or shape. The first partial derivatives of the structural response quantities with respect to the shape (or other) variables provide the essential information required to couple mathematical programming methods and structural analysis procedures. The sensitivities of responses provide the mathematical programming algorithm with search directions for optimum solutions [33].

In the present study, PLATEV_1 code uses the finite difference to calculate sensitivities. For the numerically approximation of derivatives the finite difference method uses a difference formula. The finite difference scheme is accurate and computationally efficient

4.2.6 Derivative of buckling load

The governing equation in the FS solution for buckling case may be defined as [33]

$$[\mathbf{K}^{pp} + \lambda^p \mathbf{K}_\sigma^{pp}]\overline{\mathbf{d}}^p = 0 \tag{4.5}$$

$\mathbf{K}^{pp}$ is the stiffness matrix for the pth harmonic, $\mathbf{K}_\sigma^{pp}$ is the load matrix, λ^p is the buckling factor and $\overline{\mathrm{d}}_p$ is the buckling mode shape which is normalized so that

$$\overline{\boldsymbol{d}}_p^T \mathbf{K}_\sigma^{pp} \overline{\boldsymbol{d}}_p = 1 \tag{4.6}$$

when the eigenvalues are distinct, the expression for the buckling derivative with respect to design variable s_i can be derived from (4.5) and (4.6) so that

$$\frac{\partial \lambda^p}{\partial s_i} = \overline{\mathbf{d}}_p^T \left(\frac{\partial \boldsymbol{K}^{pp}}{\partial s_i} - \lambda^p \frac{\partial \mathbf{K}_\sigma^{pp}}{\partial s_i}\right)\overline{\boldsymbol{d}}_p \tag{4.7}$$

The derivatives are computed by re-calculating $\mathbf{K}^{pp}$ and $\mathbf{K}_\sigma^{pp}$ for a small perturbation Δs_i of the design variable (coordinates or thicknesses). The derivatives of the stiffness matrices with respect to the design variable s_i may then be written as

$$\frac{\partial \mathbf{K}^{pp}}{\partial s_i} \approx \frac{\mathbf{K}^{pp}(s_i + \Delta s_i) - \mathbf{K}^{pp}(s_i)}{\Delta s_i} \tag{4.8}$$

$$\frac{\partial \mathbf{K}_\sigma^{pp}}{\partial s_i} \approx \frac{\mathbf{K}_\sigma^{pp}(s_i + \Delta s_i) - \mathbf{K}_\sigma^{pp}(s_i)}{\Delta s_i} \tag{4.9}$$

4.2.7 Derivative of volume

A forward finite difference approximation is used to evaluate the volume derivative [33].

$$\frac{\partial V}{\partial s_i} \approx \frac{V(s_i + \Delta s_i) - V(s_i)}{\Delta s_i} \tag{4.10}$$

Where the volume V of the whole structure (or cross-sectional area of the structure may also be used) can be calculated by adding the volumes of numerically integrated finite strips.

4.3 Mathematical Programming

SQP is used as a mathematical programming to generate shapes with improved objective function values using the information derived from the analysis and design sensitivities. No effort has been made to study the mathematical programming methods used for structural optimization procedures and the SQP algorithm is used here essentially as a ‘black box’.

CHAPTER 5

OPTIMIZATION OF PLATES

5.1 Introduction

FS analysis and SQP optimization is to be used to find an optimal stiffened plate design using prismatic, rectangular substiffeners, pads and linearly varying plate skin thickness running parallel to the primary straight and T shaped stiffeners. The starting point for these designs is the baseline panel from which the initial values of parameters is developed. A complete description of the baseline design is outlined later in this document.

The main interest of this study is maximizing the buckling load carrying capacity of stiffened plates by optimizing the plate section dimensions under constant volume constraint.

Optimization is carried out for the following types of stiffened plates that are expressed below and plate types are shown on five stiffened plate template and given in Figure 5.1.

Straight Stiffeners:

a) Straight stiffened plate

b) Straight stiffened plate with substiffeners

c) Straight stiffened plate and pads under main stiffeners

d) Straight stiffened plate with substiffeners and pads under stiffeners

e) Straight stiffened plate and pads between stiffeners

f) Straight stiffened plate and pads under stiffeners and between stiffeners

g) Straight stiffened plate with linearly varying skin

h) Straight stiffened plate with linearly varying skin and pads under stiffeners

T Shaped Stiffeners:

a) T shaped stiffened plate

b) T shaped stiffened plate with substiffeners

c) T shaped stiffened plate and pads under main stiffeners

d) T shaped stiffened plate with substiffeners and pads under stiffeners

e) T shaped stiffened plate and pads between stiffeners

f) T shaped stiffened plate and pads under stiffeners and between stiffeners

g) T shaped stiffened plate with linearly varying skin

h) T shaped stiffened plate with linearly varying skin and pads under stiffeners

5.1.1 Optimization process

It is desired that two separate linear eigenvalue optimizations are run. The first design is carried out for obtaining thickness of initial values by providing constant cross sectional area. Then second run will apply the design constraints associated with the manufacturing process and other issues. Full details of the DVs and constraints are outlined in the preceding sections.

5.1.2 Baseline design

The baseline panel is the foundation for the stiffened plate design. The plate cross section is constant along its length. The baseline plate cross section has a total are of 1172 mm^2 of skin material available for manipulation.

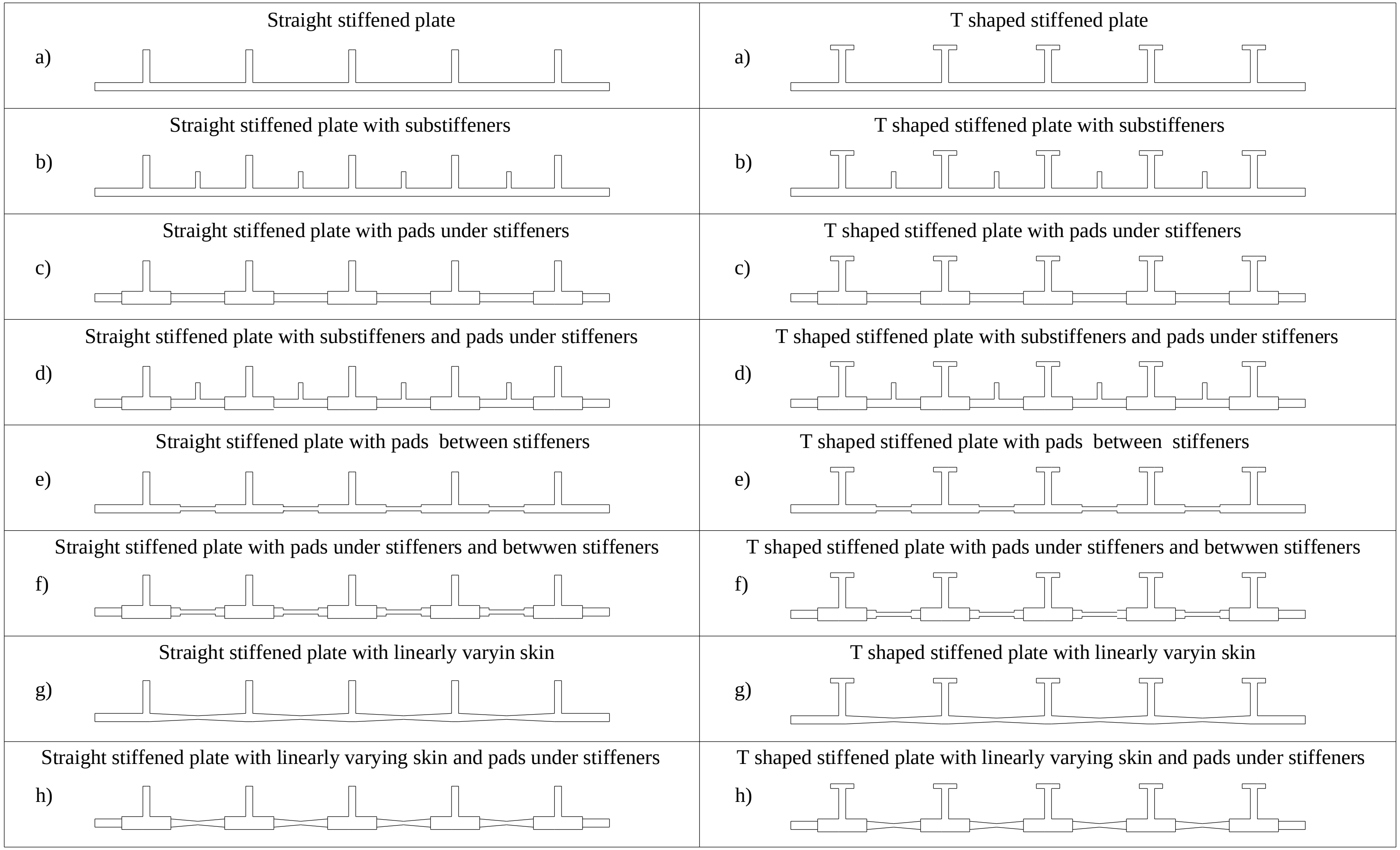

Figure 5.1 Examined plate types

5.1.3 Parameter definition

Figure 5.2 below describes the cross section and geometric (design variables) parameters associated with the prismatic blade sub-stiffened panel.

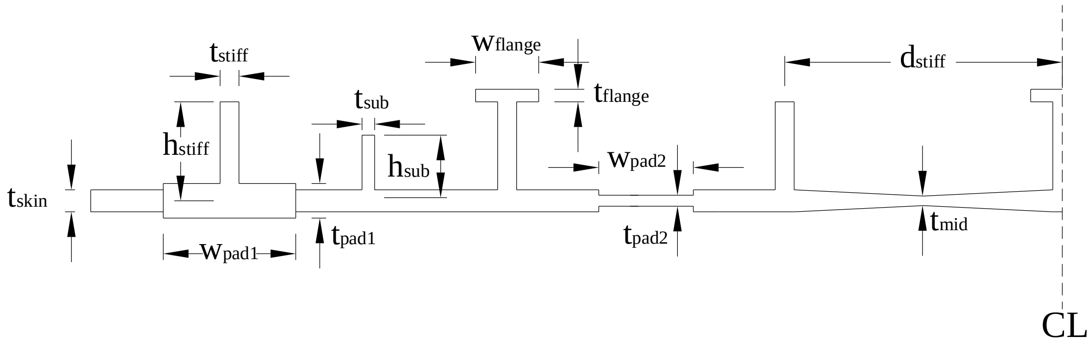

Figure 5.2 Plate variable parameters (design variables)

- t_{skin} Skin thickness
- h_{stiff} Primary stiffener height
- t_{stiff} Primary stiffener thickness
- w_{pad1} Width of pad under stiffeners
- t_{pad1} Thickness of pad under stiffeners
- h_{sub} Sub-stiffener height
- t_{sub} Sub-stiffener thickness
- w_{flange} Flange width
- t_{flange} Flange thickness
- w_{pad2} Width of pad between stiffeners
- t_{pad2} Thickness of pad between stiffeners
- t_{mid} Midspan thickness
- d_{stiff} Distance between stiffeners
- n_{stiff} Number of stiffeners

5.1.4 Optimization set up

This design has a number of sub-stiffeners running parallel to the primary stiffeners at 90 degrees to the loading plane. Only variable parameters can be changed during the optimization process.

5.1.5 Design constraints

There are a number of design constraints based on either the general design strategy or the manufacturing process as outlined below. All types of examined plates have the common fixed constraints as shown in Table 5.1. The common constraints are shown on a three dimensional aspect of five straight stiffened plate in Figure 5.3.

Table 5.1 Common constraints

Plate width	440 mm
Plate length	590 mm
Total plate volume	691480 mm³

Nevertheless, design variables have constrains (minimum and maximum limits) that are expressed in relevant sections.

5.1.6 Material properties, loading and boundary conditions

In this study eigenvalue buckling analysis is considered. This analysis only requires elastic material properties. The used material properties are.

Modulus of elasticity (E) : 73×10^9 N/m²

Poisson's ratio (ν) : 0.33

The loading direction and boundary conditions are shown in Figure 5.4

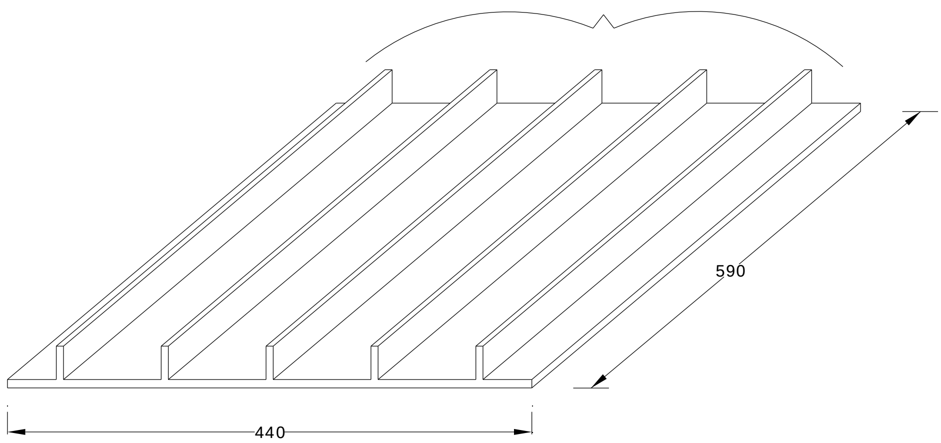

Figure 5.3 A sample three-dimensional aspect of stiffened plate (Straight stiffener with five stiffeners)

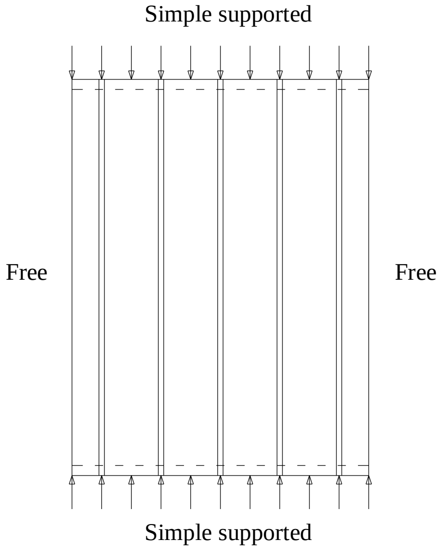

Figure 5.4 Loading and boundary conditions

The loaded sides of plate are simply supported and the other two sides are free. The plate is loaded in uniform compression in stiffeners direction.

5.2 Plate Types and Optimization Process

Straight and T shaped stiffened plates defined in section 5.1 are optimized. Optimization processes are defined, results of optimizations are presented and discussions are made in this section. All dimensions in tables are in mm and all load values in tables and figures are in N and kN unit respectively.

5.2.1 Straight stiffeners

5.2.1.1 Straight stiffened plate

Figure 5.5 shows straight stiffened plate with five stiffeners

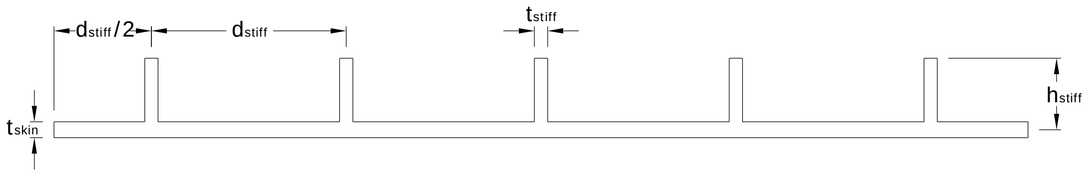

Figure 5.5 Straight stiffened plate

a) Optimization process:

i) Size optimization: Optimization is performed using thickness of plate skin (t_{skin}) and thickness of stiffeners (t_{stiff}). During this stage height of stiffeners (h_{stiff}) have constant value of 28.0 mm (See Figure 5.5).

ii) Shape optimization: Height of stiffeners (h_{stiff}) included as design variable in this stage (See Figure 5.5).

Design constraints of two stages are specified in Table 5.2. Optimization process is repeated from two to eight stiffeners.

Table 5.2 Design constraints of straight stiffened plate

		Min (mm)	Max (mm)
Thickness of plate	t_{skin}	1.4	3.0
Thickness of stiffener	t_{stiff}	1.3	4.0
Height of stiffener	h_{stiff}	8.0	40.0

b) Discussion of results

Two types of optimization are performed. These are size optimization with two design variables (t_{skin} - t_{stiff}) and shape optimization with three design variables (t_{skin} - t_{stiff} - h_{stiff}). Effect of number of stiffeners is also observed. Number of stiffeners from two to eight is optimized. Optimizations are carried out for maximization of critical buckling load subject to constant volume constraint.

i) Size optimization: Thicknesses of plate and stiffeners are kept equal at the initial design. The height of stiffeners is constant and equal to 28.0 mm. The optimum values of design variables and critical buckling load are given in Table 5.3. The highest improvement is obtained for four stiffeners case and approximately equal to 10.25 %. The stiffened panel analyzed using cubic strips. In order to obtain more accurate results the large number of degrees of freedom is taken in all analysis. The highest critical buckling load is obtained in eight stiffeners case and equal to 219833 N. The improvement of critical buckling load for eight stiffeners is 664 % compared to two stiffeners case. Moreover, it is important to note that in optimum results skin thickness is thicker than stiffener thickness except eight stiffeners case and by the increasing of number of stiffeners skin thickness is going to be thinner and stiffener thickness is going to be thicker.

Table 5.3 Size optimization of straight stiffened plate

n_{stiff}	Optimum DVs values		Buckling loads		Imp
	t_{skin}	t_{stiff}	P_i	P_{max}	(%)
2	2.49	1.30	27392.7	28749.313	4.952
3	2.41	1.30	59731.7	64479.292	7.948
4	2.32	1.34	97565.0	107542.933	10.227
5	2.19	1.47	136548.5	148318.650	8.620
6	2.08	1.52	173160.7	183581.163	6.018
7	1.96	1.57	202204.3	206859.051	2.302
8	1.75	1.79	219819.9	219833.336	0,006

ii) Shape optimization: In addition to thickness of plate and stiffeners, the height of stiffeners is also considered as design variable. (Note: During the optimization process, the height of stiffeners is equal to each other). The optimum values of design variables and critical buckling loads are presented in Table 5.4. The highest improvement, which is 41.40 %, obtained from eight stiffeners. When the number of stiffeners is increased critical buckling load is also increased similar to size optimization. The largest critical buckling load is again obtained from eight stiffeners case. The improvement is 926 % compared with two stiffeners case. Plate skin is thinner than stiffeners in optimum results and stiffener thicknesses reach upper limits.

Shape optimizations slightly gave better results compared to size optimizations as shown in Figure 5.6. For small number of stiffeners both optimizations give similar results. However when the number of stiffeners increase shape optimizations give better results. In shape optimization, stiffener thicknesses are going to be thicker than initial design values. The higher buckling loads in shape optimization type caused by the height of stiffeners. Shape optimization adds some of height to plate skin and stiffener thickness.

Table 5.4 Shape optimization of Straight stiffened plate

n_{stiff}	Optimum DVs values			Buckling loads		Imp
	t_{skin}	t_{stiff}	h_{stiff}	P_i	P_{max}	(%)
2	2.52	3.99	8.00	27392.7	30266.2	10.490
3	2.19	4.00	17.29	59731.7	66979.9	12.135
4	2.15	4.00	14.01	97565.0	114501.6	17.359
5	2.13	4.00	11.78	136548.5	171359.7	25.494
6	2.06	4.00	11.05	173160.7	237776.0	37.315
7	2.15	4.00	8.00	202204.2	283451.4	40.181
8	2.07	4.00	8.11	219819.9	310826.7	41.401

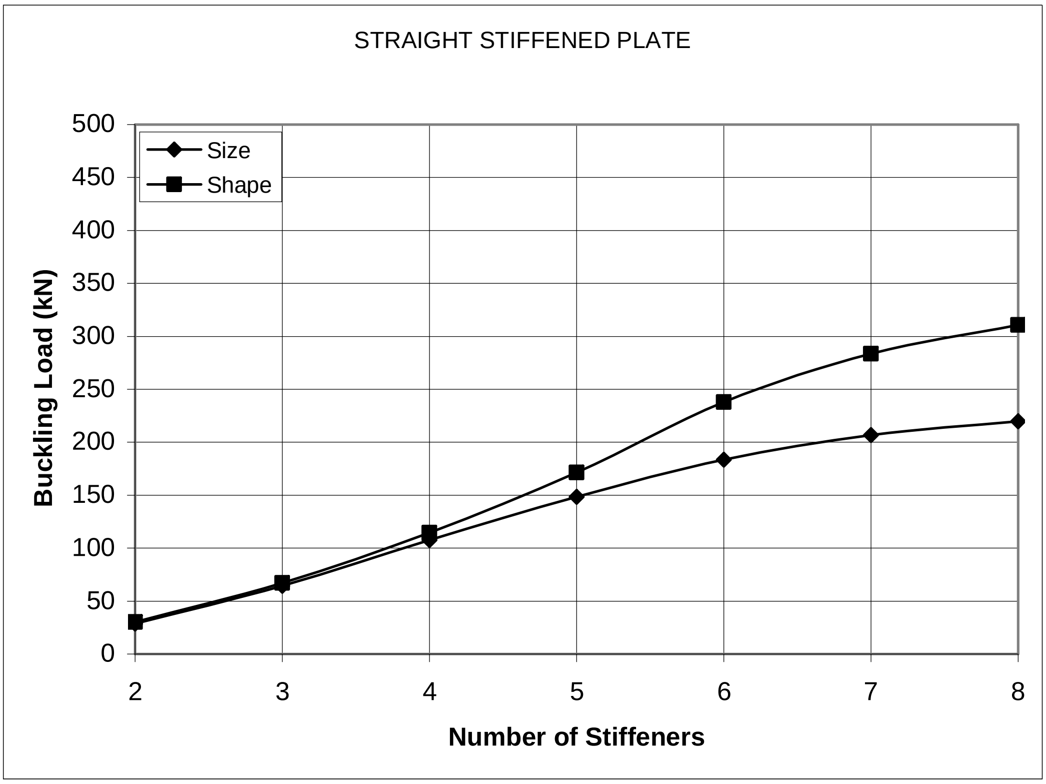

Figure 5.6 Comparison of size and shape optimizations

5.2.1.2 Straight stiffened plate with substiffeners

Figure 5.7 shows straight stiffened plate with substiffeners. Substiffeners are attached between stiffeners, which divide the distance between stiffeners two equal parts.

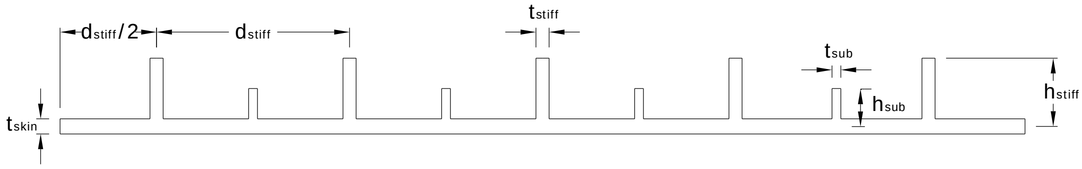

Figure 5.7 Straight stiffened plate with substiffeners.

a) Optimization Process:

i) Size optimization: Optimization is carried out using thickness of plate skin (t_{skin}), thickness of stiffeners (t_{stiff}) and thickness of substiffeners (t_{sub}). Height of stiffeners (h_{stiff}) and height of substiffeners (h_{sub}) have constant values of 28.0mm and 14.0mm in this stage (See Figure 5.7).

ii) Shape optimization: Height of stiffeners (h_{stiff}) and height of substiffeners (h_{sub}) included as design variables in this stage (See Figure 5.7).

Design constraints of two stages are specified in Table .5.5.Optimization process is carried out for two to eight stiffeners.

Table 5.5 Design constraints of straight stiffened plate with substiffeners

		Min (mm)	Max (mm)
Thickness of Plate	t_{skin}	1.4	3.0
Thickness of stiffener	t_{stiff}	1.3	4.0
Thickness of Substiffeners	t_{sub}	1.0	3.0
Height of stiffener	h_{stiff}	8.0	40.0
Height of Substiffeners	h_{sub}	5.0	20.0

b) Discussion of results

The effect of substiffeners between stiffeners to critical buckling load capacity is examined. Two types of optimization are performed. These are size optimization with three design variables (t_{skin} - t_{stiff} - t_{sub}) and shape optimization with five design variables (t_{skin} - t_{stiff} - t_{sub} - h_{stiff} - h_{sub}). The effect of number of stiffeners is also observed similar to stiffened plate.

i) Size optimization: Thickness of plate, stiffeners and substiffeners are kept equal in initial design. The height of stiffeners and height of substiffeners have constant values of 28.0 mm and 14.0 mm. The optimum values of design variables and critical buckling loads are given in Table 5.6. The highest improvement is obtained from five stiffeners case and it is approximately equal to 19.50 %. The highest critical buckling load is obtained from eight stiffeners case and equal to 218521 N. The improvement of critical buckling load is 537 % compared to two stiffeners case.

Plate skin is thicker than stiffeners in optimum solutions and except two stiffeners case and substiffeners' thicknesses decreases to lower limit.

Table 5.6 Size optimization of stiffened plate with stiffener

n_{stiff}	Optimum DVs values			Buckling loads		Imp (%)
	t_{skin}	t_{stiff}	t_{sub}	P_i	P_{max}	
2	2.42	1.39	2.07	32807.4	33704.4	2.73
3	2.35	1.30	1.02	62291.5	71102.4	14.14
4	2.23	1.33	1.00	95546.9	113592.6	18.89
5	2.09	1.40	1.00	129335.9	154533.5	19.48
6	1.97	1.40	1.00	160361.9	188273.5	17.41
7	1.78	1.55	1.00	184862.8	205626.2	11.23
8	1.59	1.66	1.00	195678.6	214763.1	9.75

ii) Shape optimization: In addition to thicknesses of plate, stiffeners and substiffeners height of stiffeners and substiffeners are included in optimization process as design variables. The optimum values of design variables and critical buckling loads are presented in Table 5.7. The highest improvement is obtained from eight stiffeners case and it is approximately 67.75 %. Also the largest critical buckling load is obtained from eight stiffeners case. The improvement of critical buckling load is about 836 % compared to two stiffeners case and it has value of 328229 N.

By the increasing of number of stiffeners, stiffener's thicknesses reach upper limit. Height of stiffeners begins with a higher value and decrease near to lower limit by the increasing of number of stiffeners. Substiffeners' height decrease to lower limit in all plates.

Shape optimizations obviously gave better results when compared size optimizations as shown Figure 5.8. Also for small number of stiffeners, both optimizations give similar results. However when the number of stiffeners increase shape optimizations give better results.

Table 5.7 Shape optimization of stiffened plate with stiffener

n_{stiff}	Optimum DVs values					Buckling loads		Imp
	t_{skin}	t_{stiff}	t_{sub}	h_{stiff}	h_{sub}	P_i	P_{max}	(%)
2	2.41	1.30	3.62	35.29	5.00	32807.4	35054.8	6.85
3	2.36	1.30	2.44	27.29	5.00	62291.5	72179.9	15.87
4	2.15	4.00	1.11	13.02	5.00	95546.9	115041.3	20.40
5	2.09	4.00	1.00	11.57	5.00	129335.9	169417.3	30.99
6	2.03	4.00	1.00	10.46	5.00	160361.9	230964.4	44.02
7	1.98	4.00	1.28	9.35	5.00	184862.8	286947.0	55.22
8	1.87	4.00	2.14	8.61	5.00	195678.6	328229.2	67.73

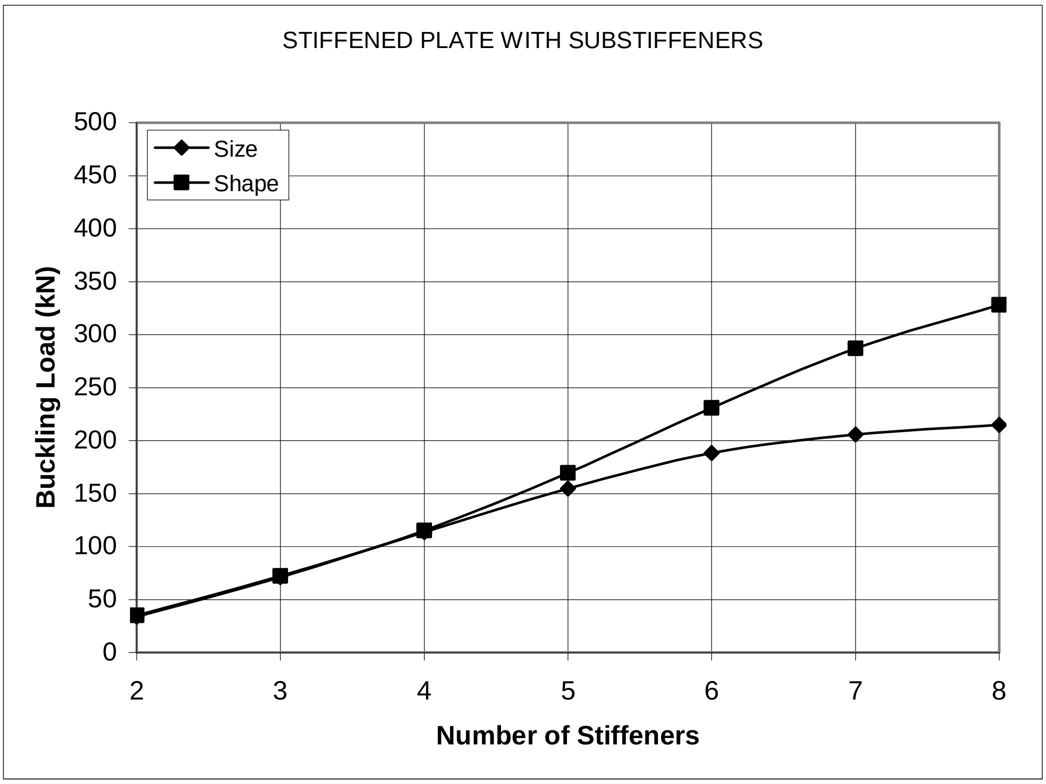

Figure 5.8 Comparison of size and shape optimizations

5.2.1.3 Straight stiffened plate and pads under main stiffeners

Pad elements are attached plate skin under straight stiffeners and Figure 5.9 shows straight stiffened plate and pads under stiffeners.

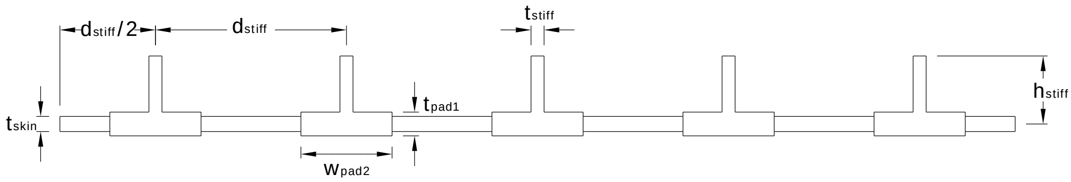

Figure 5.9 Straight stiffened plate and pads under stiffeners

a) Optimization Process:

i) Size optimization: Optimization is carried out using thickness of plate skin (t_{skin}), thickness of stiffeners (t_{stiff}) and thickness of pad (t_{pad1}). Height of stiffeners (h_{stiff}) and width of pads (w_{pad1}) have constant values of 28.0mm and $d_{stiff}/4$ (See Figure 5.9).

ii) Shape optimization: Height of stiffeners (h_{stiff}) included as design variable. Width of pads (w_{pad1}) still have constant value of $d_{stiff}/4$ (See Figure 5.9).

iii) Shape optimization: Width of pad (w_{pad1}) included as design variable in this stage (See Figure 5.9).

Design constraints of three stages are specified in Table 5.8.Optimization process is carried out for two to eight stiffeners.

Table 5.8 Design Constraints of straight stiffened plate and pads under stiffeners

		Min (mm)	Max (mm)
Thickness of Plate	t_{skin}	1.4	3.0
Thickness of stiffener	t_{stiff}	1.3	4.0
Height of stiffener	h_{stiff}	8.0	40.0
Thickness of Pad	t_{pad1}	2.0	5.0
Width of Pad	w_{pad1}	$d_{stiff}/10$	$d_{stiff}/2$

b) Discussion of results

In this type optimization the effect of pad elements under stiffeners to critical buckling load capacity is investigated. Three types optimization were performed. The first one is size optimization with three design variables ($t_{skin} - t_{stiff} - t_{pad1}$). Second is shape optimization with four design variables ($t_{skin} - t_{stiff} - t_{pad1} - h_{stiff}$). Third one is shape optimization with five design variables ($t_{skin} - t_{stiff} - t_{pad1} - h_{stiff} - w_{pad1}$). The effect of number of stiffeners also examined.

i) Size optimization: Thickness of plate and stiffeners are kept equal in initial design. Thickness of pad is kept two times of thickness of plate. The height of stiffeners and width of pads are kept constant during this stage and they have values of 28,0mm and $d_{stiff}/4$. The optimum values of design variables and critical buckling loads are given in Table 5.9. The highest improvement is obtained from three stiffeners case and the improvement is approximately 9.85 %. The highest critical buckling load is obtained from eight stiffeners case and equal to 258127 N. The improvement of this case is 593 % compared with two stiffeners case.

Skin thickness is going to be thinner and stiffener thickness is going to thicker by the increasing of number of stiffeners. There is a large difference between thicknesses of pads are and skin. Pads are thicker than skin. Skin and pad thicknesses are going to be thinner by the increasing of number of stiffeners and stiffeners thicknesses are going to be thicker.

Table 5.9 Size optimization of Straight stiffened plate and pads under stiffeners

n_{stiff}	Optimum DVs values			Buckling loads		Imp
	t_{skin}	t_{stiff}	t_{pad1}	P_i	P_{max}	(%)
2	1.84	1.30	4.48	34585.9	37248.8	7.69
3	1.85	1.30	4.11	72801.5	79991.2	9.87
4	1.72	1.44	4.04	119179.0	128100.5	7.48
5	1.62	1.57	3.80	167848.9	175648.1	4.64
6	1.49	1.65	3.65	213108.2	219021.0	2.77
7	1.40	1.66	3.50	236188.4	254098.5	7.58
8	1.40	1.66	3.07	242591.5	258127.7	6.40

ii) Shape optimization: In addition to thicknesses of plate, stiffeners and pads height of stiffeners is included in optimization process as design variables. Still width of pads has constant values of $d_{stiff}/4$. The optimum values of design variables and critical buckling loads are presented in Table 5.10. The highest improvement is obtained from eight stiffeners case and it is approximately 88.10 %. Here the height of stiffeners becomes more effective. Also the largest critical buckling load is obtained from eight stiffeners case. The improvement of critical buckling load is about 1100 % compared to two stiffeners case and it has value of 456313 N.

Stiffeners are thinner than plate skin except two stiffeners case. Pads are thicker than plate skin and skin and pads are going to be thinner but stiffeners are going to be thicker by the increasing of number of stiffeners and height of stiffeners reach lower limit.

Table 5.10 Shape optimization of straight stiffened plate and pads under stiffeners with five design variables

n_{stiff}	Optimum DVs values				Buckling loads		Imp(%)
	t_{skin}	t_{stiff}	t_{pad1}	h_{stiff}	P_i	P_{max}	
2	1.89	1.53	4.53	16.08	34585.9	38022.1	9.93
3	1.87	2.48	4.36	10.15	72801.5	82324.0	13.08
4	1.85	2.80	4.28	8.00	119179.0	139308.1	16.89
5	1.80	2.69	4.28	8.00	167848.8	207255.3	23.47
6	1.76	2.94	4.08	8.00	213108.2	283922.8	33.22
7	1.73	3.22	3.82	8.00	236188.4	364286.1	54.23
8	1.61	3.43	3.81	8.00	242591.5	456313.08	88.09

iii) Shape optimization: In addition to previous design variables width of pad included as a design variable. The optimum values of design variables and critical buckling loads are presented in Table 5.11. The highest improvement is obtained from eight stiffeners case and it is approximately 102.20 %. Largest critical buckling load also is obtained from eight stiffeners case. In this case plate has a critical buckling load of 490479 N. The improvement is 990 % compared with two stiffeners case.

Stiffeners are thicker than plate skin in all cases. Pads are going to be thinner and stiffeners are going to be thicker by the increasing of number of stiffeners in optimum results. Height of stiffeners decrease to lower limit in all plates. Width of pads reach upper limits except seven and eight stiffeners case.

Table 5.11 Shape optimization of straight stiffened plate and pads under stiffeners with six design variables

n_{stiff}	Optimum values of DVs					Buckling Loads		Imp(%)
	t_{skin}	t_{stiff}	t_{pad}	h_{stiff}	w_{pad}	P_i	P_{max}	
2	1.42	2.59	3.72	8.00	110.00	34585.9	44978.8	30.05
3	1.41	2.61	3.63	8.00	73.33	72801.5	96703.3	32.83
4	1.40	2.94	3.49	8.10	55.00	119179.0	163799.5	37.44
5	1.40	3.36	3.32	8.00	44.00	167848.8	238789.1	42.26
6	1.40	3.64	3.13	8.00	36.66	213108.2	321156.0	50.70
7	1.40	3.92	3.06	8.00	28.85	236188.4	403336.2	70.76
8	1.40	3.99	3.30	8.00	19.76	242591.52	490479.4	102.18

Shape optimizations gave better results when compared with size optimizations as shown in Figure 5.10.

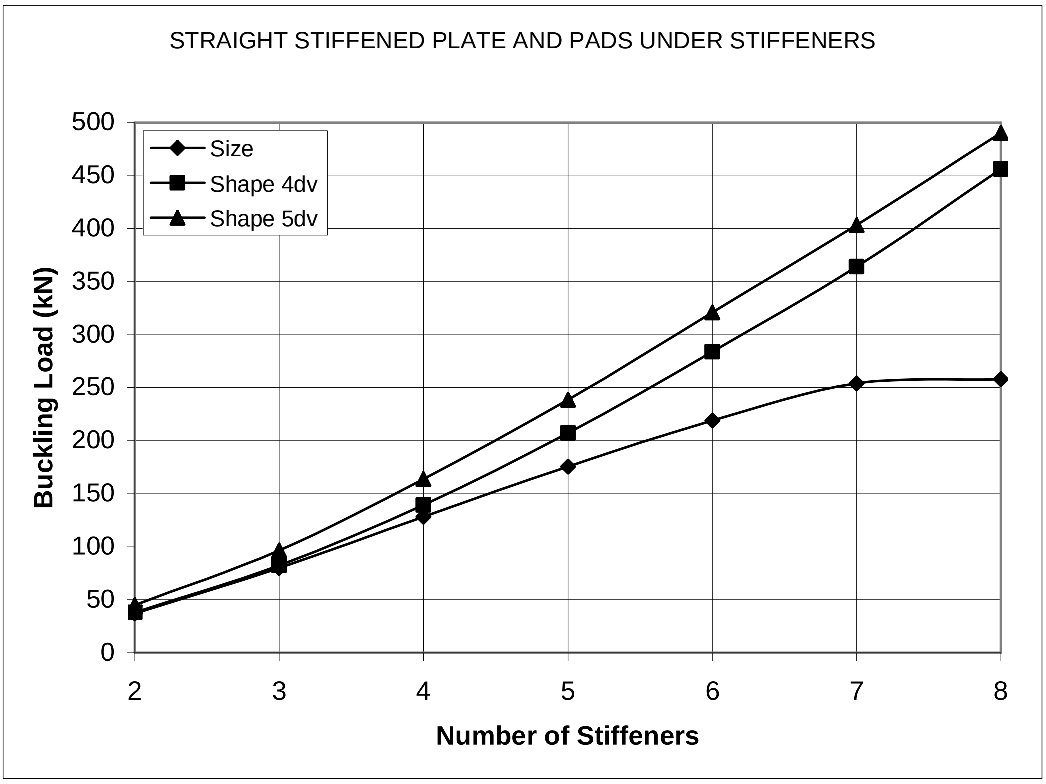

Figure 5.10 Comparison of size and shape optimizations

In this type of plates due to these results, it is very clear that the most effective elements are pads under the stiffeners. Therefore, it is obviously that the joining points of plate base and stiffeners are most critical points for critical buckling. The pads are strengthening that points and largest buckling loads are obtained.

5.2.1.4 Straight stiffened plate with substiffeners and pads under stiffeners

Substiffeners are added between stiffeners and pad elements are attached under stiffeners. Figure 5.11 shows straight stiffened plate with substiffeners and pads under stiffeners.

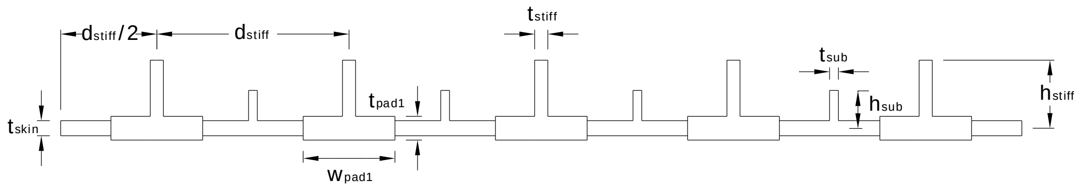

Figure 5.11 Straight stiffened plate with substiffeners and pads under stiffeners

a) Optimization Process:

i) Size optimization: Optimization is performed using thickness of plate skin (t_{skin}), thickness of stiffeners (t_{stiff}), thickness of substiffeners (t_{sub}),and thickness of pad (t_{pad1}). Height of main stiffeners (h_{stiff}), height of substiffeners (h_{sub}) and width of pads (w_{pad1}) have constant values of 28.0 mm, 14.0 mm and $d_{stiff}/4$ in this stage (See Figure 5.11).

ii) Shape optimization: Height of stiffeners (h_{stiff}) and height of substiffeners (h_{sub}) included as design variable in this stage. Width of pads (w_{pad1}) still have constant value of $d_{stiff}/4$ in this stage (See Figure 5.11).

iii)Shape optimization: Width of pads (w_{pad1}) included as design variable in this stage (See Figure 5.11).

Design constraints of three stages are specified in Table 5.12.Optimization process is carried out for two to eight stiffeners.

b) Discussion of results

The effect of substiffeners and pads are examined together in this type of plates. Three types of optimizations are performed. First one is size optimization with four design variables (t_{skin} - t_{stiff} - t_{sub} - t_{pad1}) ,second is shape optimization with six design variables (t_{skin} - t_{stiff} - t_{sub} - t_{pad1} - h_{stiff} - h_{sub}) and the third one is shape optimization with seven design variables (t_{skin} - t_{stiff} - t_{sub} - t_{pad1} - h_{stiff} - h_{sub} - w_{pad1}). The effect of number of stiffeners also examined.

Table 5.12 Design Constraints of straight stiffened plate with substiffeners and pads under stiffeners

		Min (mm)	Max (mm)
Thickness of plate	t_{skin}	1.4	3.0
Thickness of stiffener	t_{stiff}	1.3	4.0
Height of stiffener	h_{stiff}	8.0	40.0
Thickness of substiffeners	t_{sub}	1.0	3.0
Height of substiffeners	h_{sub}	5.0	20.0
Thickness of pad	t_{pad1}	2.0	5.0
Width of pad	w_{pad1}	d_{stiff}/10	d_{stiff}/2

i) Size optimization: Thickness of plate and stiffeners are kept equal in initial design. Thickness of pads and thickness of substiffeners are kept 1.5 times and 0.75 times of thickness of plate. The height of stiffeners, height of substiffeners and width of pads are kept constant during this stage and they have values of 28.0mm, 14.0mm and d_{stiff}/4. The optimum values of design variables and critical buckling loads are given in Table 5.13. The highest improvement is obtained from three stiffeners case and the improvement is approximately 13.15 %. The highest critical buckling load is obtained from eight stiffeners case and equal to 237913 N. The improvement of this case is 500 % compared with two stiffeners case.

In optimum solutions, plate skin is thicker than stiffeners, thickness of substiffeners reached to lower limits. Skin thickness is going to be thinner and stiffener thicknesses are going to be thicker by the increasing of number of stiffeners.

Table 5.13 Size optimization of straight stiffened plate with substiffeners and pads under stiffeners

n_{stiff}	Optimum DVs values				Buckling loads		Imp
	t_{skin}	t_{stiff}	t_{sub}	t_{pad1}	P_i	P_{max}	(%)
2	1.98	1.30	1.00	3.93	36316.4	39654.6	9.192
3	1.98	1.30	1.00	3.48	72736.7	81613.4	12.204
4	1.81	1.38	1.06	3.42	112890.9	127733.3	13.148
5	1.69	1.47	1.00	3.19	155308.9	172728.9	11.216
6	1.51	1.4	1.10	3.19	194556.6	208078.9	6.950
7	1.40	1.56	1.00	2.91	220346.4	233851.5	6.129
8	1.40	1.64	1.00	2.23	222514.5	237913.1	6.920

ii) Shape optimization: in addition to thicknesses of plate, stiffeners, substiffeners and pads height of stiffeners and substiffeners are included in optimization process as design variables. Still width of pads has constant values of $d_{stiff}/4$. The optimum values of design variables and critical buckling loads are presented in Table 5.14. The highest improvement is obtained from eight stiffeners case and it is approximately 97.45 %. Also the largest critical buckling load is obtained from eight stiffeners case. The improvement of critical buckling load is about 1000 % compared to two stiffeners case and it has value of 439376 N.

Skin and pad thickness are going to be thinner, height of stiffeners reach lower limit except two stiffeners case and in all cases height of substiffeners remain in lower limits.

iii) Shape optimization: In addition to previous design variables width of pad included as a design variable. The optimum values of design variables and critical buckling loads are presented in Table 5.15. The highest improvement is gained from eight stiffeners case and it is approximately 106.20 %. Largest critical buckling load also is obtained from eight stiffeners case and the plate has a critical buckling load of 458888 N. The improvement is 913 % compared with two stiffeners case.

In optimum solutions, skin is thinner than stiffeners. Skin thickness and pad thicknesses are going to be thinner and thicknesses of stiffeners are going to be thinner by the increasing of number of stiffeners. Height of stiffeners and substiffeners reach lower limits in all cases and width of pads reach upper limits except seven and eight stiffeners cases.

Table 5.14 Shape optimization of straight stiffened plate with substiffeners and pads under stiffeners with six design variables

n_{stiff}	Optimum DVs values						Buckling loads		Imp
	t_{skin}	t_{stiff}	t_{sub}	t_{pad1}	h_{stiff}	h_{sub}	P_i	P_{max}	(%)
2	1.99	1.30	1.96	4.00	25.05	5.00	36316.4	39978.0	10.08
3	1.91	3.15	1.00	4.16	8.00	5.00	72736.7	82354.9	13.22
4	1.86	2.86	1.00	4.10	8.00	5.00	112890.9	136486.8	20.90
5	1.77	2.69	1.00	4.18	8.00	5.00	155308.9	201624.5	29.82
6	1.74	3.11	1.00	3.85	8.00	5.00	194556.6	274141.2	40.90
7	1.69	3.17	1.00	3.69	8.00	5.00	220346.4	352666.9	60.05
8	1.60	3.29	1.00	3.61	8.00	5.00	222514.5	439376.4	97.46

Size optimizations and shape optimizations with six design variables gave similar results in small number of stiffeners as shown in figure 5.12. But the shape optimization more stiffeners gave higher critical buckling loads. Shape optimizations with seven design variables gave higher results starting with small number of stiffeners.

Table 5.15 Shape optimization of Straight stiffened plate with substiffeners and pads under stiffeners with seven design variables

n_{stiff}	Optimum DVs values							Buckling loads		Imp
	t_{skin}	t_{stiff}	t_{sub}	t_{pad1}	h_{stiff}	h_{sub}	w_{pad1}	P_i	P_{max}	(%)
2	1.52	2.99	1.00	3.57	8.00	5.00	110.00	36316.4	45291.6	24.71
3	1.42	2.73	1.00	3.56	8.00	5.00	73.33	72736.7	95633.7	31.47
4	1.40	2.76	1.00	3.45	8.00	5.00	55.00	112890.9	160575.7	42.24
5	1.40	3.25	1.00	3.24	8.09	5.00	44.00	155308.9	233837.0	50.56
6	1.40	3.56	1.00	3.03	8.00	5.00	36.67	194556.6	311333.6	60.02
7	1.40	4.00	1.00	2.86	8.00	5.00	29.63	220346.4	389130.8	76.60
8	1.40	3.98	1.27	3.05	8.00	5.00	19.36	222514.5	458888.3	106.22

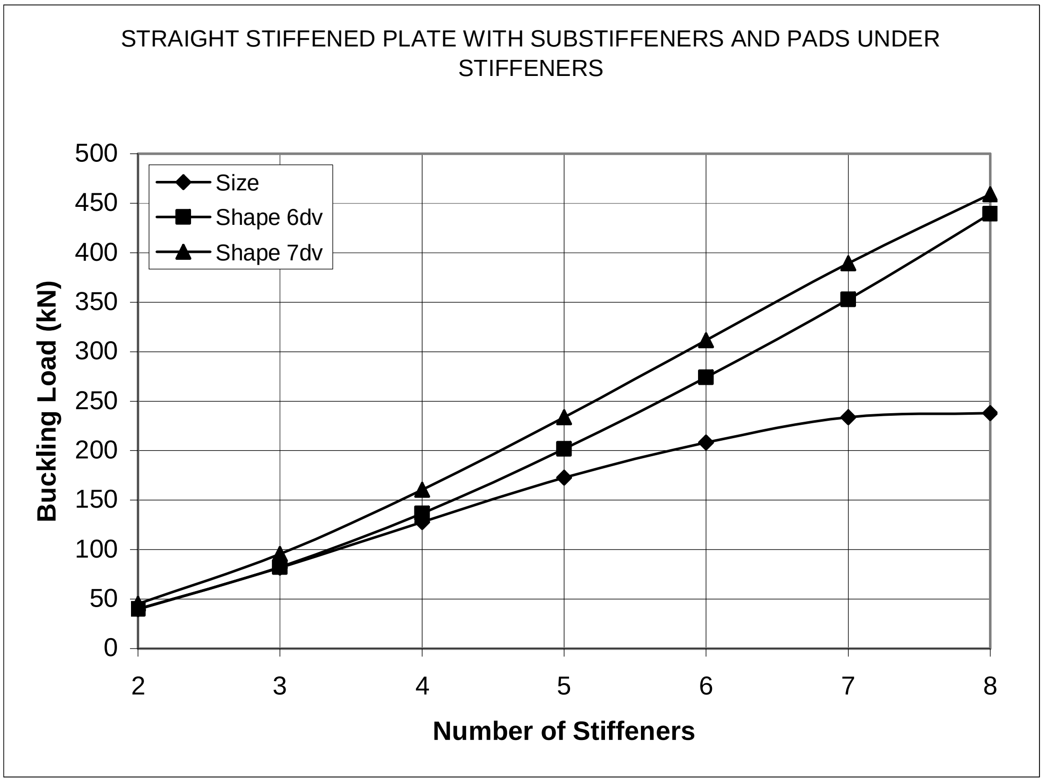

Figure 5.12 Comparison of size and shape optimizations

5.2.1.5 Straight stiffened plate and pads between stiffeners

Pad elements are added between stiffeners. Figure 5.13 shows straight stiffened plate and pads between stiffeners.

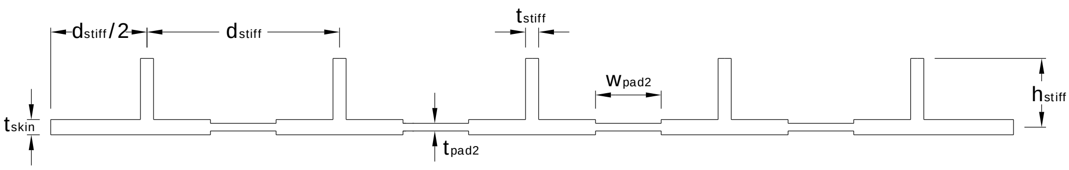

Figure 5.13 Straight stiffened plate and pads between stiffeners

a) Optimization process

i) Size optimization: Optimization is performed using thickness of plate skin (t_{skin}), thickness of stiffeners (t_{stiff}), thickness of pads between stiffeners $(t_{pad\,2})$ .Height of stiffeners (h_{stiff}) and width of pads between stiffeners $(w_{pad\,2})$ have constant values of 28,0mm and $d_{stiff}/4$ in this stage (See Figure 5.13).

ii) Shape optimization: Height of stiffeners (h_{stiff}) are included in optimization process. Width of pads between stiffeners $(w_{pad\,2})$ has still constant value of $d_{stiff}/4$ (See Figure 5.13).

iv) Shape optimization: Width of pads between stiffeners $(w_{pad\,2})$ are included as a design variable (See Figure 5.13).

Design constraints of three stages are specified in Table 5.16.Optimization process is carried out for two to eight stiffeners.

Table 5.16 Design constraints of Straight stiffened plate and pads between stiffeners

		Min (mm)	Max (mm)
Thickness of plate	t_{skin}	1.4	3.0
Thickness of stiffener	t_{stiff}	1.3	4.0
Height of stiffener	h_{stiff}	8.0	40.0
Thickness of pads between stiffeners	$t_{pad\,2}$	1.3	5.0
Width of pad between stiffeners	$w_{pad\,2}$	$d_{stiff}/10$	$d_{stiff}/2$

b) Discussion of results

The effect of pads between stiffeners on critical buckling load is investigated. Initial thickness of plate skin, stiffeners and pads between stiffeners are kept equal. The first optimization is size optimization in which three design variables are considered (t_{skin} - t_{stiff} - $t_{pad\,2}$). Secondly shape optimization with four design variables (t_{skin} - t_{stiff} - $t_{pad\,2}$ - h_{stiff}). Third one is shape optimization with five design variables (t_{skin} - t_{stiff} - $t_{pad\,2}$ - h_{stiff} - $w_{pad\,2}$). The effect of number of stiffeners also examined.

i) Size optimization: Thickness of plate, stiffeners and pads are kept equal in baseline design. The height of stiffeners and width of pads between stiffeners kept constant during this stage and they have values of 28 mm and $d_{stiff}/4$ respectively. The optimum values of design variables, obtained maximum critical buckling load and improvement are given in table 5.17. The highest improvement is gained from four stiffeners case and it is 11.78%. The highest critical buckling load is obtained from eight stiffeners case and it is 227232 N. The improvement according to number of stiffeners is 685% when compared two stiffeners case.

Skin thickness is thicker than stiffener thicknesses in optimum solutions Pads between stiffeners are thinner than skin in all cases and they are going to be thinner by the increasing of number of stiffeners and reaches to lower limit in eight stiffeners.

Table 5.17 Size optimization of straight stiffened plate and pads between stiffeners

n_{stiff}	Optimum DVs values			Buckling loads		Imp
	t_{skin}	t_{stiff}	t_{pad2}	P_i	P_{max}	(%)
2	2.55	1.30	2.14	27392.7	28923.4	5.59
3	2.51	1.30	1.94	59731.7	65599.2	9.82
4	2.48	1.39	1.56	97565.0	109060.2	11.78
5	2.33	1.51	1.58	136548.4	152406.4	11.61
6	2.18	1.58	1.60	173160.7	188909.1	9.09
7	2.06	1.58	1.59	202204.2	213925.7	5.80
8	1.90	1.76	1.30	219819.9	227232.4	3.37

ii) Shape optimization: In addition to size optimization's design variables, height of stiffeners is included in optimization procedure. Width of pads still have constant value. The optimum values of design variables, obtained maximum critical buckling loads and improvements are given in Table 5.18. the highest improvement is obtained from eight stiffeners case and it is 52.10 %. The highest critical buckling load is obtained from eight stiffeners case too and it is 334339 N. The improvement according to number of stiffeners is 994 % when compared two stiffeners case.

Skin is thinner than stiffeners and thicknesses of stiffeners reach to upper limits in all cases. Thicknesses of pads between stiffeners are thinner than skin thicknesses.

iii) Shape optimization: In addition to previous shape optimization's design variables width of pads is included in optimization process. Optimum values of design variables, obtained maximum critical buckling loads and improvements are given in Table 5.19. The highest improvement is obtained from eight stiffeners case and it is 57.62 %. The highest critical buckling load also is gained from eight stiffeners case and it has a value of 346471 N. The improvement according to number of stiffeners is 955 % when compared two stiffeners case. In optimum solutions, stiffeners are thinner than plate skin and stiffeners thicknesses reach upper limit except two stiffeners case. Widths of pads between stiffeners reach upper limits in all cases.

Table 5.18 Shape optimization of straight stiffened plate and pads between stiffeners with four design variables

n_{stiff}	Optimum DVs values				Buckling loads		Imp (%)
	t_{skin}	t_{stiff}	t_{pad2}	h_{stiff}	P_i	P_{max}	
2	2.58	4.00	2.07	8.00	27392.7	30539.1	11.49
3	2.67	4.00	1.30	8.00	59731.7	69760.8	16.79
4	2.44	4.00	1.30	11.99	97565.0	122587.9	25.65
5	2.33	4.00	1.30	11.83	136548.5	185262.4	35.68
6	2.301	4.00	1.35	10.17	173160.7	253012.9	46.11
7	2.38	4.00	1.30	8.00	202204.2	292257.2	44.54
8	2.30	4.00	1.30	8.00	219819.9	334339.5	52.10

Table 5.19 Shape optimization of straight stiffened plate and pads between stiffeners with five design variables

n_{stiff}	Optimum DVs values					Buckling loads		Imp (%)
	t_{skin}	t_{stiff}	t_{pad2}	h_{stiff}	w_{pad2}	P_i	P_{max}	
2	2.90	3.99	1.38	8.00	110.00	27392.7	32833.1	19.86
3	3.00	4.00	1.30	8.44	73.33	59731.7	76298.6	27.74
4	2.90	4.00	1.30	9.95	55.00	97565.0	132163.9	35.46
5	2.56	4.00	1.30	13.30	44.00	136548.5	206271.1	51.06
6	2.49	4.00	1.49	10.80	36.66	173160.7	260804.0	50.61
7	2.62	4.00	1.53	8.00	31.42	202204.2	300561.1	48.64
8	2.63	4.00	1.38	8.00	27.50	219819.9	346471.2	57.62

Optimization results are very close to each other between two and four stiffeners as shown in Figure 5.14. Shape optimizations gave higher results for following plates. According to results, it is clearly observed that pad zones between stiffeners are thinner than plate skin. Reference to this, pad zones between stiffeners includes less buckling risk than plate skin zones.

To obtain higher buckling loads it is important to strengthen stiffeners and plate skin joining zones. In addition, two shape optimization types gave similar results. Therefore, by the increasing of width of pads between stiffeners widths thickness of pads going to thinner but this situation does not obtain very high critical buckling loads.

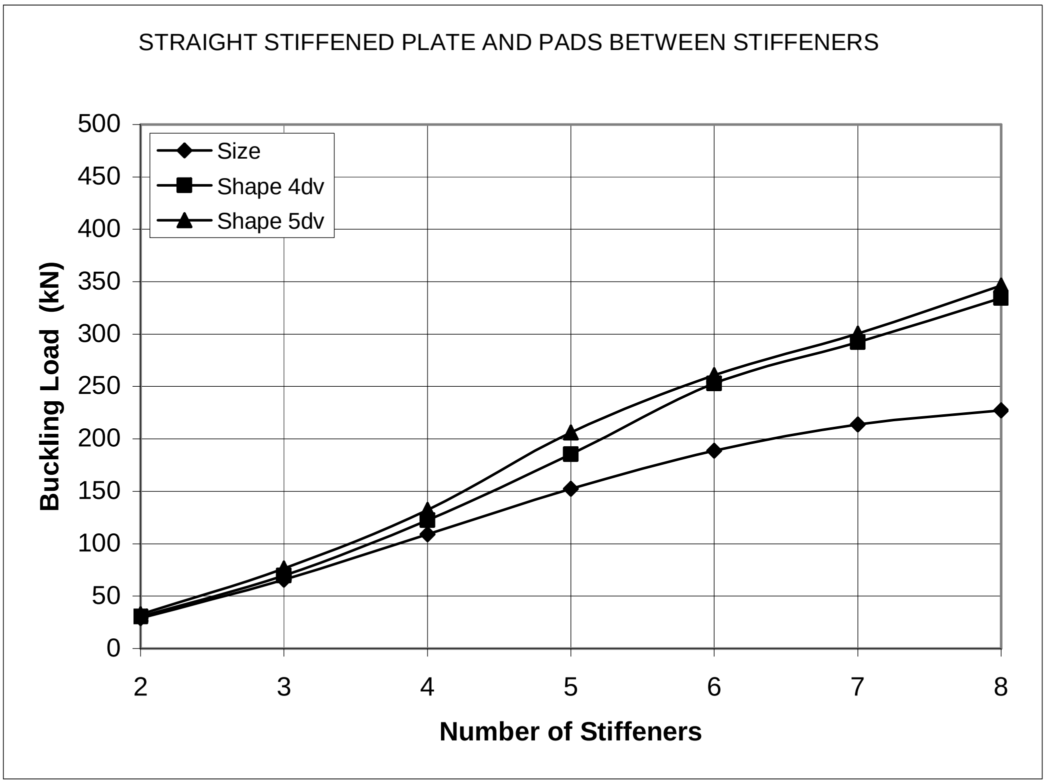

Figure 5.14 Comparison of size and shape optimizations

5.2.1.6 Straight stiffened plate and pads under stiffeners and between stiffeners

In this straight stiffened plate type pads under and between stiffeners are considered. Figure 5.15 sows straight stiffened plate and pads under stiffeners and between stiffeners.

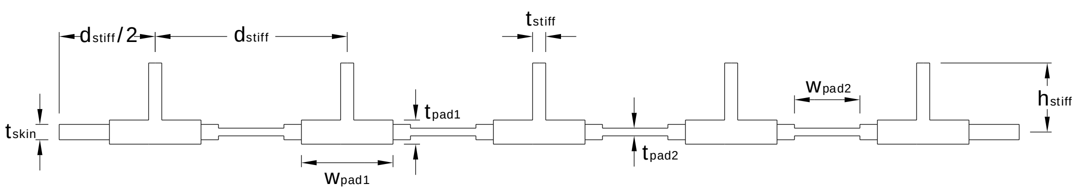

Figure 5.15 Straight stiffened plate and pads under stiffeners and between stiffeners

a) Optimization Process:

i) Size optimization: Optimization is carried out using thickness of plate skin (t_{skin}), thickness of stiffeners (t_{stiff}), thickness of pads (t_{pad1}), and thickness of pads between stiffeners (t_{pad2}) .Height of main stiffeners (h_{stiff}), width of pads (w_{pad1}) and width of pads between stiffeners (w_{pad2}) have constant values of 28,0mm, $d_{stiff}/4$ and $d_{stiff}/4$ in this stage (See Figure 5.15).

ii) Shape optimization: Height of stiffeners (h_{stiff}), are included as design variables in this stage. Width of pads under stiffeners (w_{pad1}) and width of pads between stiffeners (w_{pad2}) still have constant value of $d_{stiff}/4$ in this stage (See Figure 5.15).

iii) Shape optimization: Width of pad (w_{pad1}) and width of pads between stiffeners (w_{pad2}) are included as design variables in this stage (See Figure 5.15).

Design constraints of three stages are specified in Table 5.20. Optimization process is carried out for two to eight stiffeners

Table 5.20 Design constraints of straight stiffened plate and pads under stiffeners and between stiffeners

		Min (mm)	Max (mm)
Thickness of Plate	t_{skin}	1.4	3.0
Thickness of stiffener	t_{stiff}	1.3	4.0
Height of stiffener	h_{stiff}	8.0	40.0
Thickness of Pad	t_{pad1}	2.0	5.0
Width of Pad	w_{pad1}	$d_{stiff}/10$	$d_{stiff}/2$
Thickness of pads between stiffeners	t_{pad2}	1.3	5.0
Width of pads between stiffeners	w_{pad2}	$d_{stiff}/10$	$d_{stiff}/2$

b) Discussion of results

The effect of pads between stiffeners between stiffeners with pads is investigated. Three types of optimization is introduced. The firs one is size optimization with four design variables (t_{skin} - t_{stiff} - t_{pad2} - t_{pad1}). Second is shape optimization with five design variables (t_{skin} - t_{stiff} - t_{pad2} - t_{pad1} - h_{stiff}). Third one is shape optimization with seven design variables (t_{skin} - t_{stiff} - t_{pad2} - t_{pad1} - h_{stiff} - w_{pad2} - w_{pad1}). The effect of number of stiffeners is also examined.

i) Size optimization: Thickness of plate, stiffeners and pads between stiffeners are kept equal and the thickness of pads is kept two times of thickness of plate skin in baseline design. The height of stiffeners, width of pads between stiffeners and width of pads kept constant during this stage and they have values of 28 mm d_{stiff}/4 and d_{stiff}/4 respectively. The optimum values of design variables, obtained maximum critical buckling load and improvement are given in table 5.21. The highest improvement is gained from three stiffeners case and it is 14.07 %. The highest critical buckling load is obtained from eight stiffeners case and it is 262570 N. The improvement according to number of stiffeners is 577 % when compared two stiffeners case.

Skin thicknesses and pad thicknesses under stiffeners are going to be thinner and stiffeners thicknesses are going to be thicker and by the increasing of number of stiffeners in optimum results.

Table 5.21 Size optimization of straight stiffened plate and pads under stiffeners and between stiffeners

n_{stiff}	Optimum DVs Values				Buckling loads		Imp
	t_{skin}	t_{stiff}	t_{pad2}	t_{pad1}	P_i	P_{max}	(%)
2	1.90	1.30	1.30	4.58	34585.9	38765.5	12.08
3	1.91	1.30	1.30	4.34	72801.5	83044.9	14.07
4	1.78	1.50	1.41	4.07	119179.0	132230.3	10.95
5	1.68	1.62	1.32	3.84	167848.8	182438.2	8.69
6	1.60	1.66	1.36	3.52	213108.2	223447.6	4.85
7	1.40	1.67	1.30	3.55	236188.4	257590.3	9.06
8	1.40	1.67	1.30	3.14	242591.5	262570.4	8.24

ii) Shape optimization: in addition to size optimization's design variables, height of stiffeners is included in optimization procedure. Width of pads between stiffeners and width of pads under stiffeners have constant values. The optimum values of design variables, obtained maximum critical buckling loads and improvements are given in Table 5.22. The highest improvement is obtained from eight stiffeners case and it is 95.67 %. The highest critical buckling load is obtained from eight stiffeners case too and it is 474668 N. The improvement according to number of stiffeners is 1077 % when compared two stiffeners case.

In all cases, skin is thinner than stiffener in optimum solutions. Skin thicknesses and pad thicknesses under stiffeners are going to be thinner and stiffener thicknesses are going to be thicker by the increasing of number of stiffeners. Thicknesses of pads between stiffeners and height of stiffeners reach to lower limits in all cases.

Table 5.22 Shape optimization of straight stiffened plate and pads under stiffeners and between stiffeners with five design variables

n_{stiff}	Optimum DVs values					Buckling loads		Imp
	t_{skin}	t_{stiff}	t_{pad2}	t_{pad1}	h_{stiff}	P_i	P_{max}	(%)
2	1.99	2.66	1.30	4.63	8.00	34585.9	40310.8	16.55
3	1.94	2.96	1.30	4.61	8.00	72801.5	88180.7	21.12
4	1.93	2.85	1.30	4.50	8.00	119179.01	149191.3	25.18
5	1.89	2.99	1.30	4.35	8.08	167848.9	220955.2	31.64
6	1.81	3.15	1.30	4.27	8.00	213108.2	303625.1	42.47
7	1.79	3.35	1.30	4.01	8.00	236188.4	387708.3	64.15
8	1.72	3.63	1.30	3.74	8.00	242591.5	474668.2	95.67

iii) Shape optimization: In addition to previous shape optimization's design variables width of pads between and under stiffeners are included in optimization process. Optimum values of design variables, obtained maximum critical buckling loads and improvements are given in Table 5.23. The highest improvement is gained from eight stiffeners case and it is 108.13 %. The highest critical buckling load also is obtained from eight stiffeners case and it has a value of 504895 N. The improvement according to number of stiffeners is 1015 % when compared two stiffeners case.

In optimum solutions, skin is thinner than stiffeners in all cases. Stiffener thicknesses are going to be thicker and thicknesses of pads under stiffeners are going to be thinner by the increasing of number of stiffeners. The thicknesses of pads between stiffeners and height of stiffeners remain constant and reach to lower limits in all cases.

Table 5.23 Shape optimization of straight stiffened plate and pads under stiffeners and between stiffeners with seven design variables

n_{stiff}	Optimum DVs values							Buckling loads		Imp
	t_{skin}	t_{stiff}	t_{pad2}	t_{pad1}	h_{stiff}	w_{pad1}	w_{pad2}	P_i	P_{max}	(%)
2	1.46	2.59	1.30	3.69	8.00	110.00	22.00	34585.9	45275.8	30.91
3	1.41	2.66	1.30	3.64	8.00	73.33	14.67	72801.5	97109.1	33.39
4	1.40	2.81	1.30	3.59	8.00	55.00	55.00	119179.01	167224.0	40.31
5	1.40	3.20	1.30	3.42	8.00	44.00	44.00	167848.8	243197.4	44.89
6	1.41	3.76	1.30	3.18	8.00	36.67	36.67	213108.2	330069.2	54.88
7	1.40	3.92	1.30	3.16	8.00	28.85	31.43	236188.4	407575.9	72.56
8	1.40	3.98	1.30	3.43	8.00	19.76	27.50	242591.5	504895.3	108.13

Obtained critical buckling load results are very close to each other for two and three stiffeners as shown in Figure 5.16.

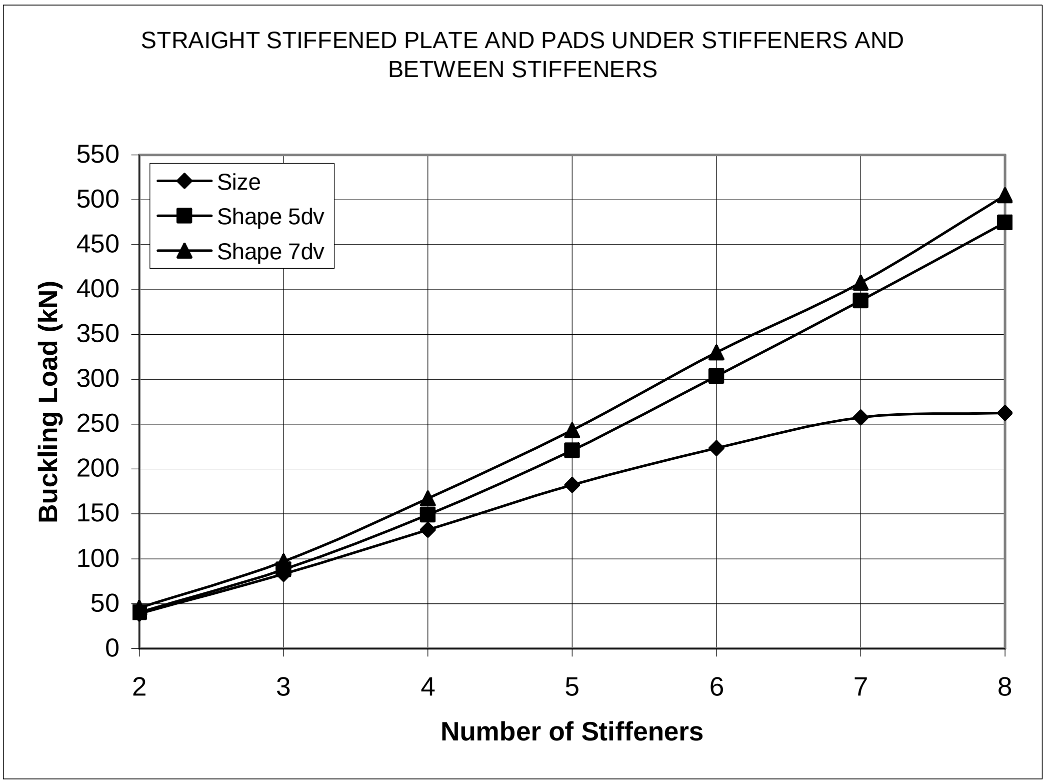

Figure 5.16 Comparison of size and shape optimizations

Shape optimizations gave higher results for the following plates. In optimized results, pad zones between stiffeners are thinner than plate skin. Therefore, the behavior of pads between stiffeners is similar to previous plate type.

5.2.1.7 Straight stiffened plate with linearly varying skin

Stiffened plate with linearly varying plate skin between stiffeners is shown in Figure 5.17.

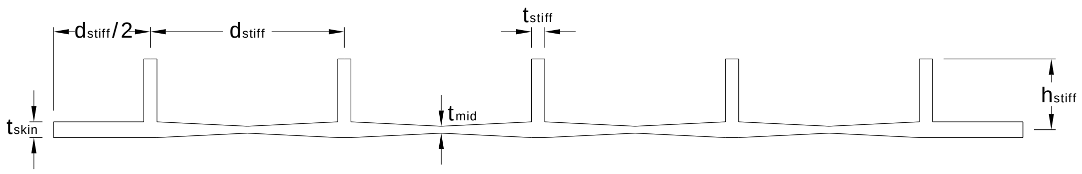

Figure 5.17 Straight stiffened plate with linearly varying skin

a) Optimization Process:

i) *Size optimization:* Optimization is performed using thickness of plate skin (t_{skin}), thickness of stiffeners (t_{stiff}) and thickness of midspan (t_{mid}). Height of main stiffners (h_{stiff}) has constant value of 28,0mm in this stage (See Figure 5.17).

ii) *Shape optimization:* Height of stiffeners (h_{stiff}) is included as design variable in this stage (See Figure 5.17).

Design constraints of two stages are specified in Table 5.24.Optimization process is carried out for two to eight stiffeners

Table 5.24 Design constraints of Straight stiffened plate with linearly varying skin

		Min (mm)	Max (mm)
Thickness of plate	t_{skin}	1.4	3.0
Thickness of stiffener	t_{stiff}	1.3	4.0
Height of stiffener	h_{stiff}	8.0	40.0
Thickness of midspan	t_{mid}	1.3	3.0

b) Discussion of results

The effect of variety of midspan thickness on critical buckling load is investigated. Two types of optimization is performed. First is size optimization with three design variables (t_{skin} - t_{stiff} - t_{mid}). Second one is shape optimization with four design variables (t_{skin} - t_{stiff} - t_{mid} - h_{stiff}). The effect of number of stiffeners is also examined.

i) Size optimization: Thicknesses of plate skin, stiffeners and midspan are kept equal at initial design. Height of stiffeners has constant value of 28 mm in this stage. Optimum values of design variables, obtained maximum critical buckling loads and improvements are given in Table 5.25. The highest improvement is obtained from four stiffeners case and it is 18.43 %. The highest critical buckling load also is gained from eight stiffeners case and it has a value of 239809 N. The improvement according to number of stiffeners is 701 % when compared two stiffeners case. In optimum solutions, skin is thinner than stiffeners

Table 5.25 Size optimization of straight stiffened plate with linearly varying skin

n_{stiff}	Optimum DVs values			Buckling loads		Imp
	t_{skin}	t_{stiff}	t_{mid}	P_i	P_{max}	(%)
2	2.90	1.30	1.30	27392.7	29937.4	9.29
3	2.24	3.85	1.30	59731.7	67954.5	13.77
4	2.84	1.58	1.30	97565.0	115546.1	18.43
5	2.47	1.64	1.65	136548.5	158121.9	15.80
6	2.49	1.76	1.30	173160.7	199366.6	15.13
7	2.38	1.67	1.30	202204.2	228295.0	12.90
8	2.12	1.77	1.30	219819.9	239809.4	9.09

ii) Shape optimization: In addition to size optimization design variables height of stiffeners are included in optimization process. Optimum values of design variables, obtained maximum critical buckling loads and improvements are given in Table 5.26. The highest improvement is obtained from four stiffeners case and it is 59.25 %. The highest critical buckling load also is obtained from eight stiffeners case and it has a value of 350065 N. The improvement according to number of stiffeners is 998 % when compared two stiffeners case.

In optimum solutions, skin is thinner than stiffeners in all cases and stiffener thicknesses are going to be thicker and reach to upper limits.

Table 5.26 Shape optimization of straight stiffened plate with linearly varying skin with four design variables

n_{stiff}	Optimum DVs values				Buckling loads		Imp
	t_{skin}	t_{stiff}	t_{mid}	h_{stiff}	P_i	P_{max}	(%)
2	2.92	3.99	1.30	8.00	27392.7	31879.6	16.38
3	2.96	4.00	1.42	8.00	59731.7	76056.0	27.33
4	3.00	4.00	1.30	8.28	97565.1	130642.2	33.90
5	2.65	4.00	1.30	12.15	136548.4	204380.6	49.68
6	2.61	4.00	1.30	10.99	173160.7	263954.9	52.43
7	2.80	4.00	1.30	8.00	202204.2	305203.5	50.94
8	2.69	4.00	1.30	8.00	219819.9	350065.4	59.25

Both optimizations gave similar results in small number of stiffeners as shown in Figure5.18.

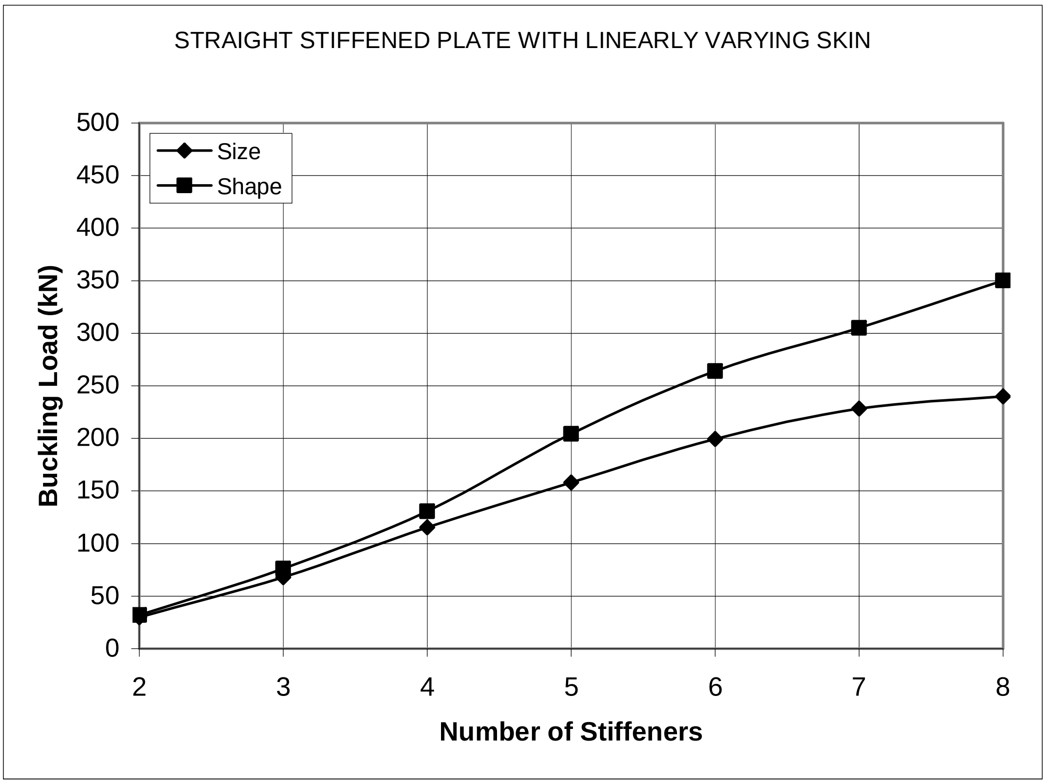

Figure 5.18 Comparison of size and shape optimizations

Optimum thickness results shows that midspan thicknesses are thinner than plate skin thickness. Because of the less buckling risk in the midspan is than the stiffener joining points, midspan thickness is going to be thinner. The difference for higher number of stiffeners between size and shape optimization results as shown Figure 5.18 is based on stiffeners' height. Shape optimization adds some of height to stiffener thickness and plate thickness.

5.2.1.8 Straight stiffened plate with linearly varying skin and pads under stiffeners

Varying plate skin with pads under stiffeners is considered and Figure 5.19 illustrates straight stiffened plate with linearly varying skin and pads under stiffeners.

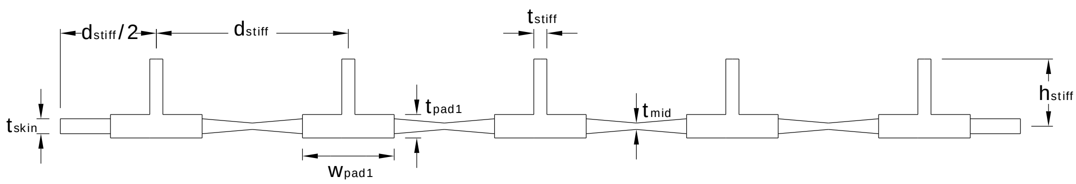

Figure 5.19 Straight stiffened plate with linearly varying skin and pads under stiffeners

a) Optimization Process

i) Size optimization: Optimization is carried out using thickness of plate skin (t_{skin}), thickness of stiffeners (t_{stiff}), thickness of pads (t_{pad1}) and thickness of midspan. (t_{mid}). Height of main stiffeners (h_{stiff}) and width of pads (w_{pad1}) have constant values of 28,0mm and $d_{stiff}/4$ in this stage (See Figure 5.19).

ii) Shape optimization: Height of stiffeners (h_{stiff}) is included as design variable in this stage. Width of pads (w_{pad1}) has still constant value of $d_{stiff}/4$ (See Figure 5.19).

iii) Shape optimization: Width of pads (w_{pad1}) is included as a design variable in this stage. (Figure 5.19)

Design constraints of three stages are specified in Table 5.27.Optimization process is carried out for two to eight stiffeners

Table 5.27 Design constraints of straight stiffened plate with linearly varying skin and pads under stiffeners

		Min (mm)	Max (mm)
Thickness of plate	t_{skin}	1.4	3.0
Thickness of stiffener	t_{stiff}	1.3	4.0
Height of stiffener	h_{stiff}	8.0	40.0
Thickness of pad	t_{pad1}	2.0	5.0
Width of pad	w_{pad1}	$d_{stiff}/10$	$d_{stiff}/2$
Thickness of midspan	t_{mid}	1.3	3.0

b) Discussion of results

The effect of variety of midspan thickness on stiffened plate with pads is examined. Three types of optimization is performed. First, size optimization with four design variables (t_{skin}-t_{stiff}-t_{mid}-t_{pad1}). Second shape optimization with five design variables (t_{skin}-t_{stiff}-t_{mid}-t_{pad1}-h_{stiff}). Third is shape optimization with six design variables (t_{skin}-t_{stiff}-t_{mid}-t_{pad1}-h_{stiff}-w_{pad1}). The effect of number of stiffeners is also examined.

i) Size optimization: Thicknesses of plate skin, stiffeners and midspan are kept equal and thickness of pads is kept two times of thickness of plate skin at initial design. Height of stiffeners and width of pads have constant values of 28 mm and $d_{stiff}/4$ respectively. Optimum values of design variables, obtained maximum critical buckling loads and improvements are given in Table 5.28. The highest improvement is obtained from three stiffeners case and it is 17.58 %. The highest critical buckling load also is obtained from eight stiffeners case and it has a value of 264873 N. The improvement according to number of stiffeners is 564 % when compared two stiffeners case.

In optimum solutions, skin thickness and pad thicknesses are going to be thinner and thickness of midspan reach lower limits.

Table 5.28 Size optimization of straight stiffened plate with linearly varying skin and pads under stiffeners

n_{stiff}	Optimum DVs values				Buckling loads		Imp
	t_{skin}	t_{stiff}	t_{mid}	t_{pad1}	P_i	P_{max}	(%)
2	1.96	1.30	1.30	4.62	34585.9	39866.6	15.27
3	1.88	1.33	1.30	4.57	72801.6	85603.6	17.58
4	1.81	1.58	1.30	4.20	119179.1	136780.9	14.77
5	1.71	1.67	1.30	3.88	167848.9	187263.3	11.57
6	1.60	1.71	1.30	3.61	213108.2	229069.6	7.49
7	1.42	1.69	1.30	3.55	236188.5	259531.6	9.88
8	1.40	1.68	1.30	3.17	242591.5	264874.0	9.19

ii) Shape optimization: In addition to size optimization design variables height of stiffeners is included in optimization process. Width of pads still has constant value of $d_{stiff}/4$. Optimum values of design variables, obtained maximum critical buckling loads and improvements are given in Table 5.29. The highest improvement is gained from eight stiffeners case and it is 102.53 %. The highest critical buckling load also is obtained from eight stiffeners case and it has a value of 491331 N. The improvement according to number of stiffeners is 1081 % when compared two stiffeners case.

In all cases, skin is thinner than stiffeners and skin thickness, skin and pads are going to be thinner, and stiffener is going to be thicker by the increasing of number of stiffeners. Midspan thickness and height of stiffeners reacht lower limit in all cases.

Table 5.29 Shape optimization of Straight stiffened plate with linearly varying skin and pads under stiffeners with five design variables

n_{stiff}	Optimum Dvs values					Buckling loads		Imp
	t_{skin}	t_{stiff}	t_{mid}	t_{pad1}	h_{stiff}	P_i	P_{max}	(%)
2	2.06	2.65	1.30	4.67	8.00	34585.9	41569.6	20.19
3	2.01	3.04	1.30	4.68	8.00	72801.6	91732.3	26.00
4	1.98	3.13	1.30	4.58	8.00	119179.1	156235.0	31.09
5	1.92	2.94	1.30	4.57	8.00	167848.9	231770.2	38.08
6	1.89	3.28	1.30	4.28	8.00	213108.2	315884.6	48.23
7	1.87	3.68	1.30	3.90	8.00	236188.5	401023.0	69.79
8	1.72	3.72	1.30	3.89	8.00	242591.5	491331.6	102.53

iii) Shape optimization: in addition to previous shape optimization's design variables, width of pads is included in optimization process. Optimum values of design variables, obtained maximum critical buckling loads and improvements are given in Table 5.30. The highest improvement is obtained from eight stiffeners case and it is 106.44 %. The highest critical buckling load also is gained from eight stiffeners case and it has a value of 500801 N. The improvement according to number of stiffeners is 994 % when compared two stiffeners case.

In optimum solutions, skin is thinner than stiffeners and skin and pads are going to be thinner nevertheless, stiffeners are going to be thicker by the increasing of number of stiffeners. Midspan thickness and height of stiffeners reach lower limits in all cases.

Table 5.30 Shape optimization of straight stiffened plate with linearly varying skin and pads under stiffeners six design variables

n_{stiff}	Optimum DVs values						Buckling loads		Imp
	t_{skin}	t_{stiff}	t_{mid}	t_{pad1}	h_{stiff}	w_{pad1}	P_i	P_{max}	(%)
2	1.46	2.66	1.30	3.71	8.00	110.00	34585.9	45765.4	32.32
3	1.42	2.63	1.30	3.66	8.00	73.33	72801.5	97877.6	34.44
4	1.43	2.85	1.30	3.53	8.00	55.00	119179.1	165164.9	38.59
5	1.40	3.22	1.30	3.38	8.00	44.00	167848.9	243720.9	45.20
6	1.40	3.59	1.30	3.24	8.00	35.54	213108.2	325627.4	52.80
7	1.40	4.00	1.30	3.15	8.00	28.02	236188.4	409495.2	73.38
8	1.40	4.00	1.30	3.35	8.00	20.00	242591.5	500801.0	106.44

In two and three stiffeners case all optimization types gave very close results as shown in Figure 5.20. In following stiffeners case shape optimizations gave higher results as shown, but they are very close each other. Observing Figure 5.20, it is obviously seen that height of stiffeners creates the difference between size and first shape optimization cases. Again, here the effect of pads under stiffeners can be seen clearly.

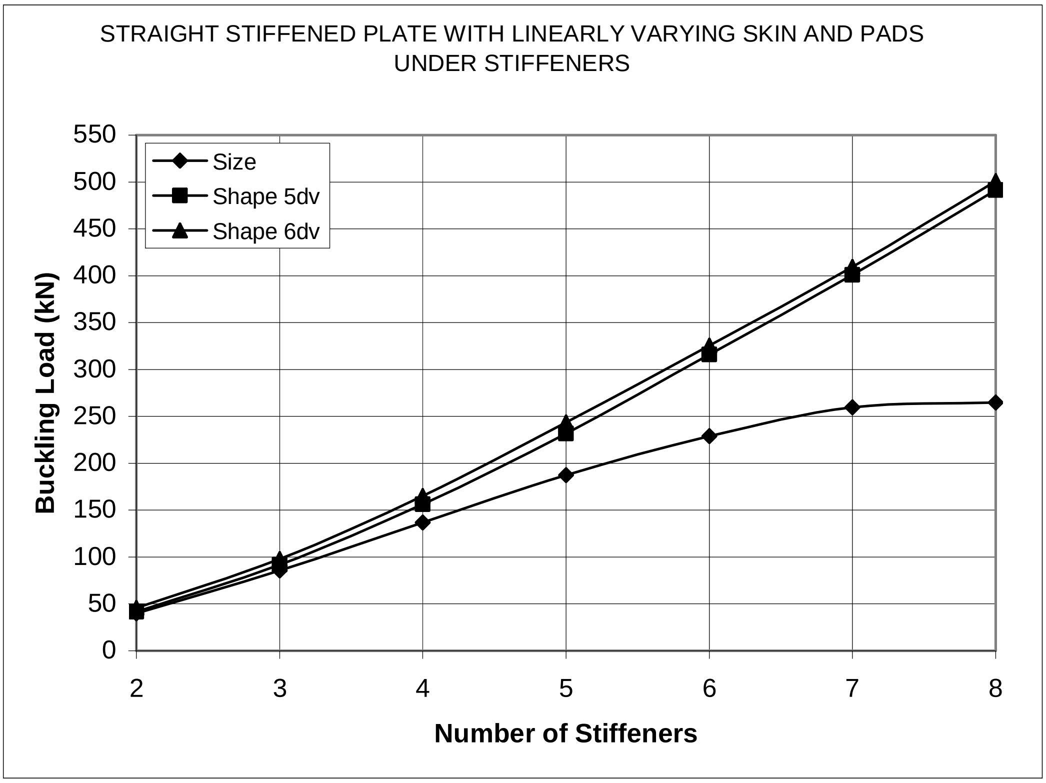

Figure 5.20 Comparison of size and shape optimizations

5.2.2 T Shaped Stiffeners

5.2.2.1 T shaped stiffened plate

Figure 5.21 shows T shaped stiffened plates.

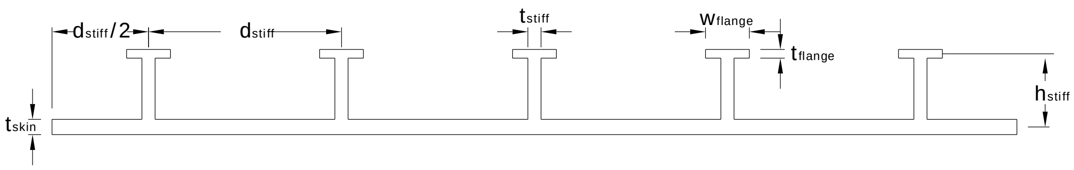

Figure 5.21 T shaped stiffened plate.

a) Optimization Process:

i) Size optimization: Optimization is carried out using thickness of plate skin (t_{skin}), thickness of stiffeners (t_{stiff}) and thickness of flange (t_{flange}). Height of stiffeners (h_{stiff}) and width of flanges (w_{flange}) have constant values of 28.0mm and 14.0mm in this stage (See Figure 5.21).

ii) Shape optimization: Height of sub stiffeners (h_{stiff}) included as design variable in this stage. Width of flanges (w_{flange}) still has constant value of 14.0mm in this stage (See Figure 5.21).

iii) Shape optimization: Width of flanges (w_{flange}) included as design variable in this stage (See Figure 5.21).

b) Discussion of results

The effect of T shaped stiffeners is examined in this type of plates. Three types of optimizations are performed. First one is size optimization with three design variables (t_{skin} - t_{stiff} - t_{flange}), second is shape optimization with four design variables (t_{skin} - t_{stiff} - t_{flange} - h_{stiff}) and the third one is shape optimization with five design variables (t_{skin} - t_{stiff} - t_{flange} - h_{stiff} - w_{flange}). The effect of number of stiffeners also examined.

Design constraints of three stages are specified in Table 5.31.Optimization process is carried out for two to eight stiffeners.

Table 5.31 Design Constraints of T shaped stiffened plate.

		Min (mm)	Max (mm)
Thickness of plate	t_{skin}	1.4	3.0
Thickness of stiffener	t_{stiff}	1.3	4.0
Height of stiffener	h_{stiff}	8.0	40.0
Thickness of flange	t_{flange}	1.0	4.0
Width of flange	w_{flange}	7.0	30.0

i) Size optimization: Thickness of plate, stiffeners and flanges are kept equal in initial design. The height of stiffeners and width of flanges are kept constant during this stage and they have values of 28.0mm and 14.0mm. The optimum values of design variables and critical buckling loads are given in Table 5.32. The highest improvement is obtained from seven stiffeners case and the improvement is approximately 20.55 %. The highest critical buckling load is obtained from eight stiffeners case and equal to 276425 N. The improvement of this case is 763 % compared with two stiffeners case. In optimum solutions, except two stiffeners case skin is thicker than stiffeners and flanges.

Also skin and stiffeners are going to be thinner and stiffeners reach lower limit by the increasing of number of stiffeners. Flanges are going to be reach lower limit too.

Table 5.32 Size optimization of T shaped stiffened plate

n_{stiff}	Optimum DVs values			Buckling loads		Imp
	t_{skin}	t_{stiff}	t_{flange}	P_i	P_{max}	(%)
2	2.16	2.81	2.25	31231.4	32020.4	2.52
3	2.24	1.66	1.10	63338.4	66268.0	4.62
4	2.20	1.30	1.00	98362.5	108236.8	10.04
5	2.09	1.30	1.00	132117.4	152763.4	15.62
6	1.98	1.30	1.00	166034.3	197633.2	19.03
7	1.86	1.30	1.00	198690.2	239519.9	20.55
8	1.75	1.30	1.00	230322.6	276425.9	20.017

ii) Shape optimization: In addition to thicknesses of plate, stiffeners and flanges, height of stiffeners are included in optimization process as a design variable. Still with of flanges are kept constant in this stage. The optimum values of design variables and critical buckling loads are presented in Table 5.33. The highest improvement is gained from eight stiffeners case and it is approximately 56.60 %. Also the largest critical buckling load is obtained from eight stiffeners case and it is equal to 360676 N. The improvement of critical buckling load is about 1026 % compared to two stiffeners case.

In optimum solutions, except two stiffeners case skin is thicker than stiffeners and flanges. Skin is going to be thinner by the increasing of number of stiffeners. Height of stiffeners begins almost initial value by two stiffeners case and reach near to lower limit in eight stiffeners case.

Table 5.33 Shape optimization of T shaped stiffened plate with four design variables

n_{stiff}	Optimum DVs values				Buckling loads		Imp
	t_{skin}	t_{stiff}	t_{flange}	h_{stiff}	P_i	P_{max}	(%)
2	2.16	2.89	2.30	27.29	31231.48	32028.64	2.55
3	2.20	2.11	1.80	20.23	63338.41	67349.93	6.33
4	2.27	1.54	1.11	18.14	98362.50	115764.81	17.69
5	2.10	2.21	1.26	14.57	132117.41	169867.32	28.57
6	2.04	2.65	1.00	11.97	166034.29	234487.83	41.22
7	1.90	3.05	1.22	10.13	198690.27	295376.08	48.66
8	1.82	3.06	1.37	8.88	230322.64	360676.41	56.59

iii) Shape optimization: In addition to previous design variables width of flanges included as a design variable. The optimum values of design variables and critical buckling loads are presented in Table 5.34. The highest improvement is gained from eight stiffeners case and it is approximately 60.50 %. Largest critical buckling load also is obtained from eight stiffeners case and the plate has a critical buckling load of 369668 N. The improvement is 1018 % compared with two stiffeners case. Height of stiffeners begins with almost initial value in two stiffeners case and reach lower limit in eight stiffeners case.

Table 5.34 Shape optimization of T shaped stiffened plate with five design variables

n_{stiff}	Optimum DVs values					Buckling loads		Imp
	t_{skin}	t_{stiff}	t_{flange}	h_{stiff}	w_{flange}	P_i	P_{max}	(%)
2	2.20	2.90	2.82	27.82	7.00	31231.4	33051.7	5.82
3	2.22	2.30	2.08	21.80	7.00	63338.4	68804.5	8.63
4	2.17	2.03	1.00	12.53	29.26	98362.5	120354.4	22.35
5	2.11	2.21	1.00	11.95	21.99	132117.4	175317.0	32.69
6	1.99	2.82	1.00	10.06	20.89	166034.3	239166.5	44.04
7	1.920	2.91	1.20	9.70	15.39	198690.2	297913.3	49.93
8	1.95	4.00	1.00	8.00	7.00	230322.6	369668.3	60.50

Shape optimizations gave better results as shown in Figure 5.22. But at small number of stiffeners critical buckling loads are approximately same for all type of optimizations. Also two type shape optimizations almost gave same results.

Reference to this, there is almost no effect of width of flanges to critical buckling load capacity in this limits of widths.

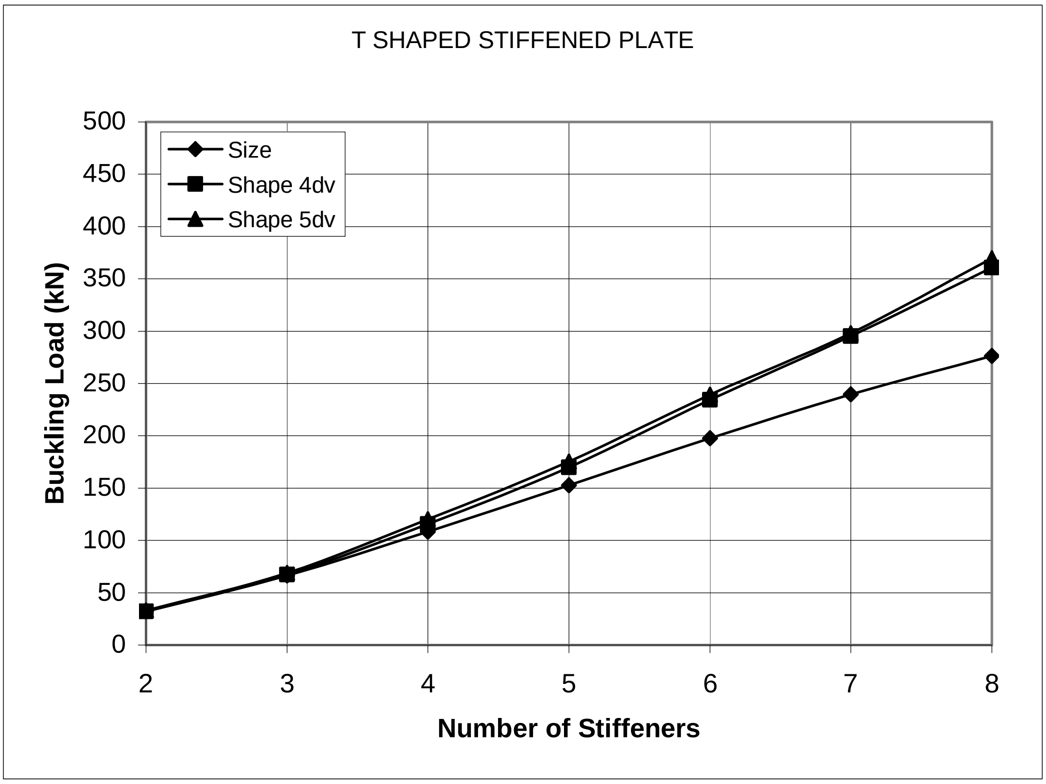

Figure 5.22 Comparison of size and shape optimizations

5.2.2.2 T shaped stiffened plate with substiffeners

Substiffeners are attached between T shaped stiffeners and Figure 5.23 shows T shaped stiffened plate wit substiffeners.

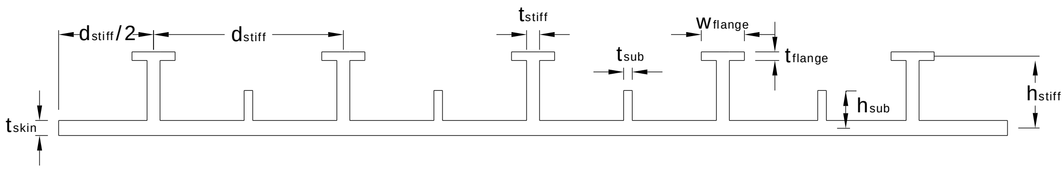

Figure 5.23 T shaped stiffened plate with substiffeners

a) Optimization Process:

i) Size optimization: Optimization performed using thickness of plate skin (t_{skin}), thickness of stiffeners (t_{stiff}), thickness of substiffeners (t_{sub}) and thickness of flange (t_{flange}). Height of stiffeners (h_{stiff}), height of substiffeners (h_{sub}) and width of flanges (w_{flange}) have constant values of 28.0mm, 14.0mm and 14.0mm in this stage (See Figure 5.23).

ii) *Shape optimization:* Height of stiffeners (h_{stiff}) and height of substiffeners (h_{sub}) included as design variables in this stage. Width of flanges (w_{flange}) still has constant value of 14.0mm in this stage (See Figure 5.23).

iii) *Shape optimization:* Width of flanges (w_{flange}) included as design variable in this stage (See Figure 5.23).

Design constraints of three stages are specified in Table 5.35Optimization process is carried out for two to eight stiffeners.

Table 5.35 Design Constraints of T shaped stiffened plate with substiffeners

		Min (mm)	Max (mm)
Thickness of plate	t_{skin}	1.4	3.0
Thickness of stiffener	t_{stiff}	1.3	4.0
Thickness of substiffeners	t_{sub}	1.0	3.0
Height of stiffener	h_{stiff}	8.0	40.0
Height of substiffeners	h_{sub}	5.0	20.0
Thickness of flange	t_{flange}	1.0	4.0
Width of flange	w_{flange}	7.0	30.0

b) Discussion of results

The effect of substiffeners between stiffeners to critical buckling load are examined in this type of plates. Three types of optimizations are performed in this type of plates. First one is size optimization with four design variables (t_{skin} - t_{stiff} - t_{sub} - t_{flange}),second is shape optimization with six design variables (t_{skin} - t_{stiff} - t_{sub} - t_{flange} -

h_{stiff} - h_{sub}) and the third one is shape optimization with seven design variables (t_{skin} - t_{stiff} - t_{sub} - t_{flange} - h_{stiff} - h_{sub} - w_{flange}). The effect of number of stiffeners also examined.

i) Size optimization: Thickness of plate and stiffeners are kept equal in initial design. Thicknesses of substiffeners and flanges are kept 0.75 times of thickness of plate. The height of stiffeners, substiffeners and width of flanges are kept constant during this stage and they have values of 28.0mm, 14.0mm and 14.0mm. The optimum values of design variables and critical buckling loads are given in Table 5.36. The highest improvement is obtained from five stiffeners case and the improvement is approximately 17.65 %. The highest critical buckling load is gained from eight stiffeners case and equal to 239774 N. The improvement of this case is 587 % compared with two stiffeners case.

In all cases, skin is thicker than stiffeners. Also stiffeners reach lower limit in all cases. Thicknesses of substiffeners and flanges reach lower limit after two stiffeners case.

Table 5.36 Size optimization of T shaped stiffened plate with substiffeners

n_{stiff}	Optimum Dvs values				Buckling loads		Imp (%)
	t_{skin}	t_{stiff}	t_{sub}	t_{flange}	P_i	P_{max}	
2	2.37	1.30	1.83	1.11	33271.0	34858.2	4.77
3	2.25	1.30	1.00	1.00	63354.9	70222.8	10.84
4	2.11	1.30	1.00	1.00	95997.8	110315.7	14.91
5	1.96	1.30	1.00	1.00	127883.6	150454.3	17.65
6	1.82	1.30	1.00	1.00	159035.8	186373.9	17.19
7	1.67	1.30	1.00	1.00	187911.6	216445.5	15.18
8	1.52	1.30	1.00	1.00	218803.6	239774.7	9.58

ii) Shape optimization: In addition to thicknesses of plate, stiffeners, substiffeners and flanges, height of stiffeners and height of substiffeners are included in optimization process as design variables. Still width of flanges is kept constant in this stage. The optimum values of design variables and critical buckling loads are presented in Table 5.37. The highest improvement is obtained from eight stiffeners case and it is approximately 57.40 %. Also the largest critical buckling load is obtained from eight stiffeners case and it is equal to 344416 N. The improvement of critical buckling load is about 877 % compared to two stiffeners case.

Skin and substiffener thicknesses are going to be thinner, stiffener thicknesses are going to be thicker and height of stiffeners decreases by the increasing of number of stiffeners.

Table 5.37 Shape optimization of T shaped stiffened plate with substiffeners with six design variables

n_{stiff}	Optimum Dvs values						Buckling loads		Imp
	t_{skin}	t_{stiff}	t_{sub}	t_{flange}	h_{stiff}	h_{sub}	P_i	P_{max}	(%)
2	2.42	1.30	2.37	1.00	25.66	5.00	33271.0	35223.1	5.86
3	2.34	1.30	2.00	1.00	21.09	5.00	63354.9	73033.5	15.27
4	2.23	1.58	1.22	1.02	17.51	5.57	95997.8	118680.3	23.63
5	2.10	2.19	1.20	1.07	13.69	5.00	127883.6	170137.8	33.04
6	2.01	2.65	1.00	1.00	11.12	5.00	159035.8	228012.9	43.37
7	1.87	2.90	1.00	1.15	10.17	5.00	187911.6	288157.5	53.34
8	1.75	2.82	1.00	1.25	9.81	5.45	218803.6	344416.7	57.40

iii) Shape optimization: In addition to previous design variables width of flanges included as a design variable. The optimum values of design variables and critical buckling loads are presented in Table 5.38. The highest improvement is obtained from eight stiffeners case and it is approximately 61.58 %. Largest critical buckling load also is gained from eight stiffeners case and the plate has a critical buckling load of 353532 N. The improvement is 884 % compared with two stiffeners case.

Skin is and substiffeners are going to be thinner and stiffeners are going to be thicker, also height of stiffeners decreases by the increasing of number of stiffeners. Height of substiffeners reach lower limit in all cases.

Shape optimizations gave better results compared with size optimizations as shown in Figure 5.24. There are no large differences between six and seven design variables. They are approximately equal to each other as shown in Figure 16. This means that width of flange in these limits has no large effect to critical buckling load.

Table 5.38 Shape optimization of T shaped stiffened plate with substiffeners with seven design variables

n_{stiff}	Optimum DVs values							Buckling loads		Imp (%)
	t_{skin}	t_{stiff}	t_{sub}	t_{flange}	h_{stiff}	h_{sub}	w_{flange}	P_i	P_{max}	
2	2.41	1.30	2.57	1.37	31.19	5.00	7.00	33271.1	35902.8	7.91
3	2.36	1.30	2.00	1.00	23.98	5.00	7.00	63354.9	73557.4	16.10
4	2.25	1.59	2.13	1.14	18.72	5.00	7.09	95997.8	119000.5	23.96
5	2.16	1.88	1.66	1.22	15.33	5.00	7.00	127883.6	171631.2	34.21
6	2.08	2.24	1.00	1.34	12.25	5.00	7.96	159035.8	228378.1	43.60
7	1.88	2.80	1.00	1.13	9.64	5.00	15.55	187911.6	290455.4	54.57
8	1.81	2.70	1.00	1.30	9.43	5.00	12.84	218803.6	353532.9	61.58

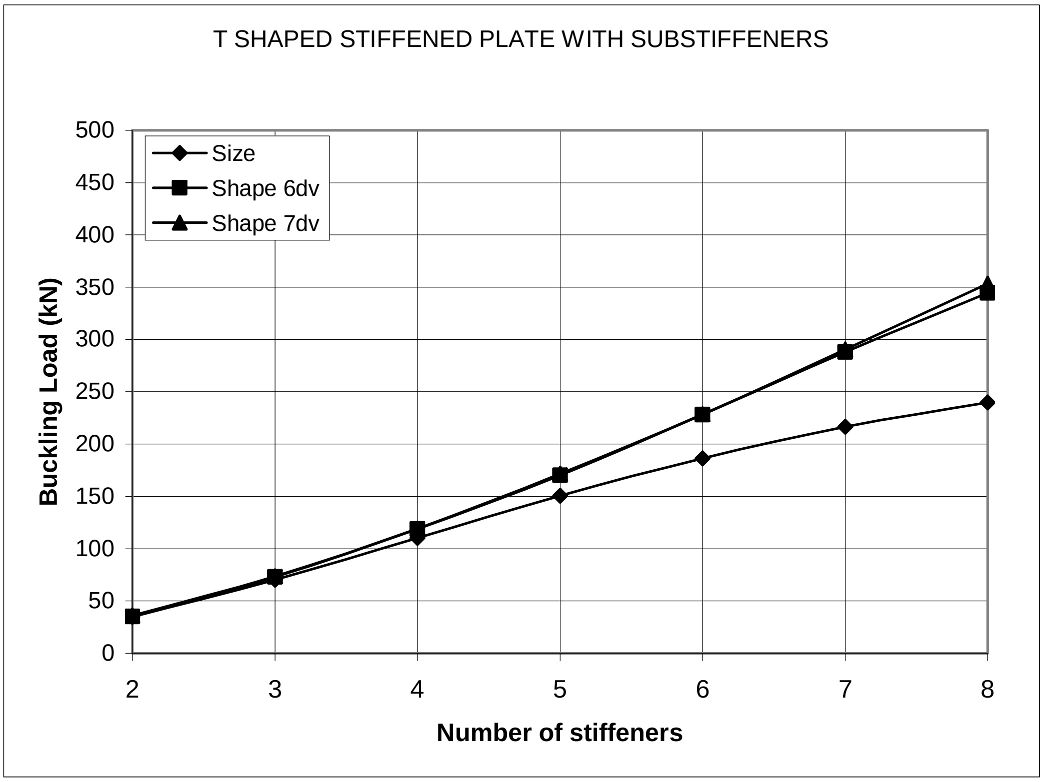

Figure 5.24 Comparison of size and shape optimizations

5.2.2.3 T shaped stiffened plate and pads under stiffeners

Figure 5.25 illustrates T shaped stiffened plate and pads under stiffeners.

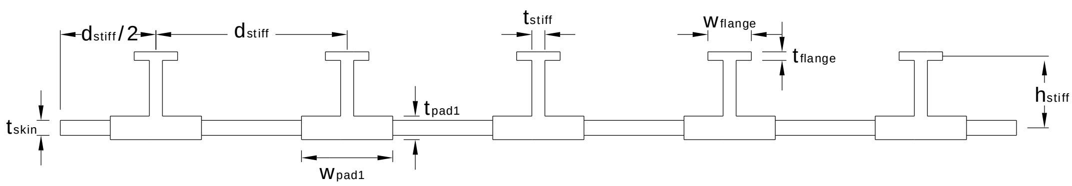

Figure 5.25 T shaped stiffened plate and pads under stiffeners

a) Optimization Process:

i) Size optimization: Optimization is performed using thickness of plate skin (t_{skin}), thickness of stiffeners (t_{stiff}) ,thickness of pads (t_{pad1}) and thickness of flange (t_{flange}). Height of stiffeners (h_{stiff}), width of pads (w_{pad1}) and width of flanges (w_{flange}) have constant values of 28.0mm, $d_{stiff}/4$ and 14.0mm (See Figure 5.25).

ii) Shape optimization: Height of stiffeners (h_{stiff}) included as design variables in this stage. Width of pads (w_{pad1}) and width of flanges (w_{flange}) still have constant value of $d_{stiff}/4$ and 14.0mm in this stage (See Figure 5.25).

i) Shape optimization: Width of pad (w_{pad1}) and width of flanges (w_{flange}) included as design variable in this stage (See Figure 5.25).

Design constraints of three stages are specified in Table 5.39. Optimization process is carried out for two to eight stiffeners.

Table 5.39 Design Constraints of T shaped stiffened plate and pads under stiffeners

		Min (mm)	Max (mm)
Thickness of Plate	t_{skin}	1.4	3.0
Thickness of stiffener	t_{stiff}	1.3	4.0
Height of stiffener	h_{stiff}	8.0	40.0
Thickness of Pad	t_{pad1}	2.0	5.0
Width of Pad	w_{pad1}	$d_{stiff}/10$	$d_{stiff}/2$
Thickness of Flange	t_{flange}	1.0	4.0
Width of Flange	w_{flange}	7.0	14.0

b) Discussion of results

Effect of pads under the T shaped stiffeners examined during this case. Three type optimizations are performed. First one is size optimization with four design variables (t_{skin} - t_{stiff} - t_{flange} - t_{pad1}), second is shape optimization with five design variables (t_{skin} -

$t_{stiff} - t_{flange} - t_{pad1} - h_{stiff}$) and the third one is shape optimization with seven design variables ($t_{skin} - t_{stiff} - t_{flange} - t_{pad1} - h_{stiff} - w_{flange} - w_{pad1}$). The effect of number of stiffeners also examined.

i) Size optimization: Thickness of plate and stiffeners are kept equal in initial design. Thicknesses of pads and flanges are kept 1.25 and 0.75 times of thickness of plate. The height of stiffeners, width of pads and width of flanges are kept constant during this stage and they have values of 28.0mm , $d_{stiff}/4$ and 14.0mm. The optimum values of design variables and critical buckling loads are given in Table 5.40. The highest improvement is obtained from seven stiffeners case and the improvement is approximately 19.82 %. The highest critical buckling load is obtained from eight stiffeners case and equal to 314117 N. The improvement of this case is 766 % compared with two stiffeners case.

Skin is thicker than stiffeners in all cases in all cases. Also stiffener thicknesses and flange thicknesses reach lower limit in all cases. Skin and pads are going to be thinner by the increasing of number of stiffeners.

Table 5.40 Size optimizations of T shaped stiffened plate and pads under stiffeners

n_{stiff}	Optimum DVs values				Buckling loads		Imp
	t_{skin}	t_{stiff}	t_{pad1}	t_{flange}	P_i	P_{max}	(%)
2	1.82	1.30	4.28	1.00	31996.5	36270.9	13.35
3	1.84	1.30	3.74	1.00	67240.3	76014.4	13.04
4	1.70	1.30	3.72	1.00	106012.8	122257.2	15.32
5	1.66	1.30	3.39	1.00	145364.8	170937.7	17.59
6	1.56	1.30	3.22	1.00	184835.5	219707.9	18.86
7	1.42	1.30	3.17	1.00	222692.2	266843.7	19.82
8	1.40	1.30	2.79	1.00	263238.4	314117.2	19.32

ii) Shape optimization: In addition to thicknesses of plate, stiffeners, pads and flanges, height of stiffeners is included in optimization process as a design variable. Still width of pads and width of flanges are kept constant in this stage. The optimum values of design variables and critical buckling loads are presented in Table 5.41. The highest improvement is gained from eight stiffeners case and it is approximately 63.20 %. Also the largest critical buckling load is obtained from eight stiffeners case and it is equal to 429679 N. The improvement of critical buckling load is about 1041 % compared to two stiffeners case.

In optimum solutions, skin and pads are going to be thinner and stiffeners are going to be thicker by the increasing of number of stiffeners. Flange thicknesses reach lower limit in all cases.

Table 5.41 Shape optimizations of T shaped stiffened plate and pads under stiffeners with five design variables

n_{stiff}	Optimum DVs values					Buckling loads		Imp
	t_{skin}	t_{stiff}	t_{pad1}	t_{flange}	h_{stiff}	P_i	P_{max}	(%)
2	1.88	1.30	4.49	1.00	10.51	31996.5	37627.5	17.59
3	1.86	1.64	4.25	1.00	9.88	67240.3	81129.1	20.65
4	1.75	1.83	4.32	1.02	8.38	106012.8	135548.8	27.86
5	1.77	2.29	3.66	1.00	10.02	145364.8	197721.4	36.01
6	1.73	2.47	3.59	1.00	8.08	184835.5	270460.3	46.32
7	1.65	2.74	3.40	1.00	8.00	222692.2	345538.5	55.16
8	1.50	2.93	3.42	1.00	8.00	263238.4	429679.8	63.22

iii) Shape optimization: In addition to previous design variables width of pads and width of flanges included as design variables. The optimum values of design variables and critical buckling loads are presented in Table 5.42. The highest improvement is obtained from eight stiffeners case and it is approximately 79.15 %. Largest critical buckling load also is obtained from eight stiffeners case and the plate has a critical buckling load of 471665 N. The improvement is 959 % compared with two stiffeners case.

In optimum solutions, pads are going to be thinner by the increasing of number of stiffeners. Height of stiffeners reaches almost lower limits in all cases.

Table 5.42 Shape optimizations of T shaped stiffened plate and pads under stiffeners with seven design variables

n_{stiff}	Optimum DVs values							Buckling loads		Impr (%)
	t_{skin}	t_{stiff}	t_{pad1}	t_{flange}	h_{stiff}	w_{flange}	w_{pad1}	P_i	P_{max}	
2	1.42	2.22	3.67	1.29	8.00	7.00	110.00	31996.5	44541.9	39.20
3	1.40	1.73	3.62	1.00	8.54	8.28	73.33	67240.3	96747.3	43.88
4	1.40	2.19	3.48	1.00	8.00	7.00	54.93	106012.8	162340.7	53.13
5	1.48	2.11	3.36	1.38	8.65	7.00	40.70	145364.8	229640.9	57.97
6	1.40	2.88	3.10	1.00	8.00	7.00	36.67	184835.5	313354.9	69.532
7	1.40	3.02	2.93	1.36	8.00	7.00	29.83	222692.2	387255.0	73.89
8	1.40	2.75	2.89	1.74	8.00	7.00	23.66	263238.4	471665.5	79.17

Shape optimizations gave better results compared with size optimizations as shown in Figure 5.26.

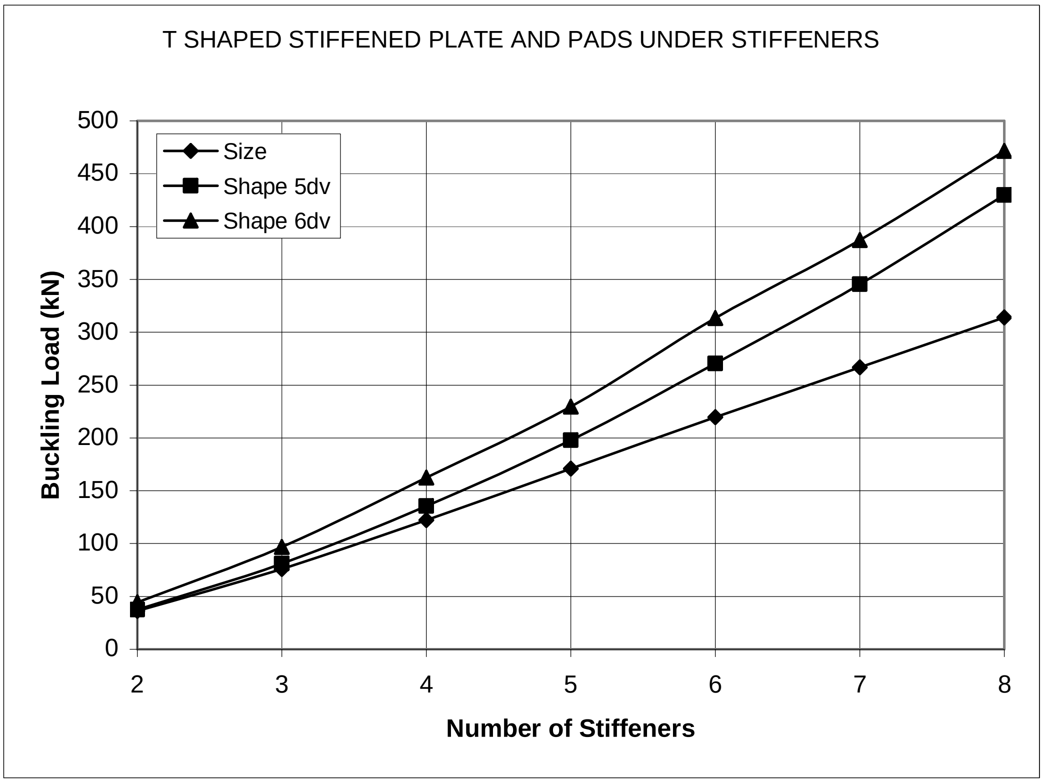

Figure 5.26 Comparison of size and shape optimizations

Size optimizations and shape optimization with five design variables gave similar results for small number of stiffeners. But size optimization with seven design variables gave higher critical buckling loads starting with small number of stiffeners. So the effect of width of pads is seen clearly.

5.2.2.4 T shaped stiffened plate with substiffeners and pads under stiffeners

Pads are added under stiffeners, substiffeners are attached between stiffeners, and Figure 5.27 shows T shaped stiffened plate with substiffeners and pads under stiffeners.

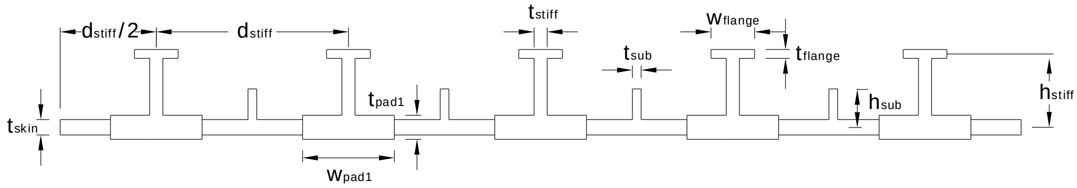

Figure 5.27 T shaped stiffened plate with substiffeners and pads under stiffeners

a) Optimization Process:

i) Size optimization: Optimization is carried out using thickness of plate skin (t_{skin}), thickness of stiffeners (t_{stiff}), thickness of substiffeners (t_{sub}), thickness of pads (t_{pad1}) and thickness of flange (t_{flange}). Height of stiffeners (h_{stiff}), height of substiffeners (h_{sub}), width of pad (w_{pad1}) and width of flanges (w_{flange}) have constant values of 28.0mm, 14.0mm, $d_{stiff}/4$ and 14.0mm in this stage (See Figure 5.27).

ii) Shape optimization: Height of stiffeners (h_{stiff}), height of substiffeners (h_{sub}) included as design variables in this stage. Width of pads (w_{pad1}) and width of flanges (w_{flange}) still have constant value of $d_{stiff}/4$ and 14.0mm in this stage (See Figure 5.27).

iii) Shape optimization: Width of pads (w_{pad1}) and width of flanges (w_{flange}) included as design variable in this stage (See Figure 5.27).

Design constraints of three stages are specified in Table5.43. Optimization process is carried out for two to eight stiffeners.

Table 5.43 Design Constraints of T shaped stiffened plate with substiffeners and pads under stiffeners

		Min (mm)	Max (mm)
Thickness of plate	t_{skin}	1.4	3.0
Thickness of stiffener	t_{stiff}	1.3	4.0
Height of stiffener	h_{stiff}	8.0	40.0
Thickness of substiffeners	t_{sub}	1.0	3.0
Height of substiffeners	h_{sub}	5.0	20.0
Thickness of pad	t_{pad1}	2.0	5.0
Width of pad	w_{pad1}	$d_{stiff}/10$	$d_{stiff}/2$
Thickness of flange	t_{flange}	1.0	4.0
Width of flange	w_{flange}	7.0	30.0

b) Discussion of results

Effect of substiffeners and pads are examined together in this type of stiffened plates. Three types of optimizations are performed. First one is size optimization with five design variables (t_{skin} - t_{stiff} - t_{sub} - t_{flange} - t_{pad1}), second is shape optimization with seven design variables (t_{skin} - t_{stiff} - t_{sub} - t_{flange} - t_{pad1} - h_{stiff} - h_{sub}) and the third one is shape optimization with nine design variables (t_{skin} - t_{stiff} - t_{sub} - t_{flange} - t_{pad1} - h_{stiff} - h_{sub} - w_{pad1} - w_{flange}). The effect of number of stiffeners also examined.

i) Size optimization: Thickness of plate and stiffeners are kept equal in initial design. Thicknesses of pads, substiffeners and flanges are kept 1.1, 0.75 and 0.75 times of thickness of plate. The height of stiffeners, height of substiffeners width of pads and width of flanges are kept constant during this stage and they have values of 28.0mm,14.0mm, $d_{stiff}/4$ and 14.0mm. The optimum values of design variables and critical buckling loads are given in Table 5.44. The highest improvement is obtained from five stiffeners case and the improvement is approximately 23.30%. The highest critical buckling load is gained from eight stiffeners case and equal to 274825 N. The improvement of this case is 605 % compared with two stiffeners case.

In optimum solutions, skin is thicker than stiffeners in all cases. Thickness of skin, substiffeners and flanges reach lower limit in all cases. In addition, skin and pads are going to be thinner by the increasing of number of stiffeners.

Table 5.44 Size optimization of T shaped stiffened plates with substiffeners and pads under stiffeners

n_{stiff}	Optimum DVs values					Buckling loads		Imp
	t_{skin}	t_{stiff}	t_{sub}	t_{pad1}	t_{flange}	P_i	P_{max}	(%)
2	1.96	1.30	1.00	3.71	1.00	34002.7	38941.0	14.52
3	1.93	1.30	1.00	3.23	1.00	65529.3	77644.7	18.49
4	1.79	1.30	1.00	3.05	1.00	98765.2	121254.2	22.77
5	1.67	1.30	1.00	2.84	1.00	132533.1	163386.2	23.28
6	1.57	1.30	1.00	2.55	1.00	164344.3	201876.8	22.84
7	1.40	1.30	1.00	2.48	1.00	195201.3	238103.1	21.97
8	1.40	1.30	1.00	2.00	1.00	274825.6	274825.6	0.00

ii) Shape optimization: In addition to thicknesses of plate, stiffeners, substiffeners, pads and flanges, height of stiffeners and height of substiffeners are included in optimization process as design variables. Still width of pads and width of flanges are kept constant in this stage. The optimum values of design variables and critical buckling loads are presented in Table 5.45. The highest improvement is obtained from seven stiffeners case and it is approximately 71.50 %. The largest critical buckling load is gained from eight stiffeners case and it is equal to 417527. The improvement of critical buckling load is about 952 % compared to two stiffeners case.

Skin and pads are going to be thinner and stiffeners are going to be thinner by the increasing of number of stiffeners. Stiffener and flange thicknesses reach lower limit in all cases.

iii) Shape optimization: In addition to previous design variables width of pads and width of flanges included as design variables. The optimum values of design variables and critical buckling loads are presented in Table 5.46. The highest improvement is obtained from seven stiffeners case and it is approximately 96.30 %. Largest critical buckling load also is obtained from eight stiffeners case and the plate has a critical buckling load of 461549 N. The improvement is 917 % compared with two stiffeners case.

Stiffeners are going to be thicker pads are going to be thinner also, skin thickness, flange thickness, height of stiffeners and height of substiffeners decrease to lower limit by the increasing of number of stiffeners. Substiffener thicknesses reach lower limit in all cases. Width of pads increases to upper limits except seven and eight stiffeners case.

Table 5.45 Shape optimization of T shaped stiffened plates with substiffeners and pads under stiffeners with seven design variables

n_{stiff}	Optimum DVs values							Buckling loads		Imp
	t_{skin}	t_{stiff}	t_{sub}	t_{pad1}	t_{flange}	h_{stiff}	h_{sub}	P_i	P_{max}	(%)
2	1.99	1.30	1.82	3.91	1.00	18.79	5.00	34002.7	39661.9	16.64
3	1.94	1.58	1.65	3.61	1.00	15.93	5.00	65529.3	82349.9	25.66
4	1.83	2.08	1.00	3.67	1.00	10.94	5.00	98765.2	134484.5	36.16
5	1.76	2.17	1.04	3.39	1.03	10.91	6.45	132533.1	194506.0	46.76
6	1.72	2.53	1.00	3.34	1.00	8.34	5.00	164344.3	263973.7	60.62
7	1.70	2.70	1.00	2.94	1.00	8.39	5.00	195201.4	334742.2	71.48
8	1.48	2.77	1.00	3.25	1.00	8.00	5.00	274825.6	417527.8	51.92

Table 5.46 Shape optimization of T shaped stiffened plates with substiffeners and pads under stiffeners with nine design variables

n_{stiff}	Optimum DVs values									Buckling loads		Imp
	t_{skin}	t_{stiff}	t_{sub}	t_{pad1}	t_{flange}	h_{stiff}	h_{sub}	w_{pad1}	w_{flange}	Pi	P_{max}	(%)
2	1.41	1.30	1.00	3.58	1.02	19.8	7.51	110.00	7.62	34002.7	45356.8	33.39
3	1.41	1.79	1.00	3.38	1.01	14.1	5.00	73.33	10.82	65529.3	94197.6	43.74
4	1.47	2.19	1.00	3.28	1.00	9.71	5.00	55.00	7.00	98765.2	158108.3	60.08
5	1.40	2.37	1.00	3.19	1.12	8.64	5.00	44.00	7.00	132533.1	232209.5	75.20
6	1.40	2.83	1.00	3.00	1.01	8.00	5.00	36.66	7.00	164344.3	307292.3	86.98
7	1.40	3.00	1.00	2.97	1.00	8.00	5.00	28.01	7.00	195201.3	383180.7	96.30
8	1.40	3.19	1.00	2.93	1.00	8.00	5.00	21.28	7.00	274825.6	461549.7	67.94

Shape optimizations gave better results again as shown in Figure 5.28. Effect of pads are seen here clearly again.

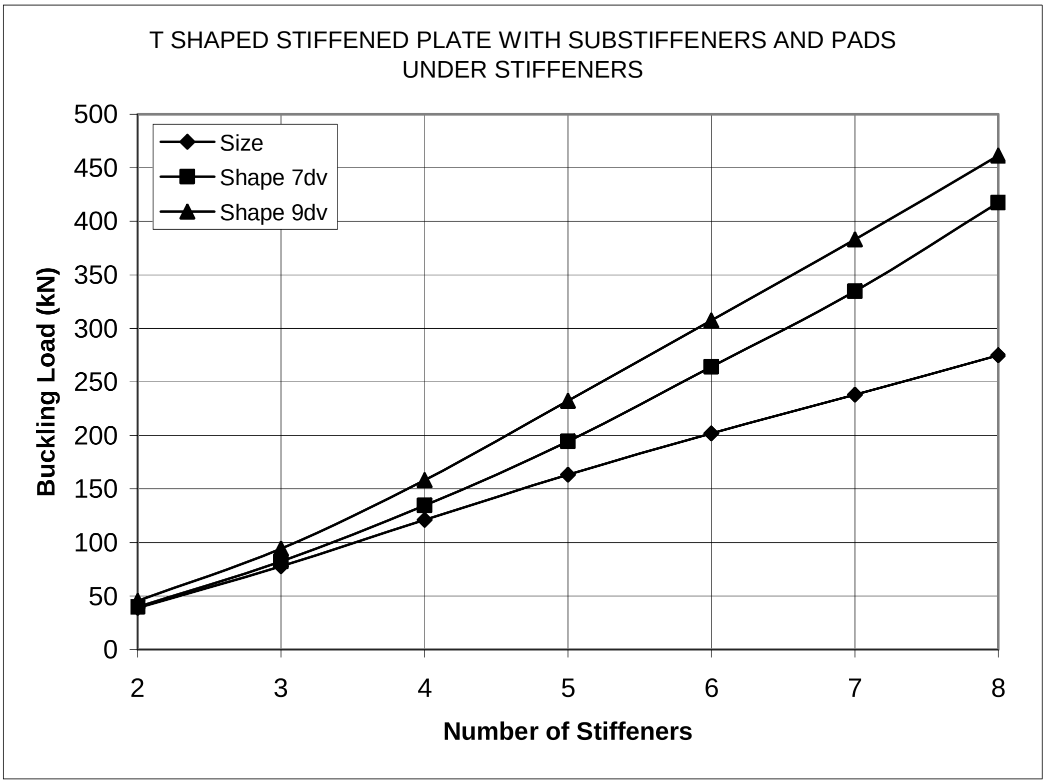

Figure 5.28 Comparison of size and shape optimizations

5.2.2.5 T shaped stiffened plate and pads between stiffeners

Pad elements are attached between T shaped stiffeners and Figure 5.29 shows T shaped stiffened plate and pads under stiffeners.

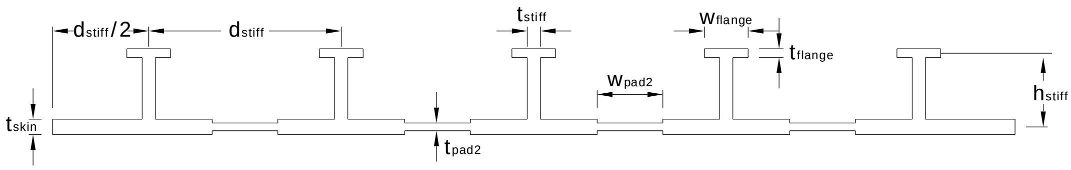

Figure 5.29 T shaped stiffened plate and pads between stiffeners

a) Optimization Process

i) Size optimization: Optimization is performed using thickness of plate skin (t_{skin}), thickness of stiffeners (t_{stiff}), thickness of pads between stiffeners (t_{pad2}) and thickness of flange (t_{flange}).Height of stiffeners (h_{stiff}), width of pads between stiffeners $(w_{pad\,2})$ and width of flanges (w_{flange}) have constant values of 28,0mm, 14,0mm, $d_{stiff}/4$ (See Figure 5.29).

ii) *Shape optimization:* Height of substiffners (h_{stiff}), is included as design variable in this stage. Width of flanges (w_{flange}) and width of pads between stiffeners $(w_{pad\,2})$ still have constant value of 14,0mm and $d_{stiff}/4$ in this stage (See Figure 5.29).

iii) *Shape optimization:* Width of flanges (w_{flange}) and width of pads between stiffeners $(w_{pad\,2})$ included as design variable in this stage (See Figure 5.29).

Design constraints of three stages are specified in Table 5.47. Optimization process is carried out for two to eight stiffeners

Table 5.47 Design constraints of T shaped stiffened plate and pads between stiffeners

		Min (mm)	Max (mm)
Thickness of plate	t_{skin}	1.4	3.0
Thickness of stiffener	t_{stiff}	1.3	4.0
Height of stiffener	h_{stiff}	8.0	40.0
Thickness of pads between stiffeners	$t_{pad\,2}$	1.3	5.0
Width of pads between stiffeners	$w_{pad\,2}$	$d_{stiff}/10$	$d_{stiff}/2$
Thickness of flange	t_{flange}	1.0	4.0
Width of flange	w_{flange}	7.0	30.0

b) Discussion of results

Effect of pads between stiffeners on Critical buckling load of T shaped stiffened plate is examined. Three types of optimizations are performed. First one is size optimization with four design variables $(t_{skin} - t_{stiff} - t_{flange} - t_{pad\,2})$, second is shape optimization with five design variables (t_{skin} - t_{stiff} - t_{flange} - $t_{pad\,2}$ - h_{stiff}) and the third one is shape optimization with seven design variables (t_{skin} - t_{stiff} - t_{flange} - $t_{pad\,2}$ - h_{stiff} - w_{flange} - $w_{pad\,2}$). The effect of number of stiffners also examined.

i) Size optimization: Thickness of plate, stiffeners, flanges and pads between stiffeners are kept equal in initial design. The height of stiffeners, width of flanges and width of pads between stiffeners and are kept constant during this stage and they have values of 28.0mm, 14.0mm, d_{stiff}/4 respectively. The optimum values of design variables and critical buckling loads are given in Table 5.48. The highest improvement is obtained from eight stiffeners case and the improvement is approximately 28.90 %. The highest critical buckling load is gained from eight stiffeners case and equal to 296898 N. The improvement of this case is 787 % compared with two stiffeners case.

In optimum solutions, stiffener thicknesses and flange thicknesses are going to be thinner and reach lower limit by the increasing of number of stiffeners. In all cases thicknesses of pads between stiffeners reach lower limits.

Table 5.48 Size optimization of T shaped stiffened plate and pads between stiffeners

n_{stiff}	Optimum DVs values				Buckling loads		Imp
	t_{skin}	t_{stiff}	t_{flange}	t_{pad2}	P_i	P_{max}	(%)
2	2.21	3.20	2.58	1.30	31231.5	33470.3	7.17
3	2.24	2.30	1.44	1.30	63338.41	69670.9	10.00
4	2.29	1.70	1.00	1.30	98362.50	113768.1	15.66
5	2.29	1.30	1.00	1.30	132117.4	163476.5	23.74
6	2.15	1.30	1.00	1.30	166034.3	212015.9	27.69
7	2.01	1.30	1.00	1.30	198690.2	258621.0	30.16
8	1.87	1.30	1.00	1.30	230322.6	296898.0	28.91

ii) Shape optimization: Height of stiffeners is included in optimization process as design variables in this stage. Still width of flanges and width of pads are kept constant in this stage. The optimum values of design variables and critical buckling loads are presented in Table 5.49. The highest improvement is obtained from eight stiffeners case and it is approximately 67.18 %. The largest critical buckling load is gained from eight stiffeners case and it is equal to 385057. The improvement of critical buckling load is about 1050 % compared to two stiffeners case.

Except five stiffeners case skin is thinner than stiffeners and flanges are going to be thinner by the increasing of number of stiffeners. Thicknesses of pads between stiffeners reach lower limits in all cases.

Table 5.49 Shape optimization of T shaped stiffened plate and pads between stiffeners with five design variables

n_{stiff}	Optimum DVs values					Buckling loads		Imp
	t_{skin}	t_{stiff}	t_{flange}	t_{pad2}	h_{stiff}	P_i	P_{max}	(%)
2	2.20	3.26	2.61	1.30	17.52	31231.4	33470.3	7.17
3	2.20	2.81	2.03	1.30	21.76	63338.4	71411.5	12.75
4	2.22	2.37	1.63	1.30	19.09	98362.5	121001.8	23.02
5	2.26	2.18	1.29	1.30	15.61	132117.4	182042.9	37.79
6	2.12	2.84	1.18	1.30	12.55	166034.2	247709.2	49.19
7	1.97	3.38	1.33	1.30	9.99	198690.2	315390.1	58.73
8	1.90	3.42	1.44	1.30	8.48	230322.6	385057.9	67.18

iii) Shape optimization: In addition to previous design variables width of flanges and width of pads are included as design variables. The optimum values of design variables and critical buckling loads are presented in Table 5.50. The highest improvement is obtained from eight stiffeners case and it is approximately 79.70 %. Largest critical buckling load also is gained from eight stiffeners case and the plate has a critical buckling load of 413894 N. The improvement is 997 % compared with two stiffeners case.

Skin is thinner than stiffeners in all cases in optimum solutions. Thicknesses of skin and height of stiffeners decrease and stiffeners are going to be thicker by the increasing of number of stiffeners. Thicknesses of pads between stiffeners reach lower limit in all cases. Widths of pads between stiffeners reach upper limits in all cases.

Shape optimizations gave better results again as shown in Figure 5.30. Effect of pads between stiffeners here can be seen again like in straight stiffeners.

Table 5.50 Shape optimization of T shaped stiffened plate and pads between stiffeners with seven design variables

n_{stiff}	Optimum DVs values							Buckling loads		Imp
	t_{skin}	t_{stiff}	t_{flange}	t_{pad2}	h_{stiff}	w_{flange}	w_{pad2}	P_i	P_{max}	(%)
2	2.39	3.44	3.39	1.30	28.12	7.00	110.00	31231.4	37711.7	20.75
3	2.42	3.11	2.88	1.30	22.60	7.00	73.33	63338.4	82093.3	29.61
4	2.38	2.62	1.00	1.30	17.48	30.00	55.00	98362.5	144305.8	46.71
5	2.19	3.60	1.00	1.30	12.41	28.42	44.00	132117.4	210542.8	59.36
6	2.12	3.40	1.41	1.30	11.97	17.03	36.67	166034.2	271860.7	63.74
7	2.15	4.00	1.36	1.30	11.38	7.00	31.43	198690.2	352058.9	77.19
8	1.97	4.00	1.57	1.30	9.99	9.15	27.50	230322.6	413894.6	79.70

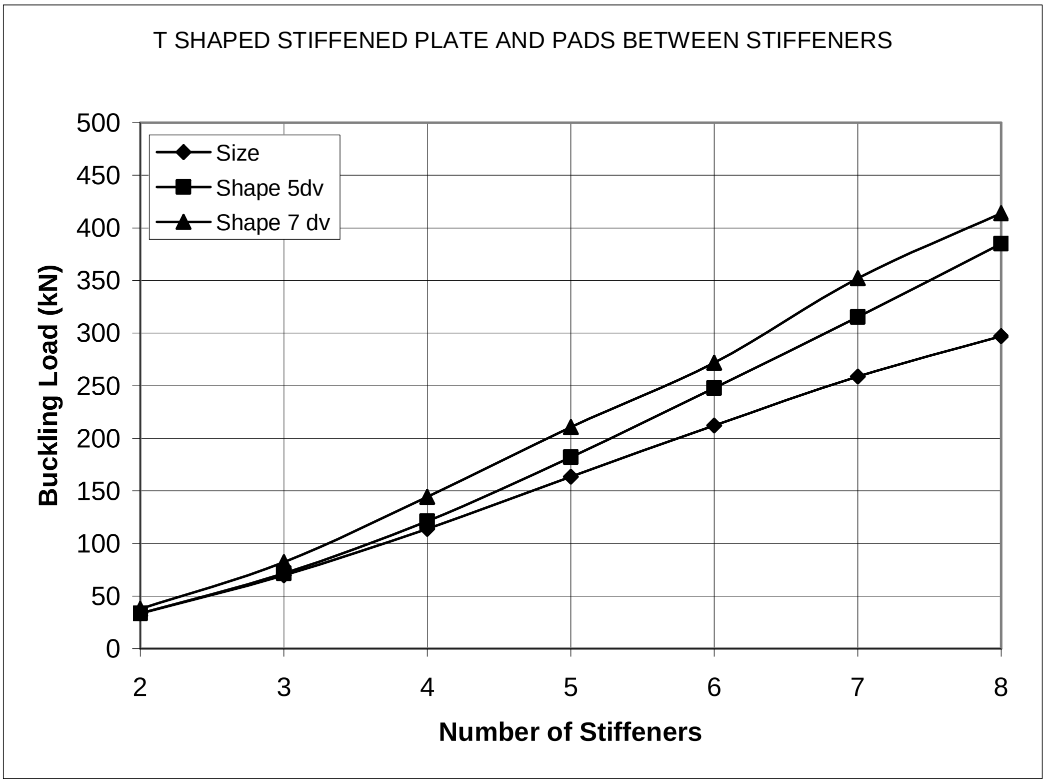

Figure 5.30 Comparison of size and shape optimizations

5.2.2.6 T shaped stiffened plate and pads under stiffeners and between stiffeners

Pad elements are attached under and between stiffeners. Figure 5.31 illustrates T shaped stiffened plate and pads under stiffeners and between stiffeners.

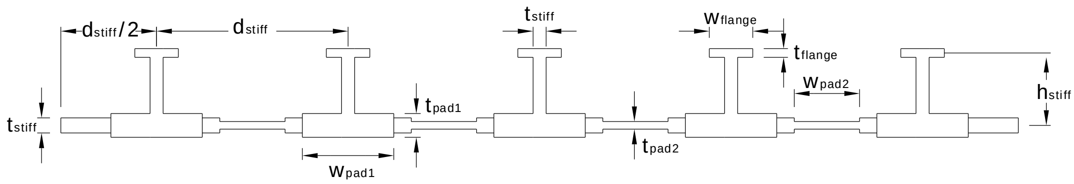

Figure 5.31 T shaped stiffened plate and pads under stiffeners and between stiffeners

a) Optimization Process

i) *Size optimization:* Optimization is carried out using thickness of plate skin (t_{skin}), thickness of stiffeners (t_{stiff}), thickness of pads (t_{pad1}) thickness of pads between stiffeners (t_{pad2}) and thickness of flange (t_{flange}). Height of stiffeners (h_{stiff}) width of pads under stiffeners (w_{pad1}), width of pads between stiffeners (w_{pad2}) and width of flanges (w_{flange}) have constant values of 28.0mm, $d_{stiff}/4$, $d_{stiff}/4$ and 14.0mm (See Figure 5.31).

ii) *Shape optimization:* Height of substiffeners (h_{stiff}), is included as design variable in this stage. Width of pads (w_{pad1}), width of pads between stiffeners (w_{pad2}) and width of flanges (w_{flange}) still have constant value of $d_{stiff}/4$, $d_{stiff}/4$ and 14.0mm in this stage (See Figure 5.31).

iii) *Shape optimization:* Width of pads (w_{pad1}), width of pads between stiffeners (w_{pad2}) and width of flanges (w_{flange}) are included as design variable in this stage (See Figure 5.31).

Design constraints of three stages are specified in Table 5.51. Optimization process is carried out for two to eight stiffeners

b) Discussion of results

Effect of pads between stiffeners on critical buckling load of T shaped stiffened plate with pads under stiffeners is examined. Three types of optimizations are performed. First one is size optimization with five design variables (t_{skin} - t_{stiff} - t_{pad1} - t_{flange} - t_{pad2}), second is shape optimization with six design variables (t_{skin} - t_{stiff} - t_{pad1} - t_{flange} - t_{pad2} - h_{stiff}) and the third one is shape optimization with nine design variables (t_{skin} - t_{stiff} -

t_{pad1} - t_{flange} - t_{pad2} - h_{stiff} - w_{pad1} - w_{flange} - w_{pad2}). The effect of number of stiffeners also examined.

Table 5.51 Design constraints of T shaped stiffened plate and pads under stiffeners and between stiffeners

		Min (mm)	Max (mm)
Thickness of plate	t_{skin}	1.4	3.0
Thickness of stiffener	t_{stiff}	1.3	4.0
Height of stiffener	h_{stiff}	8.0	40.0
Thickness of pad	t_{pad1}	2.0	5.0
Width of pad	w_{pad1}	d_{stiff}/10	d_{stiff}/2
Thickness of pads between stiffeners	t_{pad2}	1.3	5.0
Width of pads between stiffeners	w_{pad2}	d_{stiff}/10	d_{stiff}/2
Thickness of flange	t_{flange}	1.0	4.0
Width of flange	w_{flange}	7.0	30.0

i) Size optimization: Thickness of plate, stiffeners and pads between stiffeners are kept equal in initial design. Thickness of pads under stiffeners and thickness of flanges are kept 1.25 and 0.75 times of thickness of plate respectively. The height of stiffeners, width of flanges, width of pads and width of pads between stiffeners are kept constant during this stage and they have values of 28.0mm, 14.0mm, d_{stiff}/4 and d_{stiff}/4 respectively. The optimum values of design variables and critical buckling loads are given in Table 5.52. The highest improvement is gained from five stiffeners case and the improvement is approximately 24.90 %. The highest critical buckling load is obtained from eight stiffeners case and equal to 320835 N. The improvement of this case is 752 % compared with two stiffeners case. Skin is thicker than stiffeners in all cases.

Skin and pad thicknesses under stiffeners are going to be thinner by the increasing by the number of stiffeners. Stiffener thicknesses, flange thicknesses and pad thicknesses between stiffeners reach lower limits in all cases.

Table 5.52 Size optimization of T shaped stiffened plate and pads under stiffeners and between stiffeners

n_{stiff}	Optimum DVs values					Buckling loads		Imp
	t_{skin}	t_{stiff}	t_{flange}	t_{pad2}	t_{pad1}	P_i	P_{max}	(%)
2	1.88	1.30	1.00	1.30	4.38	31996.5	37642.2	17.64
3	1.89	1.30	1.00	1.30	3.99	67240.3	80286.2	19.40
4	1.80	1.30	1.00	1.30	3.79	106012.8	129230.7	21.90
5	1.73	1.30	1.00	1.30	3.51	145364.8	181490.4	24.85
6	1.65	1.30	1.00	1.30	3.25	184835.5	230252.3	24.57
7	1.53	1.30	1.00	1.30	3.05	222692.2	275319.6	23.63
8	1.40	1.30	1.00	1.30	2.88	263238.4	320835.3	21.88

ii) Shape optimization: In addition to thicknesses of plate, stiffeners, flanges, pads and pads between stiffeners, height of stiffeners is included in optimization process as design variables. Still width of flanges, width of pads between stiffeners and width of pads under stiffeners are kept constant in this stage. The optimum values of design variables and critical buckling loads are presented in Table 5.53. The highest improvement is obtained from eight stiffeners case and it is approximately 68.72 %. The largest critical buckling load is gained from eight stiffeners case and it is equal to 444142 N. The improvement of critical buckling load is about 1024 % when compared to two stiffeners case.

Skin and pad thicknesses are going to be thinner and stiffeners are going to be thicker by the increasing of number of stiffeners. Flange and pad thicknesses reach lower limits in all cases.

iii) Shape optimization: In addition to previous design variables width of pads under stiffeners, width of flanges and width of pads between stiffeners are included as design variables. The optimum values of design variables and critical buckling loads are presented in Table 5.54. The highest improvement is obtained from eight stiffeners case and it is approximately 84.26 %. Largest critical buckling load also is obtained from eight stiffeners case and the plate has a critical buckling load of 485064 N. The improvement is 961 % when compared with two stiffeners case. Skin is thinner than stiffeners in all cases in optimum solutions. Stiffeners are going to be thicker by the increasing of number of stiffeners. Flange and pad thicknesses reach lower limit in all cases.

Table 5.53 Shape optimization of T shaped stiffened plate and pads under stiffeners and between stiffeners with six design variables

n_{stiff}	Optimum DVs values						Buckling loads		Imp
	t_{skin}	t_{stiff}	t_{flange}	t_{pad2}	t_{pad1}	h_{stiff}	P_i	P_{max}	(%)
2	1.98	1.30	1.00	1.30	4.59	8.99	31996.5	39491.2	23.42
3	1.91	1.80	1.00	1.30	4.47	9.73	67240.3	86026.5	27.94
4	1.82	2.08	1.00	1.30	4.27	10.58	106012.8	142731.9	34.64
5	1.79	2.38	1.00	1.30	4.17	8.04	145364.9	211083.5	45.21
6	1.76	2.70	1.00	1.30	3.81	8.00	184835.5	286656.1	55.09
7	1.75	2.94	1.00	1.30	3.40	8.00	222692.2	365278.8	64.03
8	1.56	3.05	1.00	1.30	3.41	8.00	263238.43	444142.2	68.72

Table 5.54 Shape optimization of T shaped stiffened plate and pads under stiffeners and between stiffeners with nine design variables

n_{stiff}	Optimum DVs values									Buckling loads		Imp
	t_{skin}	t_{stiff}	t_{flange}	t_{pad2}	t_{pad1}	h_{stiff}	w_{pad1}	w_{flange}	w_{pad2}	P_i	P_{max}	(%)
2	1.52	1.81	1.00	1.30	3.82	8.00	105.31	7.00	110.00	31996.5	45705.0	42.84
3	1.43	1.85	1.00	1.30	3.65	9.20	73.33	7.00	73.33	67240.3	99412.0	47.85
4	1.42	2.28	1.00	1.30	3.53	8.00	55.00	7.00	55.00	106012.8	167017.8	57.54
5	1.43	2.62	1.00	1.30	3.43	8.21	42.32	7.00	43.98	145364.8	241814.7	66.35
6	1.58	2.89	1.00	1.30	3.47	8.00	29.26	9.57	36.67	184835.5	316008.3	70.97
7	1.53	3.09	1.00	1.30	3.49	8.00	23.24	7.00	31.43	222692.2	401147.8	80.14
8	1.47	3.20	1.00	1.30	3.54	8.00	17.87	7.00	27.48	263238.4	485064.8	84.27

Shape optimizations gave better results again as shown in Figure 5.32.Effect of pads and width of pads between stiffeners are seen here again. Pad elements causes higher buckling loads.

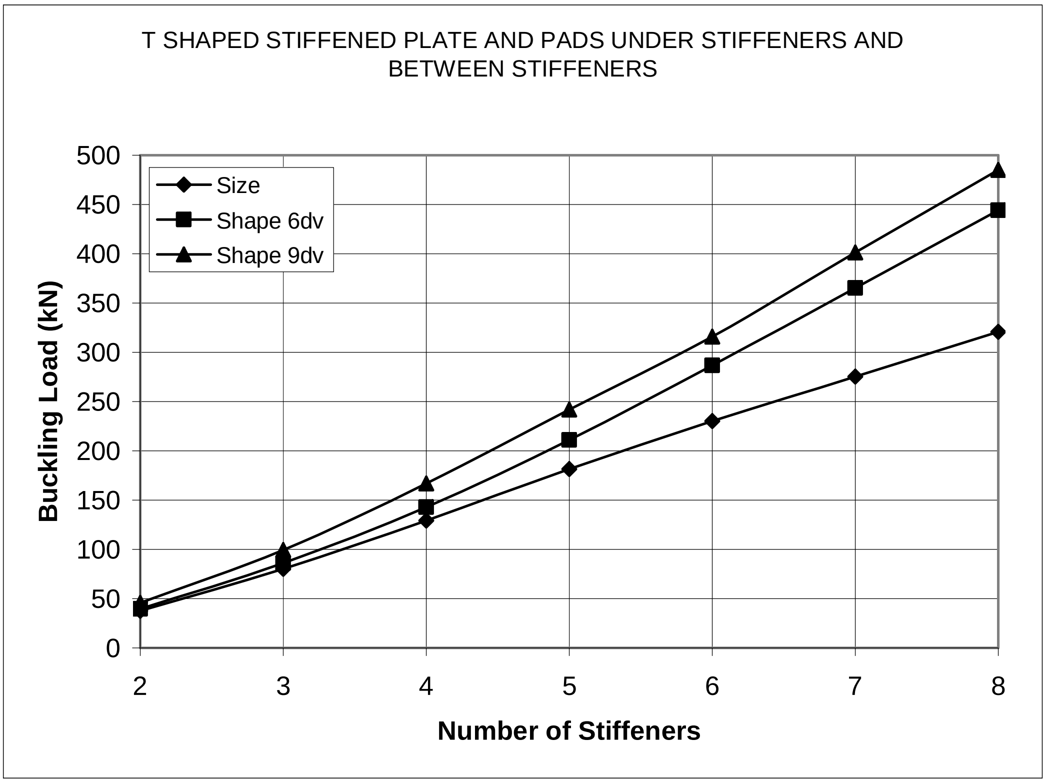

Figure 5.32 Comparison of size and shape optimizations

5.2.2.7 T shaped stiffened plate with linearly varying skin

Plate skin between T shaped stiffeners is consider linearly varying and Figure 5.33. shows T shaped stiffened plate with linearly varying skin.

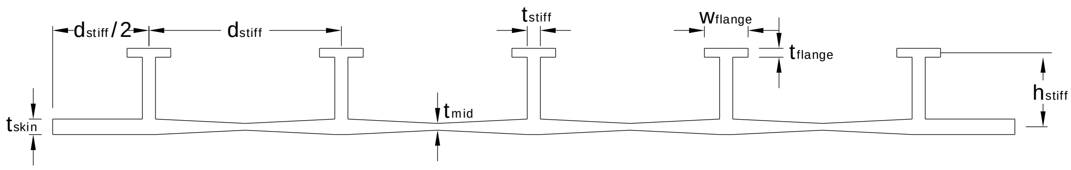

Figure 5.33 T shaped stiffened plate with linearly varying skin

a) Optimization Process

i) Size optimization: Optimization is performed using thickness of plate skin (t_{skin}), thickness of stiffeners (t_{stiff}), thickness of midspan (t_{mid}) and thickness of flange (t_{flange}). Height of stiffeners (h_{stiff}) and width of flanges w_{flange} have constant values of 28.0mm and 14.0 mm (See Figure 5.33).

ii) Shape optimization: Height of stiffeners (h_{stiff}), is included as design variable in this stage. Width of flanges (w_{flange}) still has constant value 14,0mm in this stage (See Figure 5.33).

iii) Shape optimization: Width of flanges (w_{flange}) is included as design variable in this stage (See Figure 5.33).

Design constraints of three stages are specified in Table 5.55. Optimization process is carried out for two to eight stiffeners

Table 5.55 Design constraints of T shaped stiffened plate with linearly varying skin

		Min (mm)	Max (mm)
Thickness of plate	t_{skin}	1.4	3.0
Thickness of stiffener	t_{stiff}	1.3	4.0
Height of stiffener	h_{stiff}	8.0	40.0
Thickness of midspan	t_{mid}	1.3	3.0
Thickness of flange	t_{flange}	1.0	4.0
Width of flange	w_{flange}	7.0	30.0

b) Discussion of results

The effect of variety in midspan thickness on T shaped stiffened plate is examined in this type of plates. Three types of optimizations are performed. First one is size optimization with four design variables $(t_{skin} - t_{stiff} - t_{flange} - t_{mid})$, second is shape optimization with five design variables $(t_{skin} - t_{stiff} - t_{flange} - t_{mid} - h_{stiff})$ and the third one is shape optimization with six design variables $(t_{skin} - t_{stiff} - t_{flange} - t_{mid} - h_{stiff} - w_{flange})$. The effect of number of stiffeners also examined.

i) Size optimization: Thickness of plate, stiffeners flanges and midspan are kept equal in initial design. The height of stiffeners and width of flanges are kept constant during this stage and they have values of 28.0mm and 14.0mm. The optimum values of design variables and critical buckling loads are given in Table 5.56. The highest improvement is obtained from seven stiffeners case and the improvement is approximately 41.35 %. The highest critical buckling load is gained from eight stiffeners case and equal to 318740 N. The improvement of this case is 797 % compared with two stiffeners case.

Stiffeners and flange thicknesses are going to be thinner by the increasing of number of stiffeners in optimum solutions. Midspan thickness reach lower limit in all cases.

Table 5.56 Size optimization of T shaped stiffened plate with linearly varying skin

n_{stiff}	Optimum DVs values				Buckling loads		Imp (%)
	t_{skin}	t_{stiff}	t_{flange}	t_{mid}	P_i	P_{max}	
2	2.35	3.27	2.53	1.30	31231.4	35527.2	13.75
3	2.40	2.54	1.52	1.30	63338.4	75139.3	18.63
4	2.52	1.86	1.00	1.30	98362.5	123040.4	25.09
5	2.61	1.30	1.00	1.30	132117.4	178036.8	34.76
6	2.46	1.30	1.00	1.30	166034.2	232613.4	40.10
7	2.23	1.37	1.00	1.30	198690.2	280860.5	41.36
8	2.02	1.37	1.00	1.30	230322.6	318740.4	38.39

ii) Shape optimization: In addition to thicknesses of plate, stiffeners flanges and midspan, height of stiffeners is included in optimization process as a design variable. Still with of flanges are kept constant in this stage. The optimum values of design variables and critical buckling loads are presented in Table 5.57. The highest improvement is obtained from eight stiffeners case and it is approximately 76.53 %. Also the largest critical buckling load is obtained from eight stiffeners case and it is equal to 406602 N. The improvement of critical buckling load is about 1043 % compared to two stiffeners case.

In optimum solutions, skin is thinner than stiffeners. Stiffeners are going to be thicker and height of stiffeners decreases by the increasing of number of stiffeners. Midspan thicknesses reach lower limit in all cases.

iii) Shape optimization: In addition to previous design variables width of flanges included as a design variable. The optimum values of design variables and critical buckling loads are presented in Table 5.58. The highest improvement is obtained from eight stiffeners case and it is approximately 84.74 %. Largest critical buckling load also is gained from eight stiffeners case and the plate has a critical buckling load of 452520 N. The improvement is 1126 % compared with two stiffeners case. Skin is thinner than stiffeners in all cases in optimum solutions. Stiffeners are going to be thicker by the increasing of number of stiffeners. Midspan thicknesses reach lower limit in all cases. Width of flanges reach lower limit except five stiffeners case.

Table 5.57 Shape optimization of T shaped stiffened plate with linearly varying skin with five design variables

n_{stiff}	Optimum DVs values					Buckling loads		Imp(%)
	t_{skin}	t_{stiff}	t_{flange}	t_{mid}	h_{stiff}	P_i	P_{max}	
2	2.34	2.38	2.62	1.30	27.12	31231.4	35543.6	13.81
3	2.48	2.79	2.08	1.30	20.00	63338.4	76826.6	21.30
4	2.47	2.49	1.87	1.30	16.68	98362.5	132643.6	34.85
5	2.58	4.00	1.00	1.30	9.56	132117.4	191635.8	45.05
6	2.31	4.00	1.00	1.30	10.74	166034.2	272553.8	64.15
7	2.09	4.00	1.31	1.30	9.73	198690.2	342415.6	72.34
8	1.93	4.00	1.61	1.30	8.27	230322.6	406602.9	76.54

Table 5.58 Shape optimization of T shaped stiffened plate with linearly varying skin with seven design variables

n_{stiff}	Optimum DVs values						Buckling loads		Imp
	t_{skin}	t_{stiff}	t_{flange}	t_{mid}	h_{stiff}	w_{flange}	P_i	P_{max}	(%)
2	2.41	3.33	3.49	1.30	27.57	7.00	31231.4	36902.0	18.16
3	2.47	4.00	4.00	1.30	14.41	7.00	63338.4	77250.0	21.96
4	2.47	3.29	2.07	1.30	16.7	7.00	98362.5	134966.5	37.21
5	2.35	4.00	1.00	1.30	24.00	12.87	132117.4	198629.6	50.34
6	2.45	4.00	1.00	1.30	10.98	7.00	166034.2	275153.2	65.72
7	2.26	4.00	1.41	1.30	10.34	7.00	198690.2	353184.4	77.76
8	2.11	4.00	1.75	1.30	9.44	7.00	230322.6	425520.6	84.75

Shape optimizations gave better results as shown in Figure 5.34. Nevertheless, at small number of stiffeners critical buckling loads are approximately same for all type of optimizations. Midspan thickness is going to be thinner. By this alternation, plate is going to be thicker.

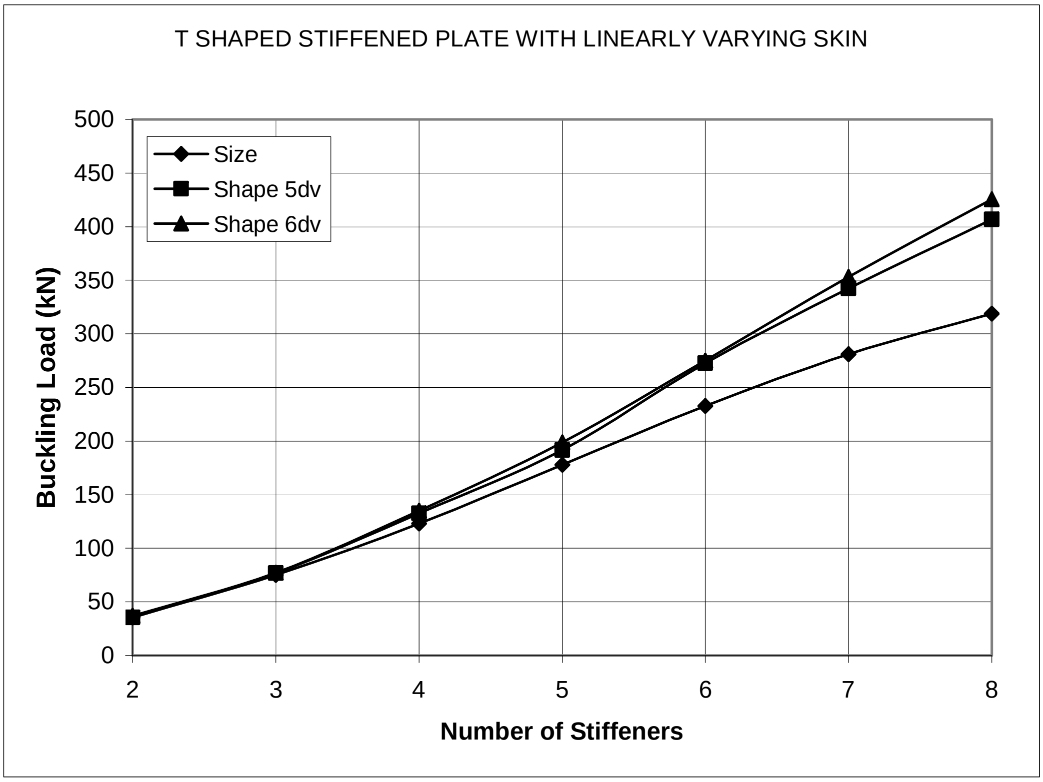

Figure 5.34 Comparison of size and shape optimizations

5.2.2.8 T shaped stiffened plate with linearly varying skin and pads under stiffeners

Linearly varying skin is considered with pads under stiffeners and Figure 5.35 shows T shaped stiffened plate with linearly varying skin and pad elements aunder stiffeners.

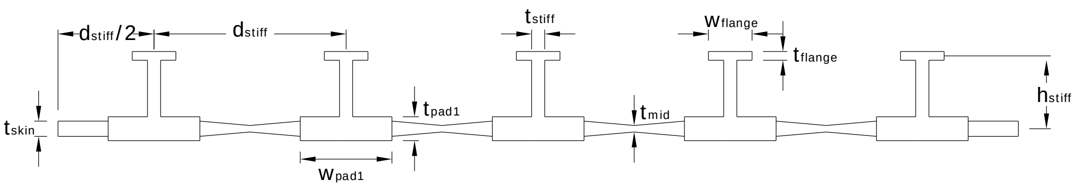

Figure 5.35 T shaped stiffened plate with linearly varying skin and pads under stiffeners

a) Optimization Process

i) *Size optimization:* Optimization is performed using thickness of plate skin (t_{skin}), thickness of stiffeners (t_{stiff}), thickness of pads (t_{pad1}) thickness of midspan (t_{mid}) and thickness of flange (t_{flange}). Height of stiffeners (h_{stiff}) width of pads (w_{pad1}), and width of flanges (w_{flange}) have constant values of 28.0mm, $d_{stiff}/4$, and 14.0mm (See Figure 5.35).

ii) *Shape optimization:* Height of substiffeners (h_{stiff}), is included as design variable in this stage. Width of pads (w_{pad1}), and width of flanges (w_{flange}) still have constant value of $d_{stiff}/4$ and 14.0 mm in this stage (See Figure 5.35).

iii) *Shape optimization:* Width of pads (w_{pad1}), and width of flanges (w_{flange}) are included as design variable in this stage (See Figure 5.35).

Design constraints of three stages are specified in Table 5.59. Optimization process is carried out for two to eight stiffeners

Table 5.59 Design constraints of T shaped stiffened plate with linearly varying skin and pads under stiffeners

		Min (mm)	Max (mm)
Thickness of plate	t_{skin}	1.4	3.0
Thickness of stiffener	t_{stiff}	1.3	4.0
Height of stiffener	h_{stiff}	8.0	40.0
Thickness of pad	t_{pad1}	2.0	5.0
Width of Pad	w_{pad1}	$d_{stiff}/10$	$d_{stiff}/2$
Thickness of Midspan	t_{mid}	1.3	5.0
Thickness of Flange	t_{flange}	1.0	4.0
Width of Flange	w_{flange}	7.0	30.0

b) Discussion of results

Effect of variety of midspan thickness on T shaped stiffeners with pads examined during this case. Three type optimizations are performed. First one is size optimization with five design variables ($t_{skin} - t_{stiff} - t_{flange} - t_{mid} - t_{pad1}$), second is shape optimization with six design variables ($t_{skin} - t_{stiff} - t_{flange} - t_{mid} - t_{pad1} - h_{stiff}$) and the third one is shape optimization with eight design variables ($t_{skin} - t_{stiff} - t_{flange} - t_{mid} - t_{pad1} - h_{stiff} - w_{flange} - w_{pad1}$). The effect of number of stiffeners also examined.

i) Size optimization: Thickness of plate, stiffeners and midspan are kept equal in initial design. Thicknesses of pads and flanges are kept 1.25 and 0.75 times of thickness of plate. The height of stiffeners, width of pads and width of flanges are kept constant during this stage and they have values of 28.0 mm, $d_{stiff}/4$ and 14.0mm. The optimum values of design variables and critical buckling loads are given in Table 5.60. The highest improvement is gained from five stiffeners case and the improvement is approximately 29.82 %. The highest critical buckling load is obtained from eight stiffeners case and equal to 324582 N. The improvement of this case is 739 % compared with two stiffeners case.

Skin is thicker than stiffeners in all cases in optimum solutions. Thickness of stiffeners, flanges and midspan reach lower limit in all cases. Skin and pad thicknesses are going to be thinner by the increasing of number of stiffeners.

Table 5.60 Size optimization of T shaped stiffened plate with linearly varying skin and pads under stiffeners

n_{stiff}	Optimum DVs values					Buckling loads		Imp (%)
	t_{skin}	t_{stiff}	t_{flange}	t_{mid}	t_{pad1}	P_i	P_{max}	
2	1.93	1.30	1.00	1.30	4.41	31996.5	38663.8	20.84
3	1.96	1.30	1.00	1.30	4.06	67240.3	83308.3	23.90
4	1.88	1.30	1.00	1.30	3.82	106012.8	134538.2	26.91
5	1.77	1.30	1.00	1.30	3.60	145364.8	188720.2	29.83
6	1.75	1.30	1.00	1.30	3.21	184835.5	238771.4	29.18
7	1.64	1.30	1.00	1.30	2.95	222692.2	283272.1	27.20
8	1.43	1.30	1.00	1.30	2.87	263238.4	324581.2	23.30

ii) Shape optimization: In addition to thicknesses of plate, stiffeners, midspan, pads and flanges, height of stiffeners is included in optimization process as a design variable. Still width of pads and width of flanges are kept constant in this stage. The optimum values of design variables and critical buckling loads are presented in Table 5.61. The highest improvement is obtained from eight stiffeners case and it is approximately 73.77 %. In addition, the largest critical buckling load is gained from eight stiffeners case and it is equal to 457431 N. The improvement of critical buckling load is about 1025 % compared to two stiffeners case.

Skin is going to be thinner and stiffeners are going to be thicker by the increasing of number of stiffeners. Thicknesses of stiffeners, flanges and midspan and height of stiffeners reach lower limit in all cases.

Table 5.61 Shape optimization of T shaped stiffened plate with linearly varying skin and pads under stiffeners with six design variables

n_{stiff}	Optimum DVs values						Buckling loads		Imp
	t_{skin}	t_{stiff}	t_{flange}	t_{mid}	t_{pad1}	h_{stiff}	P_i	P_{max}	(%)
2	2.05	1.34	1.00	1.30	4.61	8.00	31996.5	40634.6	27.00
3	1.97	1.67	1.00	1.30	4.67	8.00	67240.3	89186.9	32.64
4	1.96	2.19	1.00	1.30	4.36	8.00	106012.8	150577.3	42.04
5	1.89	2.53	1.00	1.30	4.13	8.00	145364.8	220478.8	51.67
6	1.82	2.80	1.00	1.30	3.85	8.00	184835.5	297186.0	60.78
7	1.75	3.23	1.00	1.30	3.45	8.00	222692.2	372461.7	67.25
8	1.66	3.30	1.00	1.30	3.21	8.00	263238.4	457431.1	73.77

iii) Shape optimization: In addition to previous design variables width of pads and width of flanges included as design variables. The optimum values of design variables and critical buckling loads are presented in Table 5.62. The highest improvement is obtained from eight stiffeners case and it is approximately 8.82 %. Largest critical buckling load also is gained from eight stiffeners case and the plate has a critical buckling load of 478645 N. The improvement is 950 % compared with two stiffeners case.

Skin is thinner than stiffeners in optimum solutions and skin, pads are going to be thinner and stiffeners are going to be thicker by the increasing of number of stiffeners.

Shape optimizations gave better results compared with size optimizations as shown in Figure 5.36.For two and three number of stiffeners optimizations gave very close results. For the following plates, shape optimizations gave better results. So the effect of width of pads is seen obviously. Midspan reach lower limit in all cases height of stiffeners and width of flanges reach lower limit except three stiffeners case. Also width of pads reach almost upper limits in all cases.

Table 5.62 Shape optimization of T shaped stiffened plate with linearly varying skin and pads under stiffeners with eight design variables

n_{stiff}	Optimum DVs values								Buckling loads		Imp
	t_{skin}	t_{stiff}	t_{flange}	t_{mid}	t_{pad1}	h_{stiff}	w_{pad1}	w_{flange}	P_i	P_{max}	(%)
2	1.44	1.48	1.18	1.30	3.74	8.00	110.00	7.00	31996.5	45580.1	42.45
3	1.45	1.57	1.09	1.30	3.63	9.85	72.55	7.39	67240.3	97829.4	45.49
4	1.40	2.14	1.11	1.30	3.51	8.00	55.00	7.00	106012.8	164428.9	55.10
5	1.40	2.73	1.00	1.30	3.31	8.00	43.93	7.00	145364.8	238944.5	64.38
6	1.40	3.08	1.00	1.30	3.10	8.00	36.67	7.00	184835.5	316761.3	71.37
7	1.40	3.06	1.33	1.30	2.97	8.00	29.93	7.00	222692.2	394919.8	77.34
8	1.40	2.85	1.74	1.30	2.91	8.00	23.70	7.00	263238.4	478645.1	81.83

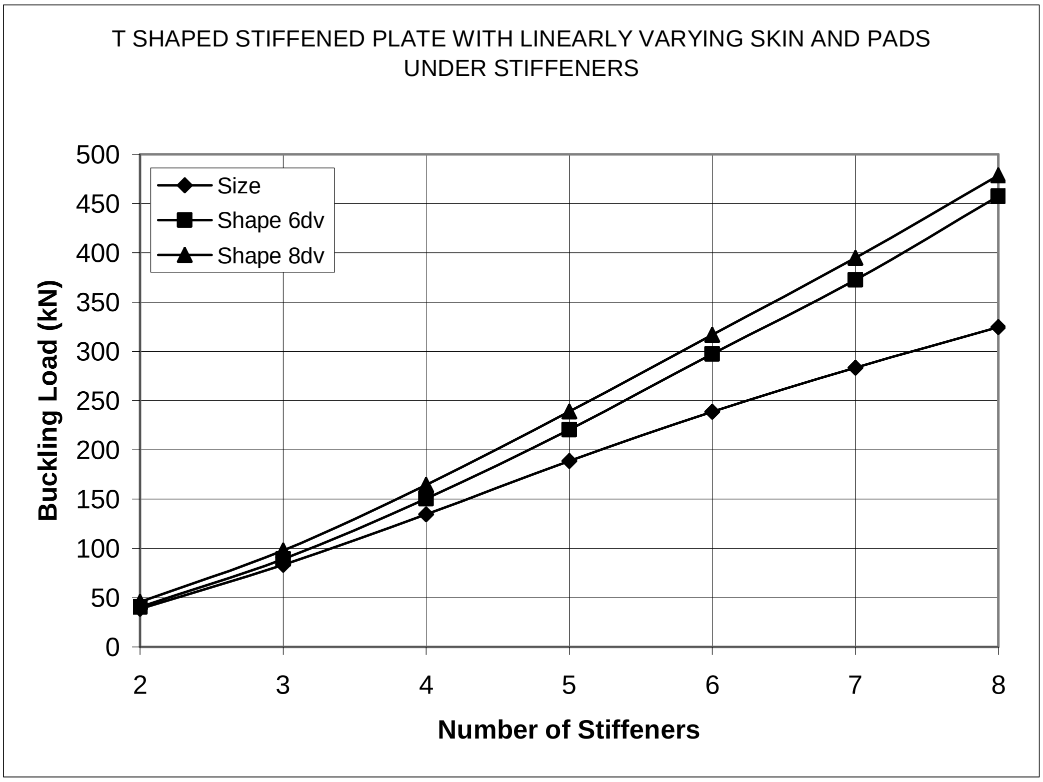

Figure 5.36 Comparison of size and shape optimizations

5.3 Discussions of all stiffened plates

If the results are glanced, it is obviously seen that in all plate types the maximum buckling load is obtained from shape optimization of eight stiffeners case. Due to this result, it can be mentioned that lengths of elements are important for buckling fails as much as element thicknesses. Figure 5.37 shows obtained maximum buckling loads of investigated eight straight stiffened plates and eight T shaped stiffened plates types.

As seen from Figure 5.37, in optimized plates maximum critical buckling load is obtained from straight stiffened plate with pad under stiffeners and between stiffeners between stiffeners. Comparing maximum obtained loads, in straight stiffeners 504895 N is obtained and from T shaped stiffeners 485064 N is obtained. This means in straight stiffeners approximately 4.01 % more critical buckling load is obtained.

The most crucial result that obtained from optimizations is the effect of the pad elements. Looking figure 5.37, it is obviously seen that in both stiffener types the obtained last four robust plate types have pad elements. For both stiffener types, plates with pads and without pads have remarkable difference of buckling loads. From this consequence, it is unquestionable that pad elements are the most effective ones against buckling. Definitely, stiffeners are strengthening flat plate behavior in bending direction. Nevertheless, the joining points of stiffener elements and plate skin become weaker because of stress concentration of corner points. By the increasing of applied inplane load, in that points stress concentration causes that points to rotate and buckling of stiffener elements take place. Pad elements prevent stress concentrations and shorten the buckling length of stiffener elements. Thus critical buckling of plate increases very sharply.

The obtained maximum load difference between straight and T shaped stiffened plates is also originated from the difference of effect of flanges and pads. In T shaped stiffened plates, flanges use somewhat volume from pads and plate skin. Therefore, the effective elements, against buckling failure become thinner. So the T shaped stiffened plates' maximum buckling load cannot reach the straights'.

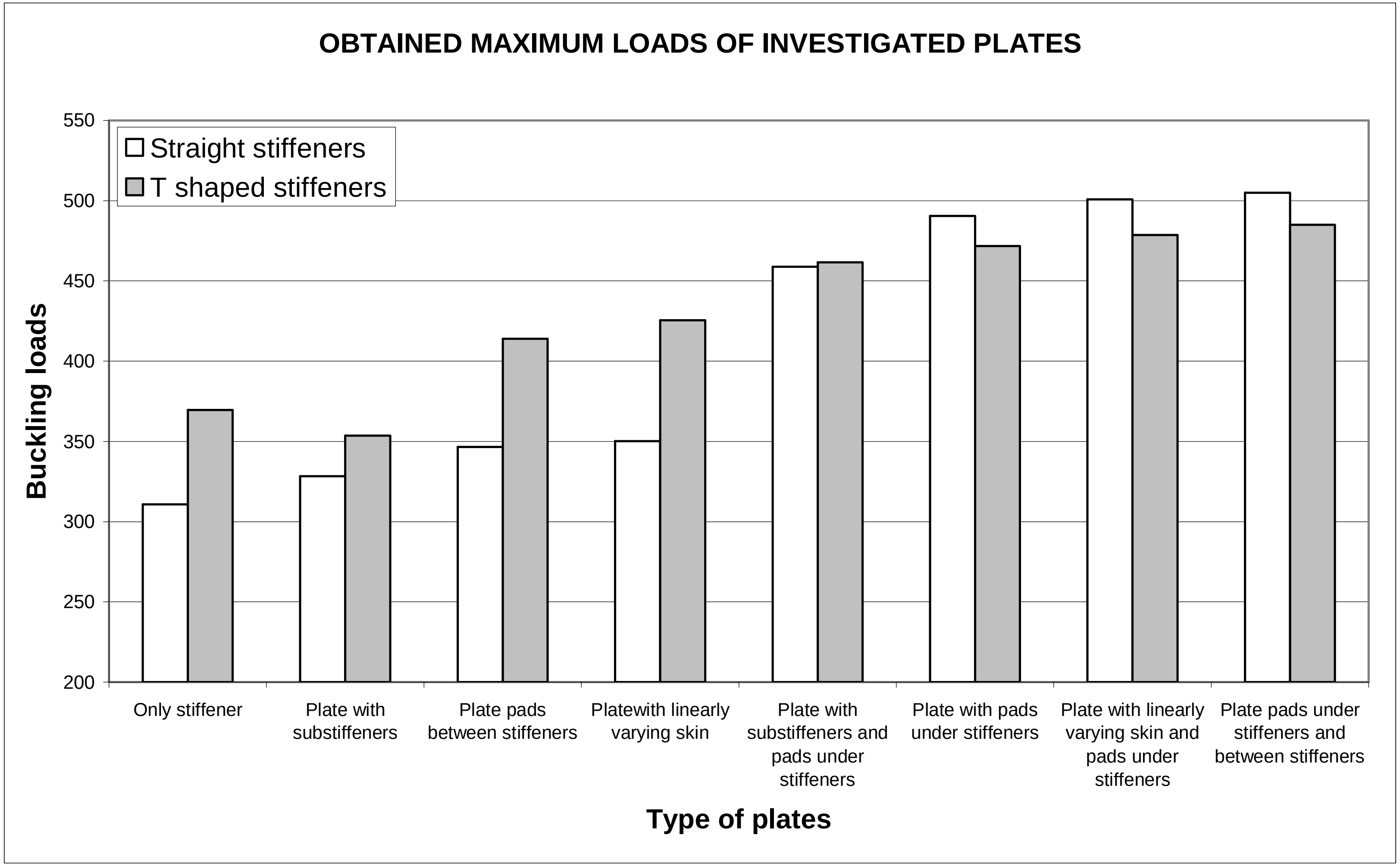

Figure 5.37 Comparison of maximum loads of plate types

Nevertheless, in plate types without pads, T shaped stiffened plates have larger critical buckling load values. This result emphasizes the effect of the flange elements. Flanges are lateral elements that are positioned top of the stiffeners. Therefore, flanges increase the moment of inertia of plate cross section in bending direction thus, critical buckling load of plate increases.

In both stiffener types, maximum loads are obtained from stiffened plates with pads under and between stiffeners. The next obtained is stiffened plate with linearly varying skin and pads under stiffeners. Reference to these it is very clear that the plate skin region between stiffeners contains less risk against buckling than other regions. Thus, some volume from this region could be used for pads, stiffeners and flanges to obtain higher critical buckling loads. Nevertheless, these types of plates have difficulty for producing because of elements varieties.

As discussed before the maximum loads are obtained from eight stiffeners case of each plate set. By the increasing of number of stiffeners, the distance between stiffeners (d_{stiff}) and the distance between stiffeners and plate sides ($d_{stiff}/2$), decrease at the same time. According to this process buckling length of plate skin regions, in other words unsupported length of plate skin decreases. Therefore, the stability of plate cross section increases remarkably and larger critical buckling loads could be gained.

Flanges include an advantage to T shaped stiffened plates. T shaped stiffened plates could be joined easily to other structural elements by their flanges.

It is necessary to mention about effect of substiffener elements finally. In straight stiffeners, plates with substiffners have a little difference of buckling load when compared only straight stiffener case. Also in T shaped stiffeners when substiffeners are added a decrease is observed in buckling load when compared only T shaped stiffener case. Thus, it is understood that flange elements are more effective than substiffener elements so that substiffeners use volume from flanges and skin then critical buckling load decreases. In straight stiffened plate because of absence of flanges, substiffeners become effective and strengthen stability of plates slightly.

For the observation of the influence of plate types Table 5.63 illustrates the percent improvement of plate types due to the only stiffener case of each stiffener types, introduced as base.

Investigating Table 5.63, it can be seen that in straight stiffeners there is a sharp increase in critical buckling load when pad elements are included plates. Nevertheless, in T shaped stiffeners the increment in critical buckling load is smooth because of existence of flange elements.

Table 5.63 Improvement of plate types according to only stiffeners case and percent differences of two types

	Buckling load of str. stif. (kN)	Imp. (%)	Buckling load of T stif.(kN)	Imp. (%)	Diff of two types (%)
Only stiffeners	310.826	Base	369.668	Base	18.93
Plate with substiffeners	328.229	5.60	353.532	-4.36	7.71
Plate with pads between stiffeners	346.471	11.47	413.894	11.96	19.46
Plate with linearly varying skin	350.065	12.62	425.520	15.11	21.55
Plate with Pads and substiffeners	458.888	47.63	461.549	24.86	0.58
Plate with Pads	490.479	57.80	471.665	27.59	-3.84
Plate with linearly varying skin and pads under stiffeners	500.801	61.12	478.645	29.48	-4.42
Plate with Pads under and between stiffeners	504.895	62.44	485.064	31.22	-3.93

Finally, the last column in Table 5.63 illustrates the percent difference of critical buckling loads between straight and T shaped stiffened plates with same elements, considering straight stiffened plates as base.

CHAPTER 6

CONCLUSION

6.1 Introduction

Structural optimization procedures are performed to obtain optimum sizes and shapes of stiffened plate types to gain maximum critical buckling load under constant volume constraint. For this purpose, totally 315 runs are carried out for considered plate types. The optimum results are obtained and detailed discussions are mentioned in Chapter 5. This chapter deals with a general look about results and discussion of the efficiencies of plate types by investigating results that are presented in Chapter 5.

6.2 Achievements

During this thesis, PLATEV_1 (finite strip structural analysis and shape optimization program), which was developed by Özakça [1] was used. During the thesis, the following purposes were achieved.

1- *Geometric modeling of plate cross section:* The plate cross section is modeled by using coordinates of key points as defined in Chapter 4. The stiffener positions governed cross section modeling procedure. To satisfy initial baseline design values, thicknesses of elements and stiffener heights were arranged according to constant volume constraints.

2- *Mesh generation of cross section:* Mesh generation of stiffened plate sections were carried out by PLATEV_1 by an automatic FS mesh generator which was adapted to program.

3- *Buckling analysis:* Eigenvalue buckling analysis were carried out using FS analysis for all investigated plates. FS method was preferred in order to suitability of analyzing simply supported prismatic structures easily.

4- *Verify the accuracy of buckling load:* To prove the accuracy of computer code and formulation used in this study, results of three examples are compared with SAP2000 structural analysis and design computer package program's results. The SAP2000 program and PLATEV_1 gave very close critical buckling load results.

5- *Optimization:* Sequential quadratic programming based algorithm was used as optimization method.

a) *Size optimization:* Size optimizations were carried out to obtain maximum critical buckling load of plate cross sections under constraints. During this procedure height and width of elements were kept constant only thickness DVs are used. The effect of thickness variation on critical buckling load is investigated.

b) *Shape optimization:* In addition to thickness of elements the height and width of elements were added as design variables to observe the variation of critical buckling load.

6- *Results and effectiveness of stiffened plate types:* By the steps mentioned above 315 runs were performed for considered plate types with desired element combinations. The obtained maximum buckling loads of plate types fluctuate in a wide interval due to the used elements that forges plate cross section. The maximum loads for the desired combinations illustrate the effectiveness of element types on critical buckling load. These consequences orientated the comments on elements effectiveness and the suggestions about manufacturing of stiffened plates in conclusion section

6.3 Conclusion

According to optimization results, the effect of elements of plate cross section is discussed in previous chapter. This section deals with some suggestions about manufacturing and use of investigated plates.

The effect of pad elements on critical buckling load is mentioned. However, including pad elements to plate cross section is difficult in practice, plates should be produced with pad elements if higher critical buckling load is desired. Without pad elements, section's stability becomes weaker and section cannot resist higher inplane loads.

When pads are attached between stiffeners and linearly varying skin is considered critical buckling load of plates' increases. Nevertheless, this increment is not remarkable. Moreover, produce plate sections like uttered is a very difficult process. According to this, producing plates with pads between stiffeners and linearly variable skin is not efficient.

If pad elements cannot be applicable due to constraints of producer, flange elements should be considered, because there is a remarkable difference between plates with flanges and without flanges, when pads are not used. As mentioned in earlier section, flange elements include connection section advantage. Plates could be connected to other structures with flange elements.

The effect of substiffeners was examined in Chapter 5. According to optimization results in T shaped stiffened plates, considering substiffeners is not effective. Instead of substiffeners, flanges and plate skin should be strengthened. In straight stiffened plate although substiffeners cause an increase in critical buckling load, it is not a remarkable one.

6.4 Recommendation of future work

In present study linear buckling analysis and optimization of stiffened plates is performed. In linear buckling analysis, critical buckling load of structure is found by buckling of a portion of stiffened plate. Nevertheless, stiffened plate keeps on resist higher loads until overall fail of structure. This situation can be investigated by performing postbuckling analysis, which requires more complex equations and more computational time. For gaining the overall resistance of structures against buckling postbuckling analysis should be investigated.

Critical buckling load of stiffened plates was evaluated by applying uniformly distributed loads to simply supported cross sections. In this way, symmetrical cross sections of stiffened plates were considered in optimization procedure. However, structures may be subjected to varying loads. In this case the behavior, resistance and optimized geometry of structure change according to applied load shape. Varying loading case may be investigated for gaining a general experience for different behaviors.

Another case that causes buckling of structures is torsional effects. In present study, only cross section axially compressive loading was considered. In practice, structures may be subjected to torsional forces and the buckling case in this situation is called as torsional buckling. Torsional effects can be investigated according to sustained structural loading types.

In this thesis, straight and T shaped stiffened plates are investigated. On the other hand, some other types of stiffeners exist in practice. Some of them are L shaped, U shaped tube, Y shaped stiffeners and etc.. It is necessary to examine these types of stiffened plates to possess general behaviors of buckling and design structures that include axially compressive loaded stiffened plates.

Investigated components of plate types also could be analyzed by different combinations. For instance in substiffened plate types only one substiffener considered between main stiffeners. Number of equally spaced substiffeners between main stiffeners may be increased.

Like the applicability of increasing number of substiffeners, number of pads between stiffeners may be increased too. Another case should be investigated that the positions of main stiffeners. In this study, the distance between stiffeners is considered as d_{stiff} according to this, the distance between stiffeners and plate edge is taken $d_{stiff}/2$. What would be the effect of changing the positions of these distances symmetrically to plate axis on critical buckling load?

In FS method, two opposite edges are simply supported and other two sides can be defined in any boundary condition. Some modifications can be made to apply any boundary conditions.

To possess general behavior of stiffened plates a wide search space like listed above should be investigated.

REFERENCES

1. Özakça, M. (1993). *Analysis and Optimal Design of Structures with Adaptivity*. Ph. D. thesis, Department of Civil Engineering University College of Swansea, U.K.

2. Szilard, R. (1974). *Theory and Analysis of Plates, Classical and Numerical Methods.* Prentice Hall.

3. Timoshenko, S. and Kreiger, S.W. (1959). *Theory of plates and shells.* McGraw Hill, New York.

4. Cheung, Y.K. (1976). *The Finite Strip Method in Structural Analysis.* Pergamon International Library of Science

5. Allman, D.J. (1975). Calculation of elastic buckling loads of thin flat plates using triangular finite element. *International Journal for Numerical Methods in Engineering,* **9**, 415-432.

6. Przemieniecki, J.S. (1973). Finite element structural analysis of local stability. *AIAA Journal,* **11**, 33-39

7. Fafard, M., Beaulieu, D. and Dhatt, G. (1987). Buckling of thin walled members by finite element method. *Computers and Structures,* **25**, 183-190

8. Anderson R.G., Irons B.M. and Zienkiewicz O.C. (1968). Vibration and stability of plates using finite elements. *International Journal of Solids and Structures,* **4**,1031-1055

9. Sheikh, I.A., Grodin, G.Y. and Elwi A.E. (2002). Stiffened steel plates under uniaxial compression. *Jornal of Constructional Steel research*, **58**, 1061-1080

10. Sridharan S. and Zeggane Matjid Z. (2001). Stiffened plates and cylindrical shells under interactive buckling. *Finite Element in Analysis and Design*, **38**, 155-178

11. Grondin, G.Y., Elwi, A.E. and Cheng, J.J.R. (1999). Buckling of stiffened steel plates-a parametric study. *Journal of Constructional Steel Research* , **50**, 151-175

12. Jiang, W., Bao, G. and Roberts, J.C. (1997). Finite Element Modelling of Stiffened and Unstiffened Orthotropic Plates. *Computers and Structures*, **63**, 105-117

13. Cheung, Y. K. (1968). The finite strip method in the analysis of elastic plates with two opposite simply supported ends. *Proc. Inst. Civ. Eng.*

14. Dawe, D.J. (1977). Finite strip buckling analysis of curved plate assemblies under biaxial loading. *Solids Structures*, **13**, 1141-1155.

15. Dawe, D. J. and Roufaeil, O. L. (1982). Buckling of rectangular Mindlin plates. *Computers and Structures*, **15**, 1249-1266.

16. Smith Graves, T.R. and Sridharan, S. (1978). A finite strip method fort he buckling of plate structures under arbitrary loading. *International Journal of Mechanical Sciences*, **20**, 685-693.

17. Tham, L.G. and Szeto, H.Y. (1990). Buckling analysis of arbitrary shaped plates by spline finite strip method. *Computers and Structures*, **36**, 729-735.

18. Dawe, D.J. and Peshkam, V. (1990). Buckling and vibration of long plate structures by complex finite strip methods. *International Journal of Mechanical Sciences*, **32**, 743-766

19. Cheung, Y.K., Au, F.T.K. and Zheng, D.Y. (2000). Finite strip method for the free vibration and buckling analysis of plates with abrupt changes in thickness and complex support conditions. *Thin Walled Structures*, **36**, 89-110

20. Xie, W.C. and Ibrahim, A. (2000). Buckling mode localization in rib-stiffened plates with misplaced stiffeners a finite strip approach. *Chaos Solutions & Fractals*, **11**, 1543-1558

21. Takahasni, K. and Nakazawa, S. (1999). Vibration and buckling of plate girders by finite strip method. *Theory and Applied Mechanics*, **48**, 127-133

22. Hinton, E. (1978). Buckling of initially Stressed Mindlin plates using Finite strip method. *Computers and Structures*, **8**, 99-105.

23. Hinton, E., Petrinic, N. and Özakça, M. (1993). Buckling analysis and shape optimization of variable thickness prismatic folded plates Part 1: Finite strip formulation. *Engineering Computations*, **10**, 483-498

24. Özakça, M., Tayşi, N. and Kolcu, F. (2003). Buckling optimization of variable thickness prismatic folded plates. *Thin Walled Structures*, **41**, 711-730

25. Özakça, M., Murphy, A. and Veen, S.V.D. (2006). Buckling and post-buckling of sub-stiffened or locally tailored aluminium panels. *25th International Congress of the Aeronautical Sciences*

26. Zienkiewicz, O.C. and Campbell, J.S. (1973). Shape optimization and sequential linear programming. *Optimum Structural Design*. John Wiley, Chichester.

27. Levy, R. and Ganz, A. (1991). Analysis of optimized plates for buckling. *Computers and Structures*, **41**, 1379-1385

28. Hojjat, A. and Kok, Y.M. (1988). Arthitecture of coupled expert system for optimum design of plate girder bridges *Engineering Applications of Artificial Intelligence*, **1**, 277-285

29. Jarmai, K., Snyman, J.A. and Farkas, J. (2006). Minimum cost design of welded orthogonally stiffened cylindrical shell *Computers and Structures*, **84**, 787-797

30. Osama, K.B. (1998). A contribution to the stability of stiffened plates under uniform compression. *Computers and Structures*, **66**, 535-570

31. Bisagni, C. and Lanzi, L. (2002). Post-buckling optimization of composite stiffened panels using neural networks. *Composite Structures*, **58**, 237-247

32. Kang., J.H. and Kim, C.G. (2005). Minimum weight design of compressively loaded composite plates and stiffened panels for postbuckling strength by Genetic Algorithm *Composite Structures*, **69**, 239-246

33. Kolcu, F. (2000). Buckling *Analysis and Shape Optimization of Variable Thickness Prismatic and Axisymmetric Plates and Shells.* Ms. Thesis, Department of Civil Engineering, University of Gaziantep

34. Stroud, W.J., Greene, W.H. and Anderson, M. S. (1984). Buckling loads of stiffened panels subject to longitudinal compression and shear: results obtained with PASCO, EAL, and STAGS computer programs, NASA, TP 2215.

35. Haftka, R.T, and Gürdal, Z., (1992) *Elements of Structural Optimization*, Kluwer Academic Publishers